UNIVERSITEIT VAN PRETORIA
UNIVERSITY OF PRETORIA
YUNIBESITHI YA PRETORIA

THE RECOVERY OF SULPHUR FROM WASTE GYPSUM

by

Ryneth Nkhangweleni Nengovhela

submitted in partial fulfilment of the requirements for the degree

Philosophiae Doctor
Chemistry

in the Faculty of Natural and Agricultural Sciences
University of Pretoria
Pretoria

ACKNOWLEDGEMENT

I would like to express my sincere gratitude and appreciation to the following people and institutions who contributed towards the completion of this study:

- My supervisors, Prof. C.A. Strydom from North West University and Dr M. Landman from University of Pretoria, for their valuable advice and support.

- Dr. J.P. Maree and Mr D. Theron from CSIR, for their supervision, interest, guidance and support in connection with this project.

- The THRIP, CSIR (STEP) and University of Pretoria, for their funding of the project.

- My colleagues, Shaan Oosthuizen, Patrick Hlabela, Priscilla Randima and Lucky Bologo for their technical assistance.

- Dr F. Carlssson and Mrs Olga Webb for the layout and editing of the thesis.

- My parents, Gladys and Simon, my sisters, Alice, Mpho and Dakalo and my brother, Khathutshelo, for their friendship, encouragement and loyal support.

- A special thanks to my husband, Njabulo and my son, Bhambatha, for their patience and understanding throughout my studies.

TABLE OF CONTENTS

PAGE

PAGE

PAGE

PAGE

PAGE

PAGE

LIST OF FIGURES

LIST OF TABLES

LIST OF ABBREVIATIONS

α :	degree of conversion
t :	time
mℓ :	millilitre
ℓ :	litre
min :	minutes
XRD :	X-ray diffraction
XRF :	X-ray fluoresence
g :	gram
M :	Molar

SUMMARY

Gypsum is produced as a waste product by various industries, e.g. the fertilizer industry, the mining industry and power stations. Gypsum waste disposal sites are responsible for the leaching of saline water into surface and underground water and create airborne dust. Gypsum waste is not only an environmental problem but has measurable economic value as well. However, all these environmental and economical concerns can be avoided should valuable/saleable by-products like sulphur and calcium carbonate be recovered from the low quality gypsum.

The aim of this project was to evaluate a process for converting waste gypsum into sulphur. The process evaluated consists of the following stages: reduction of gypsum to calcium sulphide; stripping of the sulphide with CO_2 gas and the production of sulphur.

Thermal reduction study showed that gypsum can be reduced to CaS with activated carbon in a tube furnace operating at 1100 ºC. The CaS yield was 96%. The CaS formed was slurried in water. The reaction of gaseous CO_2 with the CaS slurry leads to the stripping of sulphide to form H_2S gas and the precipitation of $CaCO_3$. The H_2S generated was then reacted in the iron (IIII) and PIPco processes to form elemental sulphur.

Sulphur with the purity between 96% and 99% was recovered from waste gypsum in this study.

CHAPTER 1

INTRODUCTION

1.1 WASTE MATERIALS

Industrial effluents rich in sulphate, acid and metals are produced when sulphuric acid is used as a raw material, and when pyrites is oxidised due to exposure to the atmosphere, e.g. in the mining industry (Jones *et al*., 1988). Acid mine waters contain high concentrations of dissolved metals and sulphate, and can have pH values as low as 2.5 (Barnes and Romberger, 1968). Acidic industrial effluents require treatment prior to discharge into sewage networks or into public watercourses. In water-rich countries the main causes for concern are the low pH and metal content of acidic effluents. Salinity is not a problem due to dilution with surplus capacity of surface water. In water-poor countries, e.g. South Africa, the high salinity associated with acidic industrial effluents is an additional concern (Verhoef, 1982).

Several processes are currently employed for sulphate removal and acid water neutralization, e.g. biological removal (Maree *et al.,* 1987*)* and chemical processes (limestone, SAVMIN (Smit, 1999), reverse osmosis and electrodialysis). Chemical treatment processes are generally the least expensive but produce the largest amounts of waste, e.g. brine, sludge and metal hydroxides.

1.1.1 Brine

Brine is water saturated or nearly saturated with salts such as sodium chloride. It is produced as a waste in membrane processes for sulphate removal (Durham *et al*., 2001). The composition of the brine will vary depending on the composition of the feed water and thus the methods of brine disposal will vary accordingly. In arid climates, the brine can be evaporated, leaving a comparatively small quantity of mixed residue. In cool or wet

climates, heating may be required to promote evaporation or alternate disposal options must be considered. Brine disposal strategies are highly site specific but may include other forms of treatment (e.g. lime addition) if metals or sulphate are sufficiently elevated (Lubelli et al, 2004).

1.1.2 Sludge

The metal precipitates resulting from the neutralisation processes of acid mine water with lime and limestone is wastes identified as sludge. The composition of sludge varies due to differences in chemical composition of drainage waters between sites and annual differences at individual sites (Simonyi *et al.,* 1977). Generally the sludge is comprised of hydrated iron and aluminium oxides, phosphate, manganese, copper, magnesium, zinc and large amounts of gypsum.

The amount and consistency of sludge also varies greatly with the chemical composition of acid mine water and the treatment process used. These factors greatly influence disposal and recycling options. Sludge settleability, which is a function of both the settling rate and final sludge volume is influenced by the chemical reagents used to treat acid mine water. Studies have shown that limestone, as opposed to lime, precipitates sludge rapidly. However, lime treatment oxidizes iron completely, and ferric hydroxide is largely responsible for the poor settleability of sludge due to its hydrous nature and electrostatic charge (Ackman, 1982).

Legislation requires that sludge from neutralisation plants be disposed in an environmentally acceptable manner to prevent metals from leaching and entering the environment. Ackman (1982) showed that sludge disposal represents a major fraction of the cost during treatment of mining effluents.

1.2 SLUDGE DISPOSAL PROCESSES

Common methods of sludge disposal are deep mine disposal, permanent retention in a pond, haulage to and disposal at a coal refuse area and on site burial.

1.2.1 Deep mine disposal

This is accomplished by pumping sludge into inactive deep mines or inactive parts of mines in use. Deep mines disposal appears to be the best disposal method environmentally. Since sludge is alkaline, it can neutralize acidity in abandoned mines. The iron hydroxide resulting from the treatment does not readily redissolve and the water portion of the sludge can filter into the groundwater (Ackman, 1982). However, the problem with this method is that surface access to abandoned mines may be prohibited or structures used to retain sludge may fail and sludge enters active mines. This latter situation could inhibit future mining operations or recontaminate the treated water.

1.2.2 Permanent retention in pond

The method requires no transportation. However, large surface areas are required for affected areas, and reclaiming this land can be very difficult (Ackman, 1982). Sludge drying can take several years and the pond may only be covered once the drying is complete. These ponds may also fill up fairly quickly and offer much less disposal volume compared to deep mines. As ponds fill with sludge, washout of pollutants increases due to decreased settling distance. Ponds created by damming a valley are hazardous since in the case of a dam failure, land and streams can be devastated.

1.2.3 Coal refuse area

Sludge disposal at a coal refuse area has some advantages. The areas are already disturbed and the alkaline sludge can reduce seepage. Also, existing runoff collection systems collect all water from these sites for treatment. Disadvantages of this method are the long distances that sludge may need to be transported for disposal. However, if a refuse pile runoff collection site is nearby this may be very viable option.

1.2.4 On site burial

This method requires a dried sludge. If the sludge is disposed of on site through burial, an appropriate cover and capping system should be designed to:

- Provide erosional stability.
- Provide optimum surface water run-off and routing.
- Provide in-place physical stabilization.
- Provide optimum evaporation (use of soil materials, vegetation, engineering design, etc.)
- Minimize infiltration through sludge burial system with geosynthetic liners.

1.3 RECOVERY PROCESS

The enormous volumes of sludge produced, limited disposal sites and the future environmental problems that could be associated with sludge disposal are the major environmental and economic concerns that face acid mine water treatment. Technologies to treat sludge are the only options to solve disposal problems. Sludge rich in gypsum create environmental concerns such as airborne dust as well as effluent problems as gypsum is slightly soluble (2 000 mg/ℓ) in water. Therefore, a need exists to develop methods to convert low quality gypsum into a useful product, namely sulphur.

Sulphur is used in a number of industries and forms, for example:

- Manufacture of sulphuric acid.
- Fertilizers in agriculture.
- Fungicides.
- Vulcanising of rubber.
- Production of matches, gunpowder and fireworks.
- Sewage and waste water treatment.
- Electrodes in alkali metal batteries.
- Corrosion resistant concretes.

As far as the supply and demand for sulphur is concerned, Africa is a major importer of sulphur (Maree *et al.,* 2005). Countries like Zambia and the DRC import large tonnages of sulphur at high cost to manufacture sulphuric acid for the reduction of oxidized ores. These costs are inflated by the cost of transportation whilst sulphur is a cheap product. The South African consumption of sulphur in all forms in 2002 was 1 080 000 tons per annum of which 700 000 tons were imported at a landed cost of about R450/t (Ratlabala, 2003).

Prospects for sulphur recovery are positive with an increasing world-wide demand. In South Africa the fertilizer industry is by far the largest consumer of sulphur. The demand is also expected to increase in line with increased fertilizer usage and exports (Agnello *et al.,* 2003)

In view of serious shortages of foreign exchange, it is becoming increasingly difficult for these African countries to import sulphur. Consequently, industries depending on the use thereof are facing shut–down unless cheaper sources are identified. Most African countries have large amounts of waste gypsum generated by industrial activity. Even the costly sulphuric acid produced from imported sulphur mostly ends up as gypsum once used. Gypsum is a good source for the recovery of sulphur (Wewerka *et al*., 1982).

Thermal decomposition of gypsum was first practised commercially in Germany, during World War II, when the imported sulphur supply was disrupted by the Allied blockade. While numerous process modifications have been proposed and practised since that time, the basic requirements for successfully applying this technology remains unchanged (Lloyd, 1985). All processes require at a minimum:

1) Gypsum: Natural or by-product gypsum can be used.
2) Heating unit: Any heating unit can be used to heat the gypsum to reaction temperature, e.g. a furnace.
3) Reducing agent: This is required for reaction with gypsum at elevated temperature (Reddy *et al*., 1967; Ali *et al.,* 1968), for example, coal or

activated carbon (reaction 1), natural gas (reaction 2), carbon monoxide (reaction 3) and hydrogen (reaction 4).

$CaSO_4\,(s) + 2C\,(s) \rightarrow CaS\,(s) + 2CO_2\,(s)$ (1)

$3CaSO_4\,(s) + 4CS_2\,(g) \rightarrow 3CaS\,(s) + 4COS\,(g) + 4SO_2\,(g)$ (2)

$CaSO_4\,(s) + 4CO\,(g) \rightarrow CaS\,(s) + 4CO_2\,(g)$ (3)

$CaSO_4\,(s) + 4H_2\,(g) \rightarrow CaS(s) + 4\,H_2O\,(aq)$ (4)

The CaS produced (reaction 1 to 4) is slurried with water. Next the slurry is reacted with the CO_2 to strip the sulphide and form hydrogen sulphide (H_2S) and limestone ($CaCO_3$) (reaction 5). The H_2S gas formed after stripping is converted to elemental sulphur via the PIPco process (reaction 6) or the iron(III) route (reaction 7),

$CaS\,(s) + H_2O\,(aq) + CO_2\,(g) \rightarrow CaCO_3\,(s) + H_2S\,(g)$ (5)

$2H_2S\,(g) + SO_2\,(g) \rightarrow 3S\,(s) + 2H_2O\,(aq)$ (6)

$H_2S\,(g) + 2Fe^{3+}\,(aq) \rightarrow S\,(s) + 2Fe^{2+}\,(aq) + 2H^{+}\,(aq)$ (7)

The PIPco process, invented and patented by PIPco Inc., is a process wherein elemental liquid sulphur is produced from SO_2 and H_2S gas (Ray *et al.*, 1990). In this process, SO_2 is absorbed in a potassium citrate buffer solution. The H_2S is then bubbled through the SO_2-rich buffer solution to first form $S_2O_3^{2-}$ (reaction 11), then sulphur in reaction 12 (Gryka, 1992).

SO_2 absorber: $SO_2\,(g) + H_2O\,(aq) \rightarrow HSO_3^{-}\,(aq) + H^{+}\,(aq)$ (8)

$Cit^{3-}\,(aq) + H^{+}\,(aq) \rightarrow Cit^{2-}\,(aq)$ (9)

H_2S reactor: $2H_2S\,(g) \rightarrow 2HS^{-}\,(g) + 2H^{+}\,(aq)$ (10)

$\frac{1}{2}\,HS^{-}\,(aq) + HSO_3^{-}\,(aq) \rightarrow \frac{3}{4}\,S_2O_3^{2-}\,(aq) + \frac{3}{4}\,H_2O\,(aq)$ (11)

$\frac{3}{2}\,HS^{-}\,(aq) + \frac{3}{4}\,S_2O_3^{2-}\,(aq) \rightarrow 3S\,(s) + \frac{9}{4}\,H_2O\,(aq)$ (12)

Overall: $2H_2S\,(g) + SO_2\,(g) \rightarrow 3S\,(s) + 2H_2O\,(aq)$ (13)

Catalytic and thermal reduction processes (Rameshni and Santo, 2005) for sulphur recovery are expensive, difficult to operate, have high fuel consumption and limited ability to control temperature and side reactions.

CHAPTER 2

LITERATURE REVIEW

2.1 OCCURRENCE OF SULPHATE

Sulphate is a common constituent of water and results from the dissolution of mineral sulphates in soil and rock, particularly calcium sulphate (gypsum) and other partially soluble sulphate minerals (Toerien and Maree, 1987). It is also one of the least toxic anions with a lethal dose for humans of 45 g potassium or zinc salt (WHO, 1996).

Mine waters can contain significant concentrations of sulphuric acid and metal sulphates due to the oxidation of pyritic material in ore bodies and effluents from the uranium leaching process (Jones *et al.,* 1988). The acidity of the water is usually neutralised, but the sulphate content of the water is often in contravention of effluent standards. Sulphates are discharged from acid mine wastes and many other industrial processes such as tanneries, textile mills and processes using sulphuric acid or sulphates (Maree *et al*., 1989). It is estimated that in South Africa, 200 Mℓ/d of mining effluent, saturated with calcium sulphate, is discharged into the public streams of the Pretoria–Witwatersrand–Vereeniging region (Maree, 1988). This represents a sulphate load of 73 000 t/a. Atmospheric sulphur dioxide, discharged on combustion of fossil fuels, can give rise to sulphuric acid in rainwater (acid rain), which in turn results in the return of sulphate to surface waters in the environment.

Typically, the concentration of sulphate in:

- Surface water is 5 mg/ℓ SO_4^{2-}, although concentrations of several hundred mg/ℓ SO_4^{2-} may occur where the dissolution of sulphate minerals or discharge of sulphate rich effluents from acid mine drainage takes place (Maree, 1988).

- Sea water has just over 900 mg/ℓ SO_4^{2-}.
- Run-off water from areas with high mining activities varies between 200 and 2000 mg/ℓ SO_4^{2-}, while in areas of low mining activities it varies between 10 and 55 mg/ℓ SO_4^{2-} (Forster, 1988).

2. 2 EFFECT OF SULPHATE IN THE ENVIRONMENT

Although sulphate is non-toxic, except at very high concentrations, it exerts a purgative effect.

- Precipitation of sulphate can cause damage to equipment through the formation of calcium sulphate scale. (Maree *et al.,* 1990).

- At high concentrations, precipitation of sulphates may affect the efficiency of many industrial processes. The corrosive effect of high sulphate waters, particularly towards concretes, is increasingly becoming a major water quality problem for mining operations (Loewenthal *et al*., 1986).

- Sulphate, especially precipitation of gypsum, may impair the quality of treated water. In many arid environments gypsum becomes the dominant contributor to salinity in the vicinity of the discharge (Verhoef, 1982).

- People consuming drinking water containing sulphate in concentrations exceeding 600 mg/ℓ commonly experience cathartic effects, resulting in purgation of the alimentary canal (WHO 1996). Dehydration has also been reported as a common side effect following the ingestion of large amounts of sulphate.

2.3 TREATMENT OF SULPHATE RICH WATER

Current legislation world-wide places a limit around 400-500 mg/ℓ SO_4^{2-} in groundwater and 2 000 mg/ℓ SO_4^{2-} in industrial effluent (Wagner and Van Niekerk, 1987). Various treatments are available for sulphates involving physical, chemical and biological processes.

Essentially, these processes operate either through separation of salts through a membrane or through precipitation of sulphate as an insoluble salt, or through water evaporation and brine saturation. The selection of the treatment option is dictated by the sulphate and calcium concentration, due to the $CaSO_4$ scaling potential (Loewenthal *et al*., 1986).

2.3.1 Membrane processes

2.3.1.1 Reverse Osmosis

When brines with different salinities are separated by a semi-permeable membrane, pure water from the less concentrated brine will diffuse through the membrane until the salt concentrations on both sides of the membrane are equal (Chamber of Mines Research Organisation, 1988). This process is called *osmosis.* With reverse osmosis, salty feed water on one side of a semi-permeable membrane is typically subjected to pressures of 200-500 lb/sq inches for brackish water, and 800-1 200 lb/sq inches for seawater (AWWA, 1999).

About 10 gallons of water will pass through a square foot of membrane each day. The percentage of incoming feed water that is recovered as product water after one pass through a reverse osmosis module ranges from about 15-80 percent, however, this percentage can be increased if necessary by passing the waste water through sequential membrane elements (Durham *et al*., 2001)

Different osmosis processes have been proposed, for example:

1) The seeded reverse osmosis which uses a suspension of salt crystals to promote precipitation, and
2) The slurry precipitation, recycle and reverse osmosis (SPARRO) which includes the precipitation of metals by increasing effluent pH to 10 as a pre-treatment step, followed by cooling, filtration and readjustment of pH to 5-6 for the protection of the membrane process (Pulles *et al*., 1992; Juby *et al*., 1996).

2.3.1.2 Electrodialysis

Electrodialysis is a process that uses a direct electrical current to remove salt, other inorganic constituents and certain low molecular weight organics from brackish water with concentrations of dissolved solids up to 10 000 ppm (Valerdi-Perez *et al*., 2001). Dialysis tends to be more economical than reverse osmosis at salinities of less than 3 000 ppm but less economical than reverse osmosis at salinities greater than 5 000 ppm (Durham *et al*., 2001).

With this technique several hundred flat, ion permeable membranes and water flow spacers are assembled in a vertical stack. Half of the membranes allow positively charged ions, or cations, to pass through them. The other half-anion-permeable membranes allow negatively charged ions to pass through them (Spiegler, 1966).

2.3.1.3 Filtration Techniques

The process involves the separation of suspended particles from fluids. Different purification schemes are defined on particle size and flow. Any filtration process treatment where coarse particles dominate the suspended load requires pre-treatment (Zeman and Zydney, 1996). Different techniques are available including screening, freezing, elutriation and irradiation.

2.3.1.4 Ion Exchange

Ion exchange occurs between solid and liquid but no change results to the solid's structure. The target ions are removed from the liquid phase and are attached to the solid structure in exchange for another ion (hydrogen or hydroxyl) to immobilise the target ion (Schoeman and Steyn, 2001). For example, sulphate in $CaSO_4$, being an anion, would be exchanged for hydroxyl on an anion exchange resin (positively charged resin) while calcium, being a cation, would be exchanged for hydrogen on a cation exchange resin (negatively charged resin).

Due to the scaling in conventional circuits, GYPCIX (Gypsum Crystallisation Ion Exchange, Chemeffco SA), which is a modified ion exchange technique, was developed. GYPCIX uses low cost reagents such as lime and sulphuric acid. These resins target calcium and sulphate to reduce gypsum levels in effluent and to reduce the total dissolved solids concentration and corrosion problem. It can be used to treat solutions containing sulphate up to 2 000 mg/ℓ and calcium up to 1 000 mg/ℓ.

2.3.2 Precipitation processes

2.3.2.1 Barium salts

Barium sulphate is highly insoluble, thus making it an excellent candidate as a removal phase for sulphate treatment. The barium salts, used to remove sulphate by precipitation, include $BaCO_3$, BaS and $Ba(OH)_2$ according to reactions (14-16):

$$BaCO_3\,(s) + H_2SO_4\,(aq) \rightarrow BaSO_4\,(s) + H_2CO_3\,(aq) \quad (14)$$

$$Ba(OH)_2\,(s) + H_2SO_4\,(aq) \rightarrow BaSO_4\,(s) + 2H_2O\,(aq) \quad (15)$$

$$BaS\,(s) + H_2SO_4\,(aq) \rightarrow BaSO_4\,(s) + H_2S\,(g) \quad (16)$$

All three barium processes can lower high sulphate concentrations down to regulatory standards concentrations. The BaS process was found to be the

most attractive process over the $BaCO_3$ and $Ba(OH)_2$ processes (Maree *et al.* , 1990) because:

1) High sulphate concentrations are removed and less gypsum is produced,
2) Acid waters can be treated directly thus eliminating the need for a pre-neutralisation step, and
3) Gypsum sludge disposal are lessened

2.3.2.2 Lime and Limestone

Lime and limestone are traditionally used for the neutralization of Acid Mine Drainage (AMD) but can also be used for the removal of sulphate from AMD through precipitation of gypsum (Bosch, 1990). After the treatment of AMD with lime or limestone, high sulphate levels remain in the treated water. Thus the process may be better suited as a pre-treatment step for AMD waters high in dissolved sulphate concentrations.

Recently, an integrated lime/limestone process was developed at the CSIR that is capable of reducing the sulphate concentration in AMD from 3 000 mg/ℓ to less than 1 200 mg/ℓ (Geldenhuys, 2001). The process consists of the following three stages:

1) Limestone neutralization to raise the pH to circum-neutrality in CO_2 production and gypsum precipitation,
2) Lime treatment to raise the pH to 12 for $Mg(OH)_2$ precipitation and enhanced gypsum precipitation, and
3) pH adjustment with CO_2 recovered from stage 1 with concurrent $CaCO_3$ precipitation.

2.3.3 Biological sulphate reduction process

The biological sulphate removal process is of interest owing to the acceptable cost and low waste production. Maree and Strydom (1985) showed that

sulphate can be removed in an anaerobic packed-bed reactor using sucrose, pulp mill effluent or molasses as carbon and energy source. Metals such as nickel, cadmium and lead were completely removed as metal sulphides. Maree and Hill (1989) showed that a three-stage process can be employed for sulphate removal, using molasses as carbon and energy source in an anaerobic packed-bed reactor.

Du Preez *et al.* (1992) were the first to demonstrate that producer gas (mixture of H_2, CO and CO_2) can be used as carbon and energy source for biological sulphate reduction. Visser (1995) investigated the competition between sulphate reducing bacteria (SRB) and methanogenic bacteria (MB) for acetate as energy and carbon source in an upflow anaerobic sludge blanket (UASB) reactor. He found that at pH values less than 7.5, SRB and MB are equally affected by the presence of H_2S, while at higher pH values SRB out-compete MB.

Van Houten (1996) showed that sulphate can be reduced to H_2S at a rate of 30 g SO_4/ℓ.d when H_2/CO_2 is used as carbon and energy source and employing pumice or basalt particles to support bacterial growth in a fluidised-bed reactor. He found the optimum pH to be 6.5-8.0; the optimum temperature between 20-35 °C; the optimum H_2S concentration to be less than 450 mg/ℓ. The system should be completely anaerobic; the biomass immobilized and the retention of the active biomass high. The gas should be in the ratio: H_2:CO_2, 80%:20% and the hydrogen mass transfer maximized and there should be a high gas hold-up (through the system recycle) and small bubble diameter.

Eloff *et al*. (2003) showed that a venturi device can be used to introduce hydrogen gas into the system as the energy source, while geotextile (a coarse, fibrous material, used in road construction) can be used as a support material for SRB growth.

2.4 THERMAL ANALYSIS

Thermal analysis is the measurement of certain characteristics of a substance as a function of temperature or time. The technique has a wide range of applications, of which some are:

- Structural changes e.g. glass transition, melting/crystallization, solid and liquid phase transitions.
- Mechanical properties e.g. elastic behaviour and expansion/shrinkage.
- Thermal properties e.g. specific heat, melting point and expansion coefficient.
- Chemical reactions e.g. decomposition and stability in various gaseous atmospheres, reaction in solution, reaction in liquid phase, reaction with purge gas and dehydration (humidity, water of crystallization).

Figure 2.1 shows the schematic diagram of a Thermal Analysis instrument.

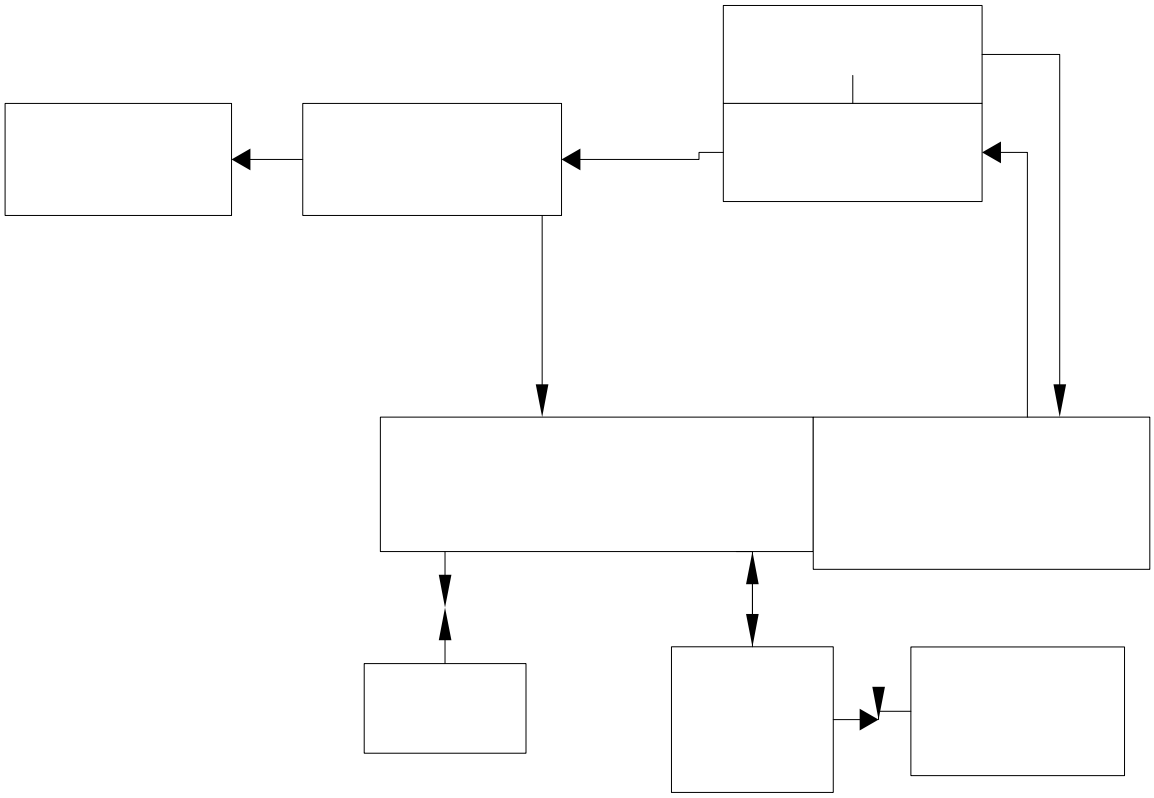

Figure 2.1 Schematic diagram of a Thermal Analysis instrument

Most important thermal analysis techniques are:

1. Thermogravimetry (TG) for measuring mass changes.
2. Differential Thermal Analysis (DTA) for measuring temperature differences.
3. Differential Scanning Calorimetry (DSC) for measuring heat flow.
4. Thermochemical Analysis (TMA) for measuring deformation.
5. Dynamic Mechanical Thermal Analysis (DMA) for measuring storage and loss moduli (Brown,1988).

2.4.1 Thermogravimetry

Thermogravimetry is the most widely used thermal technique to study heterogeneous processes. It is a limited technique, however, in that a gas-solid system must be involved in which the gaseous component is either a reactant or product of the reaction. Phase transitions such as solid to gas may also be investigated by this technique.

Three modes of thermogravimetry are:

a) isothermal or static thermogravimetry, in which the sample mass is recorded as a function of time at constant temperature,
b) quasistatic thermogravimetry or non-isothermal in which the sample is heated to constant mass at each of a series of increasing temperatures, and
c) dynamic thermogravimetry, in which the sample is heated in an environment whose temperature is changing in a predetermined manner preferably at a linear rate (Garner, 1955 and Sestak *et al*., 1973).

In the thermogravimetric curve of a single non-isothermal reaction, there are two characteristic temperatures, the initial temperature, T_i and the final temperature T_f. T_i is the lowest temperature where the cumulative weight change reaches a magnitude that a particular thermobalance can detect. T_f is

the temperature where the cumulative weight change first reaches its maximum value (Bamford and Tipper, 1980).

The development and ready availability of reliable and accurate electronic microbalances in thermogravimetry have led to their wide application in kinetic studies of the decomposition of solids (Garn, 1965).

2.4.2 Thermal decomposition reactions of solids

Thermal decomposition of solids means the breakdown of one or more constituents of the reactants into simpler atomic groupings upon heating. The thermal decomposition of a solid may be associated with physical transformations, such as melting, sublimation and recrystallization. The recrystallization of a solid may result in the production of a higher temperature lattice modification, which permits increased freedom of motion of one or more lattice constituents. The reactivity and chemical properties of solids are strongly influenced by the relative immobility of the constituent ions or molecules in the lattice of the reactant phase. The reactivity of identical chemical groupings in a solid reactant may vary with their position in the solid, as the structure may contain imperfections.

In regions of local distortion, the forces of lattice stabilization may be relatively diminished, with a consequent increase in the probability of reaction. This contrasts with the homogeneous behaviour of similar groups in the liquid or gaseous phase. In rate processes of solids it is often observed that there are localized regions or sites of preferred onset of reaction. Such initiation usually occurs at a surface, leading to the development of a zone of preferred chemical transformation, which thereafter progressively advances into adjoining volumes of unreacted material. This restricted zone of the solid is called the reaction interface (Bamford and Tipper, 1980).

The occurrence of reaction is usually regarded as being exclusively restricted to the reactant-product interface, at which local conditions markedly enhance the ease of the chemical transformation. The kinetic characteristics of the

overall process are determined by the velocity of the advance of this interface into unchanged reactant and the variation of its effective area with time (Bamford and Tipper, 1980).

The following general kinetic tenets have been used as a widely accepted basis for the interpretation of the kinetic behaviour of the decomposition reactions of solids (Bamford and Tipper, 1980):

1) the rate of reaction of a solid is proportional to the aggregate effective area of the reactant product interface,
2) the rate of interface advance is constant through an isotropic reactant under isothermal conditions and
3) the temperature dependence of the rate coefficient obeys the Arrhenius equation.

These tenets are applicable only where the reactant undergoes no melting. If no melting occurs, the shape of the fraction decomposed (α) against time (t) curve for an isothermal reaction can be related to the geometry of formation and advance of the reaction interface.

2.4.3 Kinetic rate laws for the decomposition of solids

The number of potential nucleus forming sites (N_o) and the number of molecules having the energy at least equal to the activation energy for nucleus formation determines the rate at which nuclei are formed. The laws describing the decomposition rate in decomposition reactions (Note: all these reactions are valid at constant temperature) are divided into three groups depending on the location of the maximum rate of decomposition, $(\frac{d\alpha}{dt})_{max,}$ where α is the degree of conversion and t is the time (Keattch and Dollimore, 1975):

1) α against t relationships obeyed up to $(\frac{d\alpha}{dt})_{max}$, and concerned with nuclei growth,
2) α against t relationships obeyed on both sides of $(\frac{d\alpha}{dt})_{max}$ and thus concerned with both nuclei growth and interference and
3) α against t relationships obeyed beyond $(\frac{d\alpha}{dt})_{max}$, i.e. relationships concerned with either nuclei interference or a decreasing reaction interface.

The measured thermogravimetric scan is transformed into the degree of conversion as follows:

$$\alpha_i = \frac{M_0 - M_i}{M_0 - M_f} \qquad (17)$$

where M_i = mass at time t

M_o = initial mass

M_f = final mass

The kinetics of many solid-state reactions can be represented by the general equation $f(\alpha) = kt$, where the function $f(\alpha)$ depends on the reaction mechanism and geometry of the reacting particles. Sharp *et al.* (1966) have shown that an approach based on a reduced time scale facilities comparison of experimental data with theoretical models; some theoretical equations were expressed in the form $f(\alpha) = A(t/t_{0.5})$, where $t_{0.5}$ is the time at which α = 0.5 and A is a calculable constant which depends on the form of $f(\alpha)$. Experimental data can be tabulated as α vs t for a variety of experimental conditions. Rate constants can be then be determined from linear plots of $f(\alpha)$ vs t.

The equations can be divided into groups to differentiate among equations within a group requires considerable experimental accuracy to high values of α. The groups and their equations are:

1) Diffusion-controlled reactions (Jander, 1927):

$$f(\alpha) = \alpha^2 = kt \quad (18)$$

$$(1-\alpha)\ln(1-\alpha) + \alpha = kt \quad (19)$$

$$[1-(1-\alpha)^{1/3}]^2 = kt \quad (20)$$

$$1 - 2\alpha/3 - (1-\alpha)^{2/3} = kt \quad (21)$$

2) Phase-boundary-controlled (Keattch and Dollimore, 1975): $f(\alpha) =$

$$1-(1-\alpha)^{1/2} = kt \quad (22)$$

$$1-(1-\alpha)^{1/3} = kt \quad (23)$$

3) Avrami-Erofe'ev equations (Erofe'ev, 1946): $f(\alpha) =$

$$[-\ln(1-\alpha)^{1/2}] = kt \quad (24)$$

$$[-\ln(1-\alpha)^{1/3}] = kt \quad (25)$$

2.4.4 Kinetic parameters

The temperature dependence of chemical processes can be expressed in terms of the Arrhenius equation,

$$k = Ae^{-E_a/RT} \quad (26)$$

where k is the rate constant, R is the gas constant and T is the thermodynamic temperature. The Arrhenius parameters (E_a and A) provide measures of the magnitude of the energy barrier to reaction (the activation energy, E_a) and the frequency of the occurrence of a condition that may lead to a reaction (the frequency factor, A) (Blaine and Hahn, 1998).

There is no discrete activated state in the solid state, so activation energy values need to be evaluated critically before conclusions regarding the stability of the solid reactants can be drawn (Garn, 1978). The activation energy value (E) is expressed as an energy quantity per mole ($kJ.mol^{-1}$), since the measured slope of the Arrhenius plot (lnk vs 1/T) is divided by the gas constant, R (R=8.314 $J.K^{-1}.mol^{-1}$). For the initial stages of the reaction

(α < 0.1), the relationship between the rate constants, k, and the reaction time, t, can be given as

$$\frac{d\alpha}{dt} = kt \tag{27}$$

Using the k values at different temperatures and applying them to the Arrhenius equation, an activation energy value for the nucleation process of a reaction can be obtained.

2.4.5 Determination of kinetic parameters

Any approach to the analysis of both complex (those whose kinetics cannot be described as an overall single stage process (single rate constant)) and simple (overall single- stage) processes must rely on the methods relating to complementary techniques (Vyazovkin and Lesnikovich, 1987), in other words, using generalised descriptions of the process instead of discriminating separate elementary models.

The quasi isoconversional methods can be used for determination of activation energy of the single-stage process. Among methods that are used to analyse complex processes are the isoconversional method (Flynn, 1983), method of invariant kinetic parameters (Lesnikovich and Levchik, 1983), Sestak-Berggren method (Sestak and Berggren, 1971) and Piloyan method (Piloyan *et al.,* 1966).

It has been shown by Vyazovkin and Lesnikovich, (1990) that reliable information about the mechanism and kinetics of complex processes can be obtained by isoconversional methods. One attribute to such methods is that the effective activation energy specific for a given extent of conversion can be determined if several thermal analysis experiments are performed at different heating rates.

The well known isoconversional methods used for the determination of activation energy is the Ozawa-Flynn Wall method (Dowdy, 1987). The method provides a model free approximation of the activation energy by using multiple scan analysis. It is suited for use in systems where many reactions are occurring. It does not require any assumptions concerning the form of the kinetic equation, other than that there is Arrhenius-type temperature dependence (Dowdy, 1987).

The differential methods for the calculation of the kinetic parameters are based on the use of the well known reaction rate equation:

$$\beta \frac{d\alpha}{dt} = f(\alpha) A \exp\left(\frac{-E}{RT}\right) \tag{28}$$

where β is the heating rate, T is the temperature, A is the pre-exponential factor and f(α) is the differential conversion function.

As far as the isoconversional integral methods are concerned, the above equation at constant heating can be expressed as follows:

$$g(\alpha) = \int_0^{\alpha} \frac{d\alpha}{f\alpha} = \frac{A}{\beta} \int_{T_0}^{T} \exp\left(-\frac{E}{RT}\right) dT \tag{29}$$

$$g(\alpha) = \frac{AE}{R\beta} p\left(\frac{E}{RT}\right) \tag{30}$$

where $g(\alpha)$ is the integral conversion function.

Assuming that T_0 is below the temperature at which the reaction becomes noticeable, the lower limit, T_0, can be set to zero. Then equation 30 expressed in logarithmic form is:

$$\log g(\alpha) = \log\left(\frac{AE}{R}\right) - \log\beta + \log p\left(\frac{E}{RT}\right) \tag{31}$$

Doyle, (1962) has found that for E/RT≥20, log p$\frac{E}{RT}$ may be approximated by equation 32,

$$\log p\left(\frac{E}{RT_i}\right) = -2.315 - 0.4567\left(\frac{E}{RT_i}\right) \tag{32}$$

Therefore equation 31 becomes,

$$\log g(\alpha) = \log\left(\frac{AE}{R}\right) - \log\beta - 2.315 - 0.4567\frac{E}{RT} \tag{33}$$

"Differentiating" equation 33 at constant degree of conversion results in

$$\frac{d\log\beta}{d1/T} \cong \left(\frac{0.457}{R}\right)E \tag{34}$$

For R = 1.987 cal.mole^{-1}.K^{-1}

$$E = -4.35\frac{d\log\beta}{d\frac{1}{T}} \tag{35}$$

Therefore, if a series of experiments are performed at different heating rates, this equation can be used to obtain the activation energy. A specific degree of conversion is considered, and the temperature required for this degree of conversion is determined for each heating rate. If log β is plotted against 1/T the gradient is -0.4567E/R, and so the activation energy can be determined for the particular degree of conversion (α) being considered.

2.4.6 Identifying the type of reaction/process

According to Vyazovkin and Lesnikovich, (1990) and Dowdy (1987), it was stated that for the isoconversional method, a complex process/reaction is identified by the changes in activation energy for different α, while on a single stage reaction, the activation energy does not change with α. The high sensitivity of the degree of conversion dependence of the activation energy provides a higher efficiency of its application as a criterion of a complex process. Therefore, the analysis of a complex reaction is based on the dependence of the α on the activation energy.

Vyazovkin and Lesnikovich, (1990) further showed that the increase in dependencies of activation energy on the degree of conversion occur when simultaneous/parallel reactions occur. Decreasing dependencies are typical of

complex reactions with a change in limiting stage. Among these are, in particular processes containing a reversible intermediate stage or those proceeding with a change over from kinetic to the diffusion regime.

The IKP (Invariant Kinetic Parameters) method can also be used to determine the complex character of a model process based on the shape of the Arrhenius dependence. The rate of such a process is determined by the equation,

$$\frac{d\alpha}{dt} = \beta\frac{d\alpha}{dT} = (k_1 + k_2)(1-\alpha) \tag{36}$$

where β is the heating rate, T is the temperature , t is the time, k_1 and k_2 are the rate constant. Integrating equation 36, we obtain the temperature dependence of the degree of conversion.

$$\alpha = 1 - \exp\left[-\left(\frac{1}{\beta}\right)\int_0^T (k_1 + k_2)dT\right] \tag{37}$$

Taking into account the Arrhenius shape of the temperature dependence of the rate constants, the integral can easily be calculated as Senum-Yang approximation (Senum and Yang, 1979). If the plot of lnk vs 1000/T (Arrhenius dependence) gives a concave shape then that particular process involves parallel reactions while the convex shape shows a process with a change in the limiting stage.

2.5 THERMAL DECOMPOSITION OF GYPSUM TO CALCIUM SULPHIDE

The process of converting gypsum to calcium sulphide is normally effected by passing reducing gases at elevated temperatures over gypsum and cooling the calcium sulphide produced in a non-oxidising atmosphere.

Calcium sulphide is a white powder if pure, but crude calcium sulphide called sulphurated lime, can be yellowish to pale grey (Anthony *et al.*, 1990). It has an odour of H_2S in moist air and an unpleasant alkaline taste. CaS has a very low solubility of 0.2 g/ℓ.

Calcium sulphide can be prepared in the laboratory by heating pure calcium carbonate in a stream of H_2S and H_2 at 1000 °C (Brauer, 1963). It can be used as a lubricant additive in phosphorus. Luminous CaS can be used for making luminous paints or varnishes. Pure CaS is used in electron emitters (Budavari, 1989). In industries it is used in the production of sulphur by the Chance-Claus process and as an insecticide in the treatment of waste liquor from paper mills (Ali *et al.,* 1968). It is also used in cement to achieve an increase in mechanical strength with time.

2.5.1 Description of gypsum

Gypsum can be colourless, white, grey, yellow, red or brown in colour. The crystals are prisms or flat plates, and can grow up to 1 metre (Figure 2.2). It can appear as transparent crystals (selenite); fibrous, elongated crystals (satin spar); granular and compact masses (alabaster); and in rosette-shaped aggregates called desert roses (Follner *et al*., 2002).

Figure 2.2 Crystals of natural gypsum

2.5.2 Occurrence of gypsum

Natural gypsum deposits were formed millions of years ago when salt water oceans covered most of the earth, and as they receded, many inland "dead" seas were formed which, as evaporation continued, became more salty. As those salts precipitated, they formed various compounds in turn, one of which was gypsum (natural gypsum).

Gypsum can also be produced as a waste product by various industries, e.g.

- fertilizer industry, when sulphuric acid is reacted with calcium phosphate rock, resulting in a solution of phosphoric acid and a solid calcium sulphate called phosphogypsum (Benstedt, 1979; Roode, 1996).

$$Ca_5(PO_4)_3.F(s) + 5H_2SO_4(aq) + 5x\ H_2O\ (l) \rightarrow 5CaSO_4.xH_2O(s) + 3H_3PO_4(aq) + HF(aq) \quad (38)$$

where x depends on the temperature and acid concentration and can be either 0 (anhydrite), ½ (hemihydrate) or 2 (dihydrate).

- mining industry, when acid mine water is neutralized with limestone or lime (reaction 39) .

$$CaCO_3\ (s) + H_2SO_4\ (aq) \rightarrow CaSO_4\ (s) + CO_2\ (g) + H_2O\ (aq) \quad (39)$$

- power stations, when powdered calcium carbonate is fed to the combustion chamber to react with SO_2 gas (reaction 40).

$$SO_2\ (g) + CaCO_3\ (s) + ½\ O_2\ (g) + 2H_2O \rightarrow CaSO_4.2H_2O(s) + CO_2\ (g) \quad (40)$$

Furthermore, at PPC Cleveland's Jupiter cement plant, gypsum is prepared by mixing $CaCO_3$ with diluted H_2SO_4 (Mantel and Liddell, 1988).

2.5.3 Uses of gypsum

Gypsum is used in the building and agricultural industries. As a building material, it is used

- in the manufacture of plaster walls, ceramic tiles, tombstones and partitions,
- to adjust time of setting of Portland cement, and in ceramic tiles (Mantel, 1991).

In agriculture, it is used

- as a fertilizer and soil conditioner to reduce salinity of soils,
- as an animal–food additive (Bye, 1983).

Gypsum is also used as a source for Plaster of Paris in treatment of fractured bones and as a dental plaster mold to cast the dental. It can also be sprayed in coal mines to prevent gas explosion (Mantel, 1991).

Gypsum can be ground up and calcined at a comparatively low temperature (110-120 °C) until 75% of its moisture content has evaporated. When that happens, the rock becomes a fine powder (Plaster of Paris). By returning the water to the powder, a pliable mortar can be made that can be formed into any shape and hardened. Heat treated gypsum is the only natural substance that can be restored to its original rock-like state by the addition of water alone (Murat, 1987).

2.5.4 Effect of gypsum

Gypsum wastes, not only occupy thousands of acres of land but create serious problems such as air borne dust and water pollution problems due to the release of hazardous substances such as heavy metals and acid as a result of weathering and chemical decomposition (Savostianoff, 1990).

2.5.5 Dehydration of gypsum

Waste gypsum is a mixture of calcium sulphate dihydrate ($CaSO_4$.$2H_2O$), calcium sulphate hemihydrate ($CaSO_4$.0.5 H_2O), anhydrous calcium sulphate ($CaSO_4$) and some impurities (Taylor, 1990). Dihydrate and insoluble anhydrite are stable materials found in nature, while hemihydrate and soluble anhydrite are highly unstable, and readily react with water. When the dihydrate is heated, it dehydrates in two steps to the hemihydrate and soluble anhydrite (reaction 41 and 42),

$$CaSO_4.2H_2O\ (s) \xrightarrow{>95°C} CaSO_4.0.5H_2O(s) + 1.5\ H_2O\ ((g) \quad (41)$$

$$CaSO_4.0.5H_2O\ (s) \xrightarrow{>120°C} CaSO_4\ (s) + 0.5\ H_2O\ (g) \quad (42)$$

The degree of gypsum dehydration is strongly influenced by the structure and the impurities in the material, as well as by the conditions under which the process takes place, such as temperature, heating rate, vapour pressure, humidity and particle size (Molony and Ridge, 1968). Dehydration increases with exposure time to elevated temperatures. The dehydration of the gypsum present in cement will proceed at a higher rate than dehydration of gypsum by itself as the humidity increases. Mantel and Liddell, (1988) described the kinetics differences between naturally occurring South African gypsum (used in Port Elizabeth cement companies), synthetic gypsum (which is prepared from the reaction of limestone with sulphuric acid and used in Johannesburg cement companies) and pure calcium sulphate dehydrate in different atmospheres.

2.5.5.1 Hemihydrate ($CaSO_4.0.5H_2O$)

Hemihydrate (partially dried calcium sulphate) is a fine, odourless and tasteless powder which occurs in nature as a mineral bassanite. When mixed with water, it sets to a hard mass. It is used for wall plasters, wallboard and blocks for the building industry (Ball and Norwood, 1969).

The hemihydrate exists in two forms, termed α and β. These two forms are the limiting states of this phase and are distinguished from each other by their properties, energy relationships and methods of preparation. The α-hemihydrate is produced under pressure in a humid atmosphere and consists of large primary particles. The β-hemihydrate forms flaky, irregular secondary particles which consist of small individual crystals. The solubility of the α-hemihydrate in water at 20 °C is 0.88 g/100g solution and that of the β -hemihydrate is 0.67 g/100mℓ solution. Figure 2.4 showed the crystal structure, (Bezou *et al.,* 1995**)**.

2.5.5.2 Anhydrite ($CaSO_4$)

The anhydrite (dead burned gypsum) exists in three phases (Hand, 1997):

a. soluble calcium sulphate anhydrite (γ-$CaSO_4$) (crystal structure for γ-$CaSO_4$ is given in figure 2.3, Bezou *et al*, 1995),
b. insoluble calcium sulphate anhydrite (β-$CaSO_4$)
c. high temperature calcium sulphate anhydrite phase (α-$CaSO_4$).

Insoluble anhydrite has the same crystal structure as the mineral and is obtained upon complete dehydration of the calcium sulphate dihydrate above 200 °C. It is used in cement formulations and as a paper filter (Ball and Norwood, 1969).

Soluble anhydrite is obtained in granular or powder form by complete dehydration of the calcium sulphate dihydrate above 120 °C. Because of its

strong tendency to absorb moisture, soluble anhydrite is useful as a drying agent for solids, organic liquids and gases (Ball and Norwood, 1969).

The high temperature calcium sulphate anhydrite is insoluble in water and exists at temperatures above 1 180 °C (Wirsching 1978).

2.5.5.3 Dihydrate ($CaSO_4.2H_2O$)

The dihydrate occurs in nature as a fine grained, compact mass of small crystals (crystal structure is indicated in Figure 2.5, Atoji and Rundle, 1958). It is used in the manufacturing of Portland cement, in soil treatment to neutralise alkali carbonates and to prevent loss of volatile compounds and for the manufacturing of Plaster of Paris as a white pigment (Ball and Norwood, 1969). The dihydrate is soluble in water and practically insoluble in most organic solvents. Its solubility in water is 0.21g/100g solution.

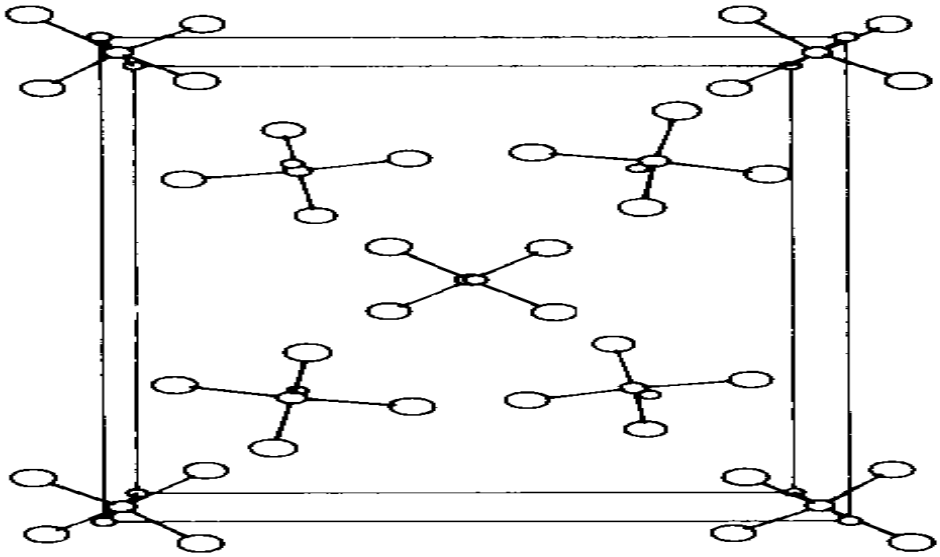

Figure 2.3 Crystal structure of γ-$CaSO_4$ (Bezou *et al*, 1995)

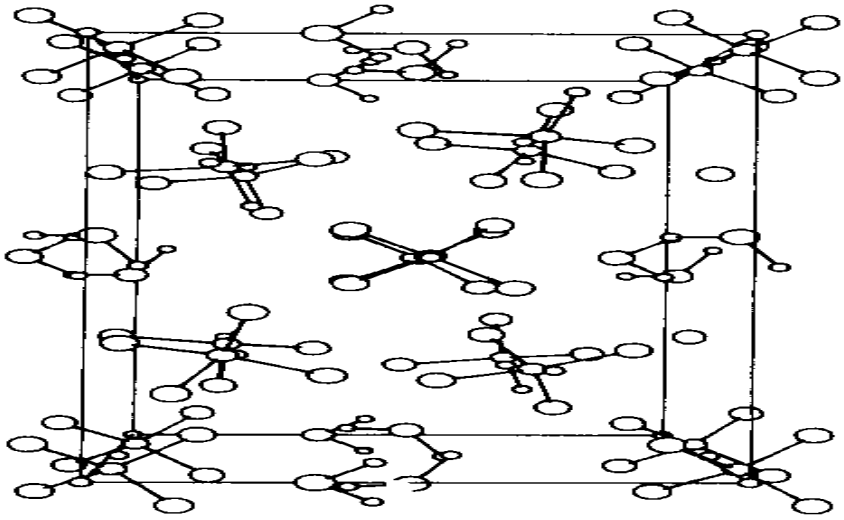

Figure 2.4 Crystal structure of $CaSO_4.0.5H_2O$ (Bezou *et al*, 1995)

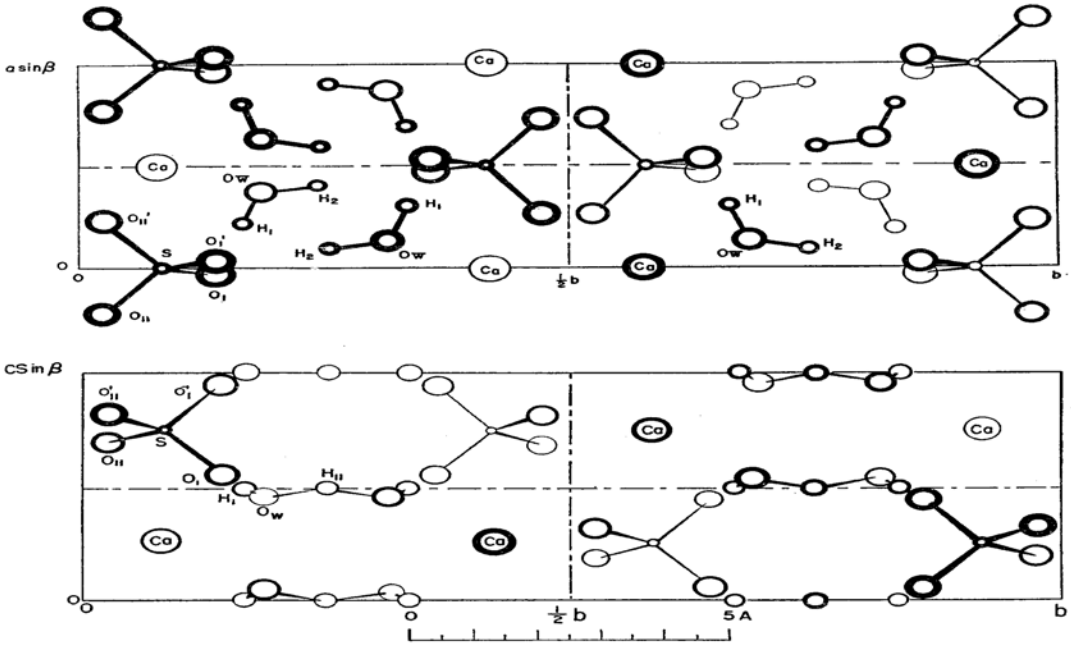

Figure 2.5 Crystal structure of $CaSO_4.2H_2O$ (Atoji and Rundle, 1958)

2.6 SULPHUR PRODUCTION PROCESS USING HYDROGEN GAS

Hydrogen sulphide (H_2S) is a highly toxic, corrosive and malodorous gas. Besides its other bad habits, it also deactivates industrial catalysts. H_2S is commonly found in natural gas and is also a by-product at oil refineries.

If water comes into contact with gas streams containing hydrogen sulphide it turns sour (Cadena and Peters, 1988). In water, sulphide (S^{2-}) has an oxygen demand of 2 mol O_2/mol S^{2-} and thus would consume oxygen and have an adverse effect on aquatic life if discharged into surface water (Kobayashi *et al*., 1983). Because H_2S is such an obnoxious substance, it is converted to non-toxic and useful elemental sulphur at most locations that produce it.

Removal of H_2S from gas streams is a familiar industrial requirement, whose economic importance will grow with the increasing utilization of fuels with higher sulphur content. Among the removal processes for H_2S, conversion to elemental sulphur is advantageous because sulphur can be used for the treatment of gases in an environmentally permissible procedure (Astarita *et al*., 1983; Kohl and Riesenfeld, 1985). It can also be applied to the treatment of gases with relatively low concentrations of H_2S in the presence of CO_2.

The conventional chemical processes for H_2S abatement and sulphur recovery (e.g. the Claus process) have some drawbacks, such as deactivation, loss of absorbent or catalyst poisoning or side reactions, unfavourable selectivity, corrosiveness, toxicity and the need to operate at a high pressure or temperature (Cork *et al*., 1986).

2.6.1 Description of the Claus process

The Claus reaction consists of H_2S and sulfur dioxide (SO_2) reacting in the vapour phase to produce sulphur and water. The H_2S is first separated from the host gas stream using amine extraction. Then it is fed to the Claus unit, where it is converted in two steps (Chandler and Isbell, 1976). The first step is the thermal step (reaction 43), where one-third of the H_2S is oxidized, producing the H_2S and SO_2 in a 2:1 ratio. This is done in a reaction furnace at high temperatures (1 000-1 400 °C).

Some sulphur is formed, but the remaining unreacted H_2S proceeds to the next step, the catalytic step. The thermal step reaction and a schematic drawing of the process are as follows:

$2H_2S\ (g) + 3O_2\ (g) \rightarrow 2SO_2\ (g) + 2H_2O\ (aq)$ (43)

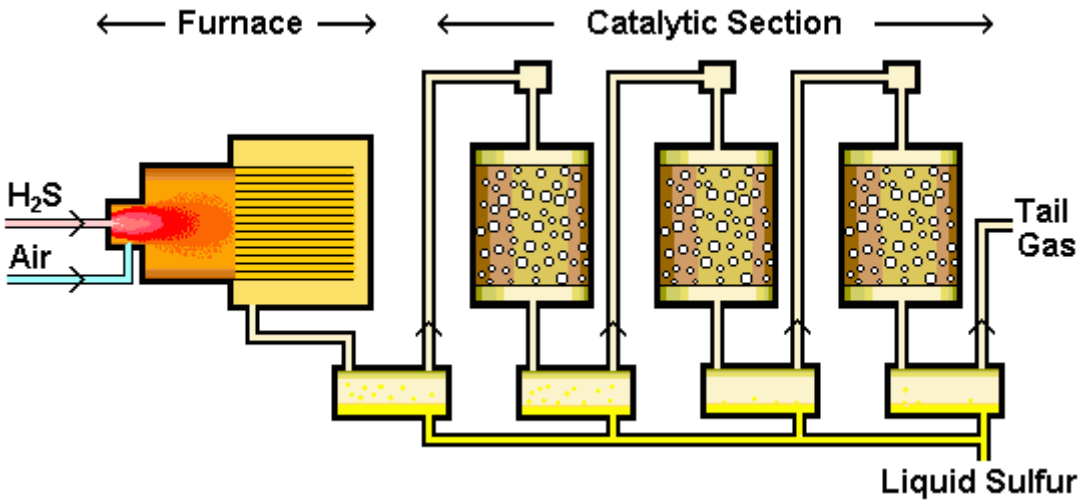

Figure 2.6 Schematic representation of the Claus technology (www.nelliott.demon.co.uk)

The liquid sulphur produced can be reused in the plant. The effluent tailgas contains SO_2, carbon disulphide (CS_2) and carbonyl sulphide (COS), which are byproducts produced in the Claus reactors.

2.6.1.1 Catalytic step

The Claus reaction continues in the catalytic step with activated alumina or titanium dioxide, and serves to boost the sulphur yield. The remaining H_2S is reacted with the SO_2 formed in the thermal step (reaction 44) at lower temperatures (200-350 °C) over a catalyst bed to make more sulphur (Shimin, *et al.,* 1997).

$2H_2S\ (g) + SO_2\ (g) \rightarrow 1.5\ S_2\ (s) + 2H_2O\ (aq)$ (44)

The catalytic recovery of sulphur consists of three substeps: heating, catalytic reaction and cooling plus condensation. The first process step in the catalytic stage is the process gas heating. It is necessary to prevent sulphur condensation in the catalyst bed, which can lead to catalyst fouling. The required bed operating temperature in the individual catalytic stages is

achieved by heating the process gas in a reheater until the desired operating bed temperature is reached (Nagl, 1997).

The typically recommended operating temperature of the first catalyst stage is 315-330 °C (bottom bed temperature). The catalytic conversion is maximized at lower temperatures, but care must be taken to ensure that each bed is operated above the dewpoint of sulphur. The operating temperatures of the subsequent catalytic stages are typically 240 °C for the second stage and 200 C for the third stage (bottom bed temperatures).

In the sulphur condenser, the process gas coming from the catalytic reactor is cooled to between 150-130 °C. The condensation heat is used to generate steam at the shell side of the condenser. Before storage and downstream processing, liquid sulphur streams from the process gas cooler, the sulphur condensers and from the final sulphur separator are routed to the degassing unit, where the gases (primarily H_2S) dissolved in the sulphur are removed (Larraz, 1999).

The tail gas from the Claus process still containing combustible components and sulphur compounds (H_2S, H_2 and CO) is either burned in an incineration unit or further desulphurized in a downstream tail gas treatment unit.

2.6.2 Fe(III) process

Dowa Mining Co. in Japan have developed a process of H_2S removal (Imaizumi, 1986). In this process, aqueous $Fe_2(SO_4)_3$ solution is used as an absorbent. H_2S is oxidized to elemental sulphur and $Fe_2(SO_4)_3$ is reduced to $FeSO_4$. The reaction is:

$$H_2S\,(g) + Fe_2(SO_4)_3\,(aq) \rightarrow S\,(s) + 2FeSO_4\,(aq) + H_2SO_4\,(aq) \qquad (45)$$

The sulphur formed is separated with a filter and the reactant $Fe_2(SO_4)_3$ is regenerated from the products $FeSO_4$ and H_2SO_4 by biological oxidation using the iron oxidising bacterium, *Thiobacillus ferrooxidans*:

$$2FeSO_4\,(aq) + H_2SO_4\,(aq) + \tfrac{1}{2}O_2\,(g) \rightarrow Fe_2(SO_4)_3\,(aq) + H_2O(aq) \qquad (46)$$

Then the overall reaction is:

$$H_2S\,(g) + \tfrac{1}{2}\,O_2\,(g) \rightarrow S\,(s) + H_2O\,(aq) \qquad (47)$$

In 1999, Pagella and Faveri developed a process of H_2S gas treatment by an iron bioprocess. The process is based on two steps corresponding to absorption with chemical reaction of the gas in a ferric solution (where the ferric ion is converted to a ferrous ion), and biological oxidation of ferrous ions in the solution to produce ferric ions again. The reactions (Satoh *et al*., 1988) are:

$$H_2S\,(g) + 2Fe^{3+}\,(aq) \rightarrow S^{o}\,(s) + 2Fe^{2+}\,(aq) + 2H^{+}\,(aq) \qquad (48)$$

$$Fe^{2+}\,(aq) \rightarrow Fe^{3+}\,(aq) + e^{-} \qquad (49)$$

The electron produced in equation 49 is transferred, through the biochemical paths of the cell, to the dissolved oxygen, which acts as the final electron acceptor:

$$2H^{+}\,(aq) + \tfrac{1}{2}\,O_2\,(g) + 2e^{-} \rightarrow H_2O\,(aq) \qquad (50)$$

The following overall reaction is performed:

$$H_2S\,(g) + \tfrac{1}{2}\,O_2\,(g) \rightarrow S\,(s) + H_2O\,(aq) \qquad (51)$$

Advantages of this process for H_2S abatement are mild pressure and temperature conditions, lower costs and closed loop operation without input of chemicals or output of wastes (Pagella and Faveri, 1999).

Asai *et al*., (1990) proposed the reaction where H_2S is absorbed with ferric monohydrate as follows:

$$H_2S\,(g) + 2FeOH^{2+}\,(aq) \rightarrow S\,(s) + 2Fe^{2+}\,(aq) + 2H_2O\,(aq) \qquad (52)$$

Reaction (52) is made up out of the following steps:

$$H_2S\ (g) + FeOH^{2+}\ (aq) \rightarrow H_2S.FeOH^{2+}\ (aq) \qquad (53)$$

$$H_2S.FeOH^{2+}\ (aq) + FeOH^{2+}\ (aq) \rightarrow S\ (s) + 2Fe^{2+}\ (aq) + 2H_2O\ (aq) \qquad (54)$$

2.6.3 PIPco process

The PIPco process is a patented process and offers a great potential to convert H_2S gas into uncontaminated liquid sulphur in an environmental friendly and economical way. The black box description of the process is given in Figure 2.7.

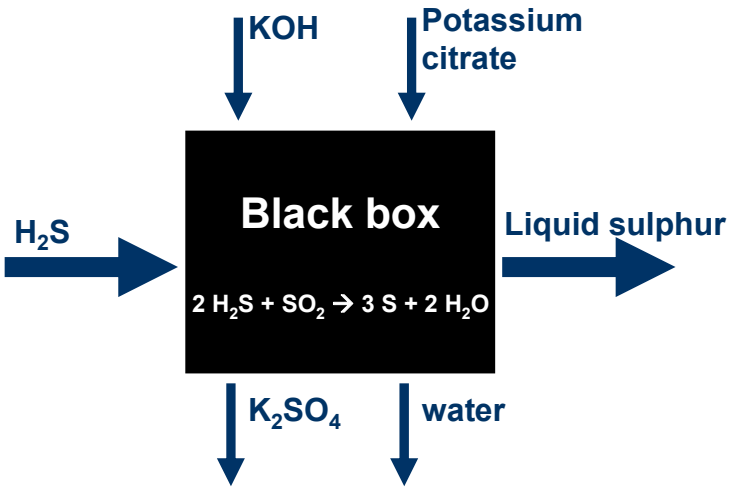

Figure 2.7 Black box description of the PIPco process

The only feedstock of the PIPco process is H_2S gas. During operation KOH and potassium citrate are added as make-up chemicals. The main by-products are potassium sulphate (which can be used as a fertilizer) and the process also produces water. The core of the process is a potassium citrate solution which is used to selectively absorb SO_2 in water. This solution is contacted with H_2S to form elemental liquid sulphur. Note that SO_2 is not added to the process from an external source but is generated within the process.

This process is closely related to processes developed by others. Comparable processes are the Sodium Phosphate Process and the Sodium Citrate Process (Bekassy-Molnar *et al.*, 2005). Both processes use a buffer (sodium phosphate and sodium citrate, respectively) to absorb SO_2 which is then used as an oxidizing agent to convert H_2S to elemental sulphur. However, in contrast to the PIPco process, these processes take place at a low temperature and produce solid elemental sulphur instead of liquid sulphur.

The advantages of the PIPco process compared to similar processes are as follows (Gryka, 1992):

- Mild conditions - the temperatures and pressures are, although slightly elevated, not very high. The temperature of the potassium citrate buffer in the absorption reactor must be as low as possible, preferable below 50 °C. The reaction is carried out at a temperature above the melting point of sulphur and below the temperature where sulphur becomes very viscous. The preferred reaction temperature is about 125 °C. A maximum of 4 bar pressure is recommended.

- Favourable economics - an engineering study carried out showed that the PIPco process costs 50% of today's preferred technology to remove H_2S from natural gas. Flexible feed is possible - the process is very flexible towards impurities in the feed. Other components besides H_2S or SO_2 are either burned in the furnace or leave the process through the vent of the absorption column as potassium citrate is a selective absorbent for SO_2.

- No liquid or solid wastes - the process does not produce any liquid or solid wastes (a big disadvantage of throwaway processes which might produce, for example, gypsum).

- Uncontaminated liquid sulphur is produced: If the PIPco process is used in a brine treatment plant, brine is converted into a very valuable feedstock for the chemical industry in general. Moreover, this enhances the economic potential of the process as industry might consider sulphur as a co-product of their activities.

The description of the PIPco process is detailed in US patent 5057298 (Ray *et al.,* 1990) and a report prepared by PIPco Inc. (Gryka, 1992) for the Gas Research Institute. Also processes that are developed by earlier workers serve as a foundation of knowledge which can be applied to the PIPco process. A schematic diagram of the PIPco process is given in Figure 2.8.

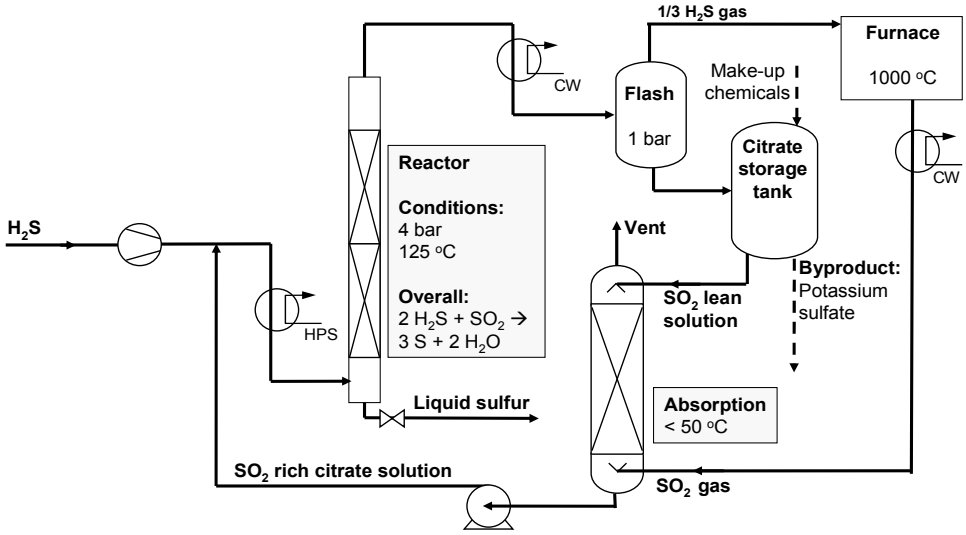

Figure 2.8 Process flow sheet for the PIPco process (Gryka, 1992)

The pressure of the H_2S feed gas is elevated to approximately 4 bar (reaction conditions) and mixed with a SO_2 rich potassium citrate solution. This gas liquid mixture is then heated to 125 °C and fed to the reactor. The H_2S gas reacts with the absorbed SO_2 to form sulphur. The network of reactions taking place in the liquid phase is very complex, but the overall (exothermic) reaction can be given as follows:

$$2H_2S\ (g) + SO_2\ (g) \rightarrow 3S\ (s) + 2H_2O\ (aq) \qquad (55)$$

The formation of sulphur proceeds through reactions of several intermediate compounds. The reaction is carried out at an elevated pressure to prevent the potassium citrate solution from boiling. In the reactor ideally 2/3 of the H_2S that enters the reactor reacts with SO_2 to form sulphur. Within the reactor, sulphur is coalesced and separated by decantation. The reaction is favoured by a low pH.

At the top of the reactor a gas liquid mixture leaves the reactor. The gas and the liquid phase are separated in a flash vessel at atmospheric pressure. The gas phase is introduced to a furnace where the unreacted H_2S is converted to SO_2 according to the following reaction:

$$2H_2S\,(g) + 3O_2\,(g) \rightarrow 2H_2O\,(g) + 2SO_2\,(g) \qquad (56)$$

The SO_2 gas is introduced into the bottom of an absorption column as shown in Figure 2.8. The liquid phase is first introduced to a citrate storage tank, where make-up chemicals can be added and by-products can be removed, before it is added to the top of the absorption column. In the absorption column the potassium citrate solution is again enriched with SO_2 gas and can be used for the reaction.

The unique aspect of a buffered process such as the PIPco process is illustrated by the following: SO_2 solubility in water at 50 °C is only 0.17 g/ℓ (with 1000 ppm SO_2 in the feed gas), while a solution buffered with citrate has a solubility of 8.7 g/ℓ (at pH = 4.5), which is a fifty-fold increase (Vasan, 1975). The task of a buffering agent like citric acid is to shift the equilibrium to the right as shown below:

$$SO_2\,(g) + H_2O\,(aq) \rightarrow HSO_3^-\,(aq) + H^+\,(aq) \qquad (57)$$

$$Cit^{3-}\,(aq) + H^+\,(aq) \rightarrow HCit^{2-}\,(aq) \qquad (58)$$

$$HCit^{2-}\,(aq) + H^+\,(aq) \rightarrow H_2Cit^-\,(aq) \qquad (59)$$

The concentration of potassium citrate in the solution should preferably be as high as possible to increase the buffering capacity, but should be below the concentration at which potassium citrate would crystallize from the solution at

the coldest or most concentrated part of the process. Generally, a concentration in the range of 1 M to about 3.5 M is suitable and about 2 M is preferred.

Sulphur plugging may be a problem for continuous operation of the PIPco process. This could be caused by two mechanisms. As mentioned previously, temperature control is important. The temperature must be above the melting point of sulphur at every part of the reactor. If the temperature is low somewhere, sulphur precipitates and may cause plugging of the equipment. Also sulphur post-formation (sulphur that is formed after the reaction mixture has left the reactor) may cause plugging of equipment. To prevent the first eventuality, careful insulation should be applied everywhere where liquid sulphur is present. To prevent the second type of plugging a different process flow sheet might be applied. The post-formation of sulphur is prevented by the introduction of some SO_2 rich solution into the SO_2 lean solution that exits the reactor.

The mechanism is described in the literature (Vasan, 1975; Rochelle and King, 1979; Korosy *et al*, 1974) and by PIPco Inc (Gryka, 1992). The most important reactions that take place in the liquid phase are given below (Gryka, 1992):

$$H_2S\ (g) \rightarrow HS^-\ (aq) + H^+\ (aq) \quad (60)$$

$$HS^-\ (aq) + 3HSO_3^-\ (aq) + 2H^+\ (aq) \rightarrow S_4O_6^{2-}(aq) + 3\ H_2O\ (aq) \quad (61)$$

$$2HS^-\ (aq) + 4HSO_3^-\ (aq) \rightarrow 3\ S_2O_3^{2-}\ (aq) + 3H_2O\ (aq) \quad (62)$$

$$HSO_3^-\ (aq) + S_4O_6^{2-}\ (aq) \rightarrow S_3O_6^{2-}\ (aq) + S_2O_3^{2-}\ (aq) + H^+\ (aq) \quad (63)$$

$$3HS^-\ (aq) + S_3O_6^{2-}\ (aq) + 3H^+\ (aq) \rightarrow S_2O_3^{2-}\ (aq) + 4S\ (s) + 3H_2O\ (aq) \quad (64)$$

$$2HS^-\ (aq) + S_2O_3^{2-}\ (aq) + 4H^+\ (aq) \rightarrow 4S\ (s) + 3H_2O\ (aq) \quad (65)$$

Under the operating conditions of the reactor, reaction 65 is the slowest and is therefore the overall reaction-rate controlling step (Gryka, 1992; Rochelle and King, 1979). The rate of reaction 65 is favoured by a low pH. Different equations that describe the rate of this reaction are given in the literature (Rochelle and King, 1979). Keller (1956) found that the rate of H_2S

consumption in concentrated buffered solutions is a function of pH and thiosulphate concentration but independent of H_2S partial pressure, as given below:

$$\text{rate of } H_2S \text{ consumption} = k\left[S_2O_3^{2-}\right]^{3/2}\left[H^+\right]^{1/2} \quad (66)$$

$$k = 3\cdot 10^{11}\exp\left(-16500/RT\right) \qquad [\text{mol}^{-1}\ \text{min}^{-1}] \quad (67)$$

Typical conditions for the experiments were, pH = 4.5, $[S_2O_3^{2-}]$ = 0.4 M and T = 25 °C. Keller's results corresponded closely with those of Johnston and McAmish (1973) on the acid decomposition of thiosulphate. They found that the rate of sulphur production in dilute solutions was given by

$$\frac{dS}{dt} = k\cdot\left[H^+\right]\cdot\left[S_2O_3^{2-}\right]^2 \quad (68)$$

$$k = 1.6\cdot 10^{11}\exp\left(-16500/RT\right) \qquad [\text{mol}^{-1}\ \text{s}^{-1}] \quad (69)$$

The literature source does not specify for which temperature range equations 66 to 69 are valid.

To understand the network of reactions better, a schematic overview of the reaction path that leads to the formation of sulphur is given in Figure 2.9.

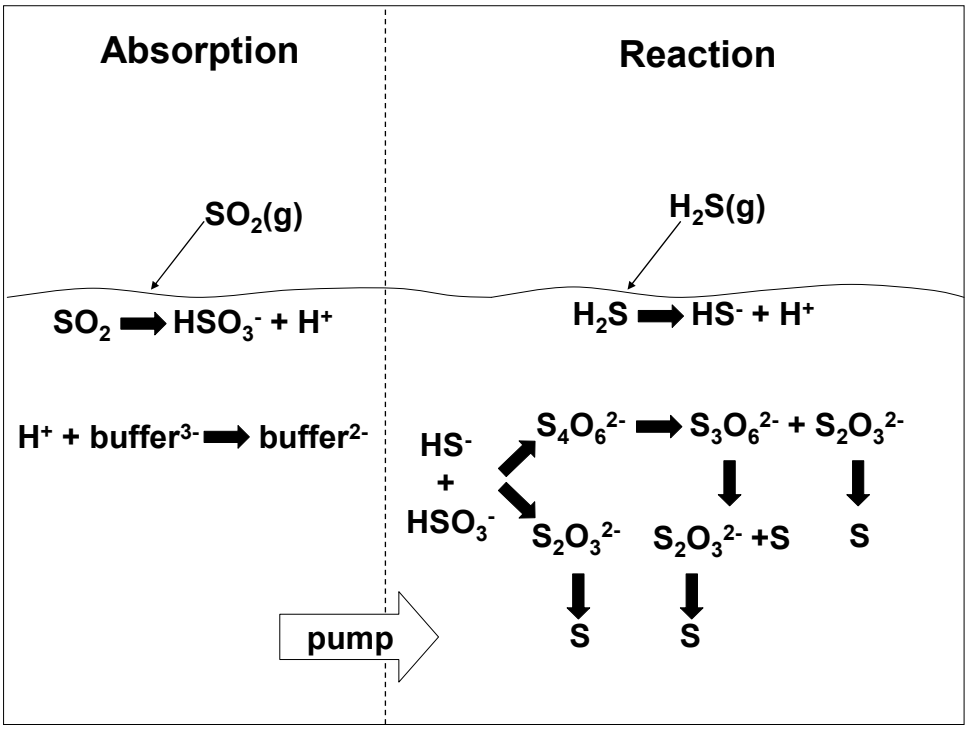

Figure 2.9 Reaction pathways of absorption and reaction leading to the formation of sulphur in the PIPco process (Gryka, 1992)

For completeness the absorption step is also included in Figure 2.9, showing why the thiosulphate concentration is important. It is the end of each pathway and leads to the formation of sulphur. Moreover, as mentioned before, this final reaction is the rate limiting step in the experiments as carried out by PIPco Inc (Gryka, 1992). Furthermore, it is mentioned that both absorption steps are favoured by a high pH, but the reaction is favoured by a low pH. A pH from 4.5 to 6.5 is recommended for the lean solution (Gryka, 1992).

Several investigators have followed the batch reaction of H_2S sparged into buffered solutions for low temperature systems. Typical results are presented in Figure 2.10.

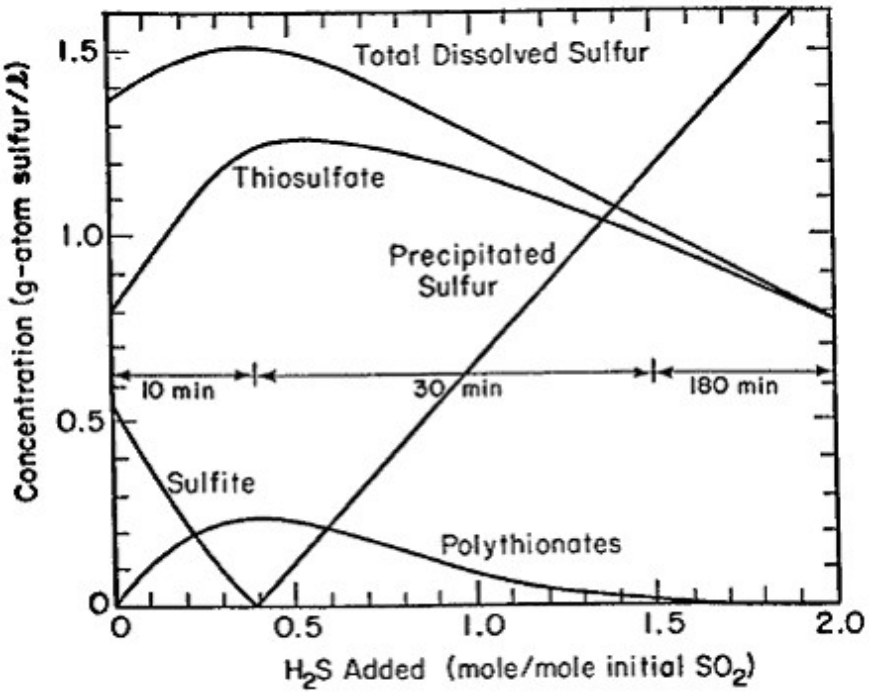

Figure 2.10 Course of H_2S/SO_2 reaction in pH = 4.4 at 25 °C .

Although the temperature is much lower than the PIPco temperature, Figure 2.10 can give some clarification of the reaction mechanisms. Three reaction phases are apparent. In the first phase there is a net consumption of bisulphite and a net production of polythionate and thiosulphate. In the second phase polythionate and some thiosulphate are consumed, with the production of sulphur. In the third and longest phase, residual thiosulphate is converted to sulphur. The sulphite is quickly converted to thiosulphate and polythionate.

The polythionate is also quickly converted to thiosulphate and finally thiosulphate is almost the only sulphur species present and is slowly converted to sulphur.

CHAPTER 3

EXPERIMENTAL TECHNIQUES

3.1 THERMOGRAVIMETRY

Thermogravimetry is the technique whereby the mass of a sample is measured as a function of time or temperature, while subjected to a controlled heating programme in a specified atmosphere.

The technique has a wide range of applications, some of which are:

- investigation of phase changes;
- evaluation of thermal stability of materials;
- investigation of chemical reactivity; and
- kinetic studies.

Figure 3.1 Thermogravimetric instrument

The thermogravimetric instrument is composed of the following:

3.1.1 Sensor

The sensor is the heart of the instrument. It provides the basic information on the sample behaviour. Usually, the output of the sensor is a small DC voltage with a value related to the measured property or an AC voltage with a frequency related to the measured property.

3.1.2 Furnace

In the instrument, the sensor is in contact with the sample, which is placed in the furnace in such a way that it can be heated easily. The construction of the furnace for thermogravimetrc instruments is designed to withstand high temperatures. The furnace has a cylindrical shape and is heated by means of resistance wire, which is wound around the outer wall.

3.1.3 Programmable temperature controller

The programmable temperature controller is linked directly to the furnace and controls the heating. The instrument can measure samples in a temperature range of 20-1 600 °C. A thermocouple that is chemically inert, measures the furnace temperature. The signal from the thermocouple is transmitted to the programmer, and the temperature it represents is compared with the temperature required by the programme. The system will respond by supplying more or less power to the furnace, depending on whether the temperature of the furnace is too low or too high. The response times of the controller and the furnace govern the thermal lag of the instrument, and the range of heating rates that is achievable. The accuracy or resolution of the controller greatly depends on the technique.

3.1.4 Instrument Control

The instrument is digitally operated and controlled by a microprocessor. The processor controls

- power supply to the furnace;
- takes care of temperature programming;
- measures the signals from the sensor;
- sends the data either to a printer or via an interface to a computer; and
- ensures the correct functioning of the instrument.

3.1.5 Amplifier

The basic signal from the sensor is frequently a small analog signal. Before it can be digitized and processed further, it must be amplified. The signal amplifier is therefore a very important part of the instrument and is largely responsible for determining the quality of the resulting curve.

3.1.6 Data acquisition device (computer)

The computer produces a record of the sample mass as a function of time and temperature. It makes the collection, interpretation, storage and retrieval of the instrumental data easier. It allows the user to calculate and compare results accurately (Brown, 1988, Charsley and Warrington, 1992)

3.1.7 Sources of error during thermogravimetry

Errors lead to inaccuracy of the results. The following precautions must be taken in the design of an accurate thermobalance:

- insulation of microbalance from furnace heat;
- accurate control of the reaction temperature;
- effective earthing of glass components to avoid electrostatic charging;

- correction of weight readings for buoyancy forces. The buoyancy effect is due to thermomolecular flow that can occur when the balances are operating at low pressure. As the sample is heated, the density of the atmosphere around the sample decreases, and the upthrust, caused by the gas, will decrease. The crucible will therefore show an apparent gain in measured mass.
- use of a narrow reaction tube and smaller sample masses to minimize turbulence.

3.1.8 Operational conditions

The measurement in this instrument is performed in a defined atmosphere, usually in inert conditions (nitrogen) or in an oxidative environment (air or possibly oxygen). The mass is measured with a highly sensitive electronic balance. Currently, electronic balances are available having sensitivities as low as 0.1 µg. The sample is mostly suspended from the balance by long platinum or quartz wires and hangs in a furnace that can be heated or cooled at a given rate.

3.2 X-RAY ANALYSIS

X-rays were first discovered by the German physicist W.E Roentgen in 1895 (Graham, 1995). X-rays can be defined as wave or electromagnetic radiation of relative short wavelengths, high energy. All electromagnetic radiation is characterized by its wave character using its *wavelength* λ (the distance between the peaks), its *frequency* ν (the number of points that pass a point in unit time) or by its photon *energy* E. The relationships between these quantities are as follows:

$$\nu = \frac{c}{\lambda} \tag{70}$$

and

$$E = h\nu \tag{71}$$

c = the speed of light, h = the Planck's constant

From these two equations (70 and 71) it follows that the energy equivalent to an X-ray photon is:

$$E = \frac{hc}{\lambda} \tag{72}$$

They are produced when any electrically charged particle of sufficient kinetic energy is rapidly decelerated. The radiation is produced in an X-ray tube containing a source of electrons and two metal electrodes. Figure 3.2 shows a cutaway view of an X-ray tube. The tungsten filament is heated by the filament current producing a cloud of electrons, which are accelerated along the focussing tube by the potential difference between the filament and the anode. The generated X-rays then pass through the window to the outside. The conversion of electrons to X-rays is a very inefficient process because most of the energy is converted to heat. The tube must therefore be cooled with water.

The high voltage maintained across the tube electrodes rapidly draws the electrons to the anode or target which they strike at high velocity. The x-rays are produced as the electrons strike the atoms of the target material and radiate in all directions (Figure 3.3).

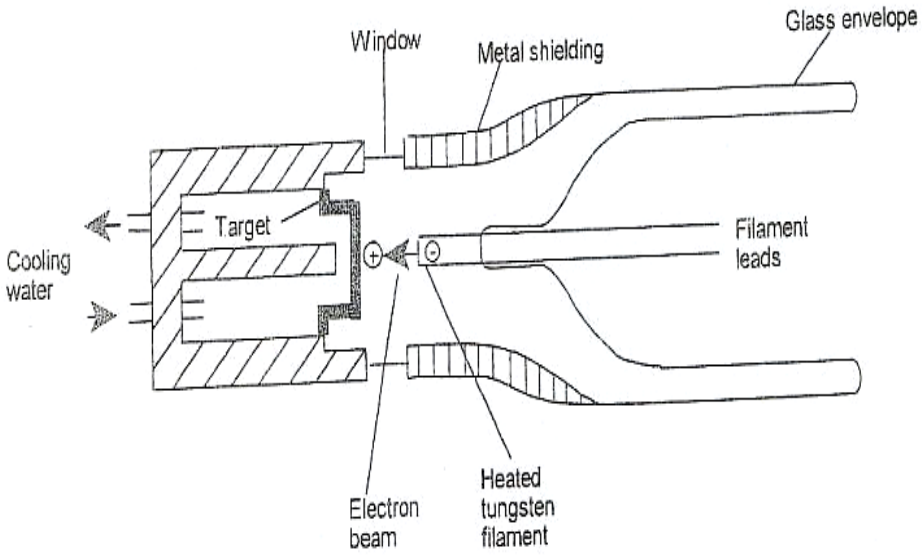

Figure 3.2 Schematic diagram of X-ray tube (courtesy: Shimadzu Corp.)

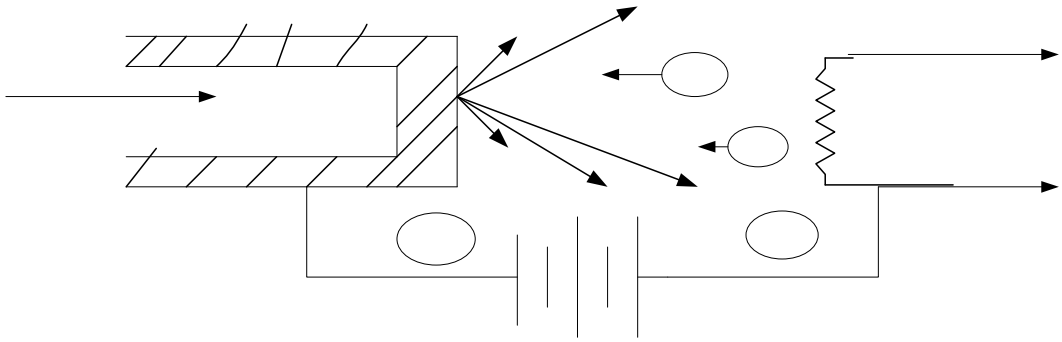

Figure 3.3 Schematic diagram of X-ray generation

Rays coming from a target consist of a mixture of different wavelengths and the tube spectrum consists of two parts:

1) Continuous spectrum

It is caused by the deceleration of the electrons hitting the target and in that way emitting their energy or by the stepwise loss of energy of bombarding electrons in a series of encounters with atoms of the target material.

X-RA

TARGET

COOLING WATER

No X-rays are produced before the minimum voltage is not reached for the specific target material. The intensity of the X-rays at a specific voltage also depends on the target material.

When the voltage on an X-ray tube is raised above a certain critical value, sharp intensity maxima, characteristic of the target metal, appear at certain wavelengths. These lines fall into several sets referred to as K, L, M, etc. lines. The K lines are useful in X-ray diffraction, because the larger wavelength lines L and M are too easily absorbed. The intensities of the lines are dependant on the X-ray tube current and the voltage. The continuous spectrum consists of “bremsstrahlung” radiation: radiation produced when high energy electrons passing through the tube are progressively decelerated by the material of the tube anode (the "target").

2) Characteristic spectrum

It is produced through interaction between the atomic electrons of the target and the incident particles, which can be high voltage electrons, an X-ray photon, a gamma ray or a photon. Each will produce similar effects if the energy of the particle is greater than the energy binding the electrons to the nucleus. The radiation is generated when the bombarding electrons have sufficient energy to dislodge electrons from the inner electron shells in the atoms of the target material. There are two de-excitation processes, the photoelectric and the Auger effects.

The photoelectric effect is produced when an electron is removed form its original position leaving the atom in an ionized state. The free electron, called the photoelectron will leave the atom with a kinetic energy $E - E_0$ (where $E =$ energy of the incident photon and $E_0 =$ the binding energy of the electron). This leaves the atom with a vacancy, which can be filled by transferring an outer orbital electron to fill its place. Following the transfer and lowering of the ionized energy of the atom is the production of a fluorescent X-ray photon with an energy $E_{X\text{-}ray}$. The final resting place of the transferred

electron determines the type of radiation, i.e K, L, M etc. If a K electron is ejected, the atom is in the high energy K^+ state. Transfer of an electron from the L shell reduces the electron energy state from K^+ to L^+ and the excess energy is emitted as Kα radiation. L radiation is produced in a similar way. Each element has a unique set of binding energies and unique energy state differences.

- ***Absorption of X-rays***

X-rays, unlike ordinary light, are invisible but travel in straight lines. They have a significant attribute which is the ability to penetrate different materials to different depths. When a monochromatic beam of radiation of wavelength λ and intensity I_0 falls onto an absorber of thickness t and density ρ, a certain portion, I, of the radiation may pass through the absorber. The wavelength of the transmitted beam is unchanged and the intensity is lower depending on the thickness and the mass absorption coefficient.

Some rays do not pass through the material and are reflected by the surface causing coherent and incoherent scattering. When X-rays strike an atom in the material, tightly bound electrons in the atom also scatter X-rays of the same wavelength as that of the incident beam (coherent scatter), and loosely bound electrons scatter X-rays of the slightly increased wavelength (incoherent scatter) (Azaroff, 1968).

3.2.1 X- ray Fluorescence analysis

X-ray fluorescence (XRF) is the emission of characteristic "secondary" (or fluorescent) X-rays from a material that has been excited by bombarding with high-energy X-rays or gamma rays (Beckhoff *et al.,* 2006). The phenomenon is widely used for chemical analysis, particularly in the investigation of metals, glass, ceramics and building materials, and for research in geochemistry, forensic science and archaeology.

When materials are exposed to short-wavelength X-rays or to gamma rays, ionization of their component atoms may take place. Ionisation consists of the ejection of one or more electrons from the atom, and may take place if the atom is exposed to radiation with the energy greater than its ionization potential. X-rays and gamma rays can be energetic enough to expel tightly-held electrons from the inner orbitals of the atom. The removal of an electron in this way renders the electronic structure of the atom unstable, and electrons in higher orbitals "fall" into the lower orbital to fill the hole left behind. In falling, energy is released in the form of a photon, the energy of which is equal to the energy difference of the two orbitals involved. Thus, the material emits radiation, which has energy characteristic of the atoms present. The term fluorescence is applied to phenomena in which the absorption of higher-energy radiation results in the re-emission of lower-energy radiation.

The fluorescent radiation can be analysed either by sorting the energies of the photons (energy-dispersive analysis) or by separating the wavelengths of the radiation (wavelength-dispersive analysis). Once sorted, the intensity of each characteristic radiation is directly related to the amount of each element in the material (Van Grieken and Markowicz, 2002).

3.2.1.1 Energy dispersion

In energy dispersive analysis, the fluorescent X-rays emitted by the material sample are directed into a solid-state detector which produces a continuous distribution of pulses, the voltages of which are proportional to the incoming photon energies. This signal is processed by a multichannel analyzer (MCA) which produces an accumulating digital spectrum that can be processed to obtain analytical data. In wavelength dispersive analysis, the fluorescent X-rays emitted by the material sample are directed into a diffraction grating monochromator. The diffraction grating used is usually a single crystal. By varying the angle of incidence and take-off on the crystal, a single X-ray wavelength can be selected. The wavelength obtained is given by the Bragg equation (Buhrke *et al*., 1998):

$$n.\lambda = 2d.\sin(\theta) \quad (73)$$

where d is the interplanar spacing

θ is the angle between the planes and the X-ray beam (Bragg angle),

λ is the X-ray wavelength and

n is the order of reflection.

3.2.1.2 Wavelength dispersion

In wavelength dispersive spectrometers (WDX or WDS), the photons are separated by diffraction on a single crystal before being detected. Although wavelength dispersive spectrometers are occasionally used to scan a wide range of wavelengths, they are usually set up to make measurements only at the wavelength of the emission lines of the elements of interest. This is achieved in two different ways:
"Simultaneous" spectrometers have a number of "channels" dedicated to analysis of a single element, each consisting of a fixed-geometry crystal monochromator, a detector, and processing electronics.

This allows a number of elements to be measured simultaneously, and in the case of high-powered instruments, complete high-precision analyses can be obtained in under 30 s. "Sequential" instruments have a single variable-geometry monochromator (but usually with an arrangement for selecting from a choice of crystals), a single detector assembly (but usually with more than one detector arranged in tandem), and a single electronic pack. The instrument is programmed to move through a sequence of wavelengths, in each case selecting the appropriate X-ray tube power, the appropriate crystal, and the appropriate detector arrangement.

3.2.1.3 Sample analysis by XRF

- ***Qualitative analysis by XRF***

For qualitative analysis, the crystal is rotated so that all angles between approximately 15 ° and 145 ° are presented to the x-ray beam. Detected X-rays are amplified and recorded as a series of peaks. A scale of 2θ is automatically recorded, and elements are identified from their 2θ values in conjunction with an appropriate set of tables.

- ***Quantitative analysis by XRF***

For quantitative analysis, the crystal remains stationary, set at the appropriate angle to reflect a particular element's radiation. The recorded intensity is related to the element's concentration in the sample.

3.2.2 X-ray Diffraction

X-ray diffraction is coherent elastic scattering of X-rays by atoms or ions in a crystal. Because the wavelength of photons with energy of order 10 KeV is a little smaller than the spacing of atoms in solids, a crystal will act as a diffraction grating for X-ray. As a crystal is three dimensional, the diffraction conditions are more stringent than for a two-dimensional grating. This technique is widely used in chemistry and biochemistry to determine the structures of an immense variety of molecules, including inorganic compounds, DNA, and proteins. X-ray diffraction is commonly carried out using single crystals of a material, but if these are not available, microcrystalline powdered samples may also be used.

3.2.2.1 Principle of X-ray diffraction

The principle involved is, that a beam of X-rays striking a crystal will pass through it, but with scattering or diffraction of the photons in the beam. Since the particles in the crystal are in a regular or symmetrical arrangement, the X-

rays will be scattered in a regular pattern. X-rays wavelength used in diffraction lie between approximately 0.5 and 2.5 Aº.

When X-rays are incident on any form of matter, they are partly scattered in all directions by the atoms in the matter. When these atoms have three dimensionally regular arrangements, these scattered X-rays mutually reinforce one another to show the phenomenon of diffraction.

X-ray diffraction by crystals can simply be explained by the Bragg model (equation 78). Measuring distances (d) between units in crystals by X-ray diffraction is done by the Bragg method. The units in each Bragg plane act as the X-ray scattering sources and the X-ray beam striking the crystal will act as if it had been reflected from these evenly spaced planes. This will give rise to reinforcement of the beam at certain angles and destruction at others, so that the spacing between the planes can be determined.

3.2.2.2 Methods in Quantitative XRD

In a multicomponent crystalline mixture, each component of the mixture produces its characteristic pattern independently of the others, making it possible to identify the various components. Additionally, the intensity of each component pattern is proportional to the amount present. Absorption corrections, however, have to be performed, so that a quantitative analysis for the various components may be developed. The following three quantitative methods will be discussed: Reference Intensity Ratios (RIR) method, Whole Pattern Method and Rietveld Method.

- ***Reference Intensity Ratios***

The ratio has been given the notation I / I_c, meaning 'analyte intensity I over corundum intensity I_c'.

Two methods are used to measure the RIR:

1) measuring intensities of the strongest peaks from samples prepared by mixing the analyte and standard together in a known weight ration; and
2) measuring separately the intensities for the analyte peak and the reference standard peak from pure phase preparations and by correcting the intensities with mass absorption coefficients. Both methods are independent of the difference in mass absorption coefficients between analyte and standard (Davis, 1992).

The general RIR definition for component j, when components j and c are mixed together in a 1:1 weight ratio or are corrected from the known value of w_c is (Davis *et al.*, 1990):

$$I_j = \frac{I_j}{I_c}, \qquad w_j = w_c \tag{74}$$

- ***Whole Pattern Method***

The method uses the full diffraction pattern collected over a specified 2θ range preselected to cover all the major peaks of all the phases analyzed (Smith *et al.,* 1987). The key feature of this method is that all the information in the diffraction pattern is used for the analysis.

- ***Quantitative Phase Analysis using the Rietveld Method***

Rietveld method is used in the characterisation of crystalline materials and needs a complete structure model (Bish and Howard, 1988).

This method fits calculated rather than measured reference patterns to the pattern from the unknown. It can also use a pattern-fitting algorithm where all lines for each phase are considered. This method allows to correct for preferred orientation, but corrections only appear to work in samples with minor amounts of preferred orientation (Bish and Howard, 1988). The use of an internal standard will allow the determination of total amorphous phase content in a mixture. Hill (1991) states that the Rietveld method of phase

analysis is only as accurate as the modelling provided in the pattern calculation.

In the Rietveld Method, an entire calculated diffraction pattern is compared with the observed pattern, point by point. Six factors affecting the relative intensity of the diffraction lines of a powder pattern (Klug and Alexander, 1974):

- Polarization factor when radiation is scattered or diffracted.
- Structure factor – the ratio of the amplitude scattered by the plane relative to the amplitude scattered by a single electron.
- Multiplicity factor – the number of different planes in a form having the same spacing.
- Lorentz factor – a reflection time factor
- Absorption factor-factor affecting the intensities of diffracted rays
- Temperature factor – when atoms undergo thermal vibration. The amplitude of this vibration increases as the temperature increases.

Basic equation of the Rietveld method (Wiles and Young, 1981):

$$y_i = \sum \left[S_p \sum_k \left[APL\Psi M_k \left| F_k \right|^2 G(\Delta\Theta_{ik}) po_k \right] \right] + y_{bi} \qquad (75)$$

where,

y_i - Intensity of the angular position, i in the powder pattern

S_p - Scale factor of the phase p, relates the phase intensities to the pattern

APL - Absorption, polarisation, Lorenz factor

Ψ - Geometrical factor (powder-ring - factor)

M - Plane multiplicity factor

F - Structure factor

G - Profile shape function

po - Preferred orientation correction factor

y_{bi} - Background intensity

3.3 TUBE FURNACE

A tube furnace is designed to heat a tube that is usually 50 to 100 cm in length and from 25 to 100 mm in diameter. Samples are placed inside the tube in ceramic or metal boats using a long push rod. The tube is surrounded by heating elements which may also incorporate a thermocouple (a thermocouple can also be inserted down the tube if desired).

Different types of elements are single zone wirewound, silicon carbide and multi zone wirewound. Tube furnaces also have a significant advantage over other types of furnaces. The ends of the furnace tubes (which usually protrude 10 or more centimeters from each end of the furnace) do not get very hot and so a variety of different adapters may be placed on the ends. Furnace tubes can be made out of a variety of materials. Quartz is commonly used for temperatures below 1 200 °C and alumina or yttria-stabilized zirconia can be used for higher temperatures. The ceramics, quartz silica and metals are the worktubes suitable for this instrument. Figure 3.4 shows the picture of a tube furnace used in this study.

Figure 3.4 Tube furnace (Model TSH12/38/500)

3.4 MUFFLE FURNACE

The controller can be used in Automatic mode in which the output power is automatically adjusted to hold the temperature at the required value. It is ideal for ashing organic and inorganic samples, cement testing, heat treating small steel parts, ignition tests, gravimetric analysis, and determination of volatiles and suspended solids. Heating elements are embedded in refractory cement on top and both sides to reduce energy consumption and for structural strength. The furnace is insulated with ceramic fibre insulation which improves furnace temperature uniformity. Unit can heat up to 2 000 °C.

Figure 3.5 Muffle furnace (Model TSH12/38/500)

CHAPTER 4

AIM OF STUDY

The aim of this project was to investigate and optimize various stages of the sulphur recovery process on laboratory scale to the stage prior to pilot and full-scale implementation. Figure 4.1 shows the process flow diagram of the sulphur recovery process. The following individual stages were studied:

- Thermal decomposition of gypsum to calcium sulphide (A)
- Stripping of the H_2S from calcium sulphide slurry with CO_2 to form $CaCO_3$ (which can also be recovered as a by-product and used for neutralization of acid mine water) (B)
- Sulphur production (C)

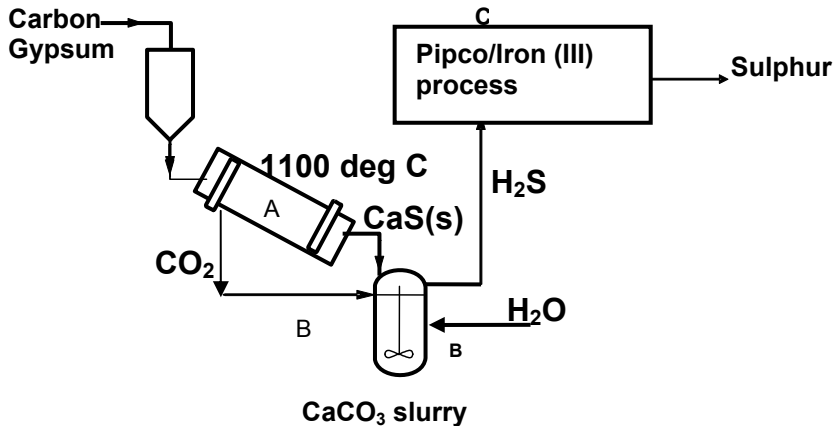

Figure 4.1 Process flow diagram for the sulphur recovery process

4.1 THERMAL STUDIES (A)

The effects of the following parameters on the reduction of gypsum to calcium sulphide were investigated

- Reaction time: Different time periods ranging from 5 min to 60 min were evaluated to optimize the time needed to thermally decompose gypsum into calcium sulphide in the furnace.

- Temperature of the furnace: The conversion of gypsum to calcium sulphide occurs at high temperature. The temperatures were varied from 900 °C to 1100 °C to obtain the optimum temperature.

- Molar ratio: The molar ratios of gypsum to activated carbon were varied from 1:0 to 1:3. The aim was to investigate the stoichiometric amount of activated carbon needed to react with gypsum for effective reduction.

- Particle sizes of gypsum: As reactivity also depends on particle size, different particle sizes of gypsum were studied (1 250 µm, 630 µm and 380 µm).

- Type of furnace: The muffle furnace, which contained oxygen, and tube furnace, which was oxygen deficient, were investigated to identify which heating unit is more efficient.

- Gypsum compounds: Gypsum from three sources were tested. Pure gypsum, Anglo gypsum and Foskor gypsum were compared in respect of CaS yield.

- Reducing agent: Two different reducing agents (activated carbon and Duff coal) were compared with respect to yields of CaS and for cost effectiveness.

Thermogravimetric analysis was conducted under isothermal and non-isothermal conditions with the aim of elucidating the influence of different kinetic parameters on the mechanism of the process. Carbon monoxide and activated carbon were used as reducing agents. The following parameters were studied:

- Heating rate: The aim of this investigation was to use the isoconversional method to estimate/calculate the activation energy. These allow the dependence of activation energy on the degree of conversion to be observed. Six different heating rates between 1 °C/min and 10 °C/min were studied using gypsum from three different sources (pure gypsum, Anglo gypsum and Foskor gypsum) and two different reducing agents (carbon monoxide and activated carbon).

- The effect of heating mixtures of gypsum and activated carbon at a constant temperature for a certain period was investigated by conducting isothermal studies using pure gypsum and activated carbon. Isothermal temperatures were between 850 °C to 1 000 °C.

- The molar ratio between gypsum and activated carbon was varied from 1:0.5 to 1:3. The aim was to investigate the optimum amount of activated carbon needed to react with gypsum for effective reduction.

- The two different reducing agents (activated carbon and Duff coal) were compared with the aim of obtaining a suitable reducing agent to use on a full-scale plant

4.2 SOLUBILITY OF CaS

Due to the low solubility of CaS, the influence of the following parameters on the solubility of CaS were studied:

- Stirring: The influence of stirring on the solubilisation of CaS solution was studied by stirring the CaS slurry for 180 minutes.

- Temperature: The effect of temperature on the solubility of CaS was investigated by heating the CaS solution from 30 °C to 90 °C.

4.3 SULPHIDE STRIPPING AND ABSORPTION (B)

The effect of the following parameters on the stripping of sulphide using CO_2 was investigated:

- CO_2 flow rate: To obtain the equivalent amount of CO_2 gas required to strip hydrogen sulphide gas from a CaS slurry, different CO_2 flow rates (2 200 mℓ/min to 3 300 mℓ/min) were studied.
- CO_2 pressure: The effect of 100 kPa and 200 kPa CO_2 pressure on the system was studied. This work was done to identify if the effect of doubling the partial pressure of CO_2 in the system would increase the amount of CO_2 in solution, thereby displacing/reacting with more of the remaining sulphide.
- Hydrodynamics: These experiments were conducted to investigate whether increasing the agitation would speed up the liquid-gas-solid reaction and if more of the gas in the headspace would result in more gas being circulated through the mix, resulting in a greater volume of CO_2 being cycled through the liquid per unit time. Stirring rates of 500 rpm and 1000 rpm were tested.

4.4 H_2S GAS ABSORPTION AND SULPHUR FORMATION (C)

Two methods were tested for sulphur recovery to establish the more effective method:

- Iron (III) process: In this process, H_2S gas was absorbed into Fe(III) solution. A sample from the iron (III) reactor was analysed, using XRD, with the aim of identifying compounds formed other than sulphur.

- The PIPco process: In this process H_2S gas was absorbed into a SO_2 rich potassium citrate solution. The sulphur recovered was assayed for purity.

CHAPTER 5

MATERIALS AND METHODS

5.1 THERMAL STUDIES

5.1.1 Feedstock

Gypsum. Three different gypsum samples were utilised in the reduction studies.

- Pure gypsum (AR grade) was obtained from Merck.
- Anglo gypsum from Anglo Coal (Landau Colliery) was prepared from the desalination stages of a mine water treatment pilot plant.
- Foskor gypsum obtained from Foskor (Phalaborwa) was prepared by leaching of calcium phosphate, with sulphuric acid.

The results of X-ray fluorescence (XRF) analyses of the gypsum samples used are summarised in Table 5.1.

Carbon. Two types of carbon were used as the reducing agents.

- Activated carbon obtained from Merck with a carbon content of 98.7%.
- Duff Coal from Anglo Coal with 68.5% carbon content.

Analysis of the activated carbon and Duff coal is given in Table 5.2.

Carbon monoxide. 5% CO gas diluted with pure 95% nitrogen obtained from Air Liquide was used for the reduction of gypsum.

Table 5.1 XRF analyses of pure gypsum, Anglo gypsum and Foskor gypsum

Compounds	Composition (%)		
	Pure gypsum	Anglo gypsum	Foskor gypsum
SiO_2	0.01	0.01	0.17
TiO_2	0.01	0.00	0.00
Al_2O_3	0.01	0.01	0.01
Fe_2O_3	0.00	0.09	0.05
MnO	0.00	0.12	0.00
MgO	0.00	4.37	0.00
CaO	41.6	34.74	37.47
Na_2O	0.01	0.01	0.01
K_2O	0.01	0.00	0.01
P_2O_5	0.04	0.13	0.78
SO_3	56.0	50.48	53.76
Loss On Ignition	0.89	9.10	6.64
Total $CaSO_4$	97.6	85.2	91.2

Table 5.2 XRF analyses of the activated carbon and Duff coal

Sample composition	Composition (%)	
	Activated carbon	Duff Coal
Moisture	0.5	1.6
Ash	0.5	13.5
Volatile Matter	0.3	15.2
% Carbon	98.7	68.5

5.1.2 Equipment

For the thermal study, a Mettler Toledo Star e System was used for execution of thermogravimetric analysis. A tube furnace, model TSH12/38/500 and a muffle furnace model 2216e controller were used for thermal decomposition of gypsum (refer to Chapter 3). A silica tube was used for the reduction reaction.

Samples were contained in silica boats, A_1 clay graphite crucibles and a platinum sample holder during the thermal studies.

5.1.3 Experimental procedure

5.1.3.1 Tube and Muffle furnace

The gypsum and carbon mixtures were thoroughly mixed by hand to ensure homogeneity. The mixtures were placed in silica boats/clay crucibles and heated in the tube furnace and muffle furnace for various times. The amounts of activated carbon or Duff coal used for the different carbon to gypsum ratios are summarized in Table 5.3. The gypsum amount was kept constant at 5 g.

The Anglo gypsum and Foskor gypsum were dried first at 150 °C - 180°C to remove excess moisture (anhydrous gypsum) as they tend to form lumps when wet and thereafter grounded to a fine powder. Nitrogen gas (50 mℓ /min) was passed through the reaction tube as an inert gas in the tube furnace. In the muffle furnace some oxygen was present. Reaction products from the tube furnace were allowed to cool in a nitrogen atmosphere.

X-Ray Diffraction (XRD) analysis was used to determine the composition of samples (described in 5.1.4).

The effect of the following parameters on the reduction of gypsum to calcium sulphide using a tube or muffle furnace were investigated:

- Reaction time (5 min, 20 min, 30 min and 60 min).
- Temperature of the furnace (900 °C, 1 000 °C, 1050 °C and 1 100 °C, 1150 °C).
- Carbon to gypsum molar ratio (0, 0.025, 0.5, 1, 2 and 3).
- Particle sizes of Foskor gypsum (1 250 µm, 630 µm and 380 µm).
- Type of furnace (muffle furnace (oxygen present) or tube furnace (oxygen deficient)).

- Gypsum compounds (pure gypsum, Anglo gypsum and Foskor gypsum).
- Reducing agent (duff coal and activated carbon).

Table 5.3 Compositions of various gypsum/carbon ratios

Gypsum compound (5g)	Ratio	Activated carbon (g) (98.7 % C)	Duff coal (g) (68.5 % C)
Pure gypsum dihydrate (97.6 %)	0.25:1	0.09	
	0.5:1	0.17	
	1:1	0.35	
	2:1	0.70	
	3:1	1.04	1.5
Anglo gypsum (anhydrite) (85.2 %)	3:1	1.14	1.6
Foskor gypsum (91.2 %)	3:1	1.22	1.7

5.1.3.2 Thermogravimetry Analysis

Carbon monoxide and activated carbon were used for the reduction of gypsum. Nitrogen gas was used as inert atmosphere at a flow rate of 50 mℓ/min. The nitrogen gas was also utilized as a diluent gas for carbon monoxide. Carbon monoxide (5% in nitrogen) was used unless otherwise stated. Samples with masses between 10 and 20 mg were held in a platinum sample holder during the thermogravimetric studies. The percentage conversion was calculated based on measured mass loss. Kinetic analysis was done using the Ozawa Flynn Wall method (Ozawa, 1965; Flynn and Wall, 1966).

For the kinetic studies on the reduction of gypsum to calcium sulphide, using carbon monoxide or activated carbon as reducing agents, the influence of following parameters were studied:

- Heating rates (1, 2, 4, 6, 8, 10 °C/min) on the reaction between pure gypsum and carbon monoxide.

- Temperature from 25 ºC to 1 260 °C for the reaction between activated carbon and pure gypsum.
- Molar ratio of activated carbon to pure gypsum (0.5:1 to 3:1).
- Gypsum compounds (pure gypsum, Anglo gypsum and Foskor gypsum)
- Reducing agent (activated carbon or Duff coal) using pure gypsum, Anglo gypsum and Foskor gypsum)
- Heating rate (1, 2, 4, 6, 8 and 10 °C/min) on the reaction between the three gypsum compounds and activated carbon.
- Isothermal studies on the reaction between pure gypsum and activated carbon. The temperature of the furnace was 850 °C, 875 °C, 900 °C, 950 °C and 1000 °C. The samples were allowed to remain at each temperature for 15 minutes.

5.1.4 Analytical Procedure

To identify the composition of the samples before and after thermal treatment, XRF and XRD analyses were carried out.

5.1.4.1 XRF analyses

Analysis of the gypsum and Duff coal samples were done using the ARL 9400XP+ XRF spectrometer. Samples were prepared as pressed powder briquettes and introduced into the spectrometer. Analyses were executed using the UniQuant software that detects and quantifies all elements in the periodic table between Na and U. Only elements present above the detection limits were reported.

5.1.4.2 XRD analyses

An automated Siemens D501 XRD spectrometer was used to analyse the composition of samples. Samples were milled in a swing mill using a WC-milling vessel and prepared for analysis using a back loading preparation method. A PANalytical X'Pert Pro powder diffractometer with X'Celerator

detector and variable divergence- and receiving slits with Fe filtered Co-K_α radiation was used to analyse the samples. Phases were identified using X'Pert Highscore Plus software. Quantification (Rietveld method) was perfomed by Autoquan/BGMN software (GE Inspection Technologies) employing the Fundamental Parameter Approach.

5.2 SOLUBILITY OF CaS

5.2.1 Feedstock

CaS. Calcium sulphide (purity of 90%) was a product obtained from the thermal process (described in 5.1).

5.2.2 Equipment

A 1 ℓ reactor, a magnetic stirrer with temperature controller and a magnetic stirrer bar were used for this study.

5.2.3 Experimental procedure

The study was conducted by adding CaS to water. For the stirring studies, the CaS slurry was stirred for 180 minutes. The slurry was heated from 30 °C to 90 °C when the effect of temperature on solubility was investigated. Samples were taken at different time and temperature intervals and analysed for sulphide and pH (described in 5.3.4).

The influence of the following parameters on the solubility of CaS was investigated:

- Stirring (the CaS slurry was stirred for 180 minutes).
- Temperature (30 °C to 90 °C).

5.3 SULPHIDE STRIPPING AND SULPHUR PRODUCTION

5.3.1 Feedstock

CaS. Calcium sulphide was obtained from the thermal process (described in 5.1).

CO_2. Pure CO_2 was obtained from Air Liquide and used for the stripping of the sulphide gas.

Ferric sulphate solution. A $Fe_2(SO_4)_3$ solution with a concentration of 200 g/ℓ was used for absorption of the H_2S gas. The chemical was obtained from Merck.

Potassium citrate solution. Potassium citrate buffer solution rich in SO_2 was used for the absorption of the stripped H_2S-gas. The potassium citrate solution was prepared from 2 M citric acid (refer to 4.3.4) and 45% KOH added to raise the pH to 6.8.

5.3.2 Equipment

5.3.2.1 Sulphide stripping using a pressurized reactor

Figure 5.1 shows a 5 ℓ pressurised reactor, containing a hollow shaft stirrer (Figure 5.2) capable of a maximum pressure of 140 bar and a maximum operating temperature of 300 °C.

Figure 5.1 The 5 ℓ jacketed, pressurised & continuously stirred reactor used in CaS stripping experiments.

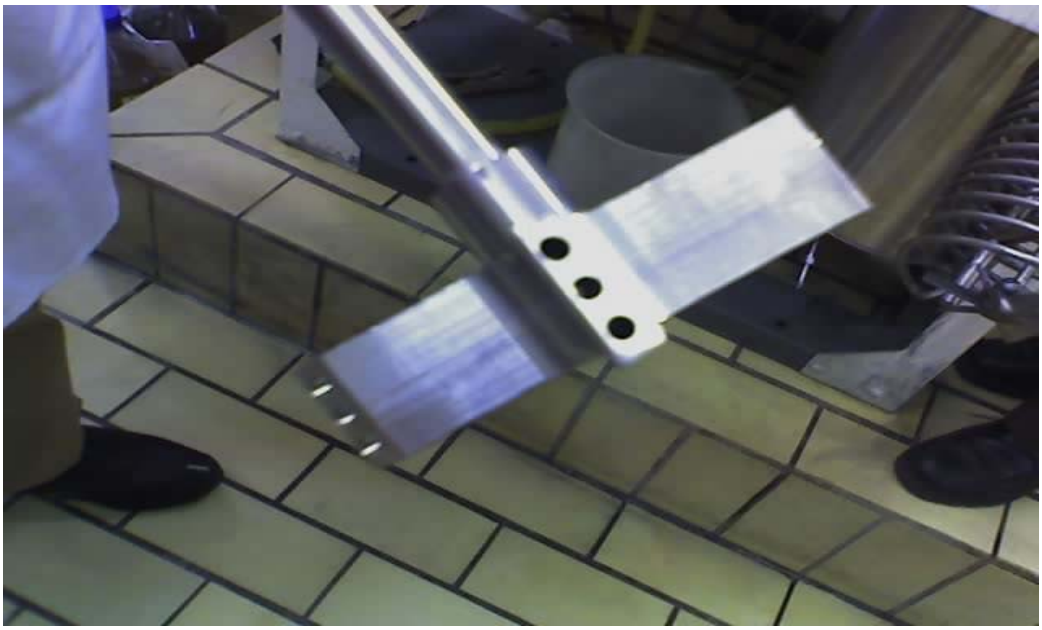

Figure 5.2 The hollow shaft stirrer used to inject pressurised CO_2 into the CaS slurry

5.3.2.2 Sulphide stripping and sulphur formation

Figure 5.3 shows the laboratory set-up used for H_2S-stripping and sulphur formation under atmospheric pressure. It consisted of three reactors connected in series and equipped with glass spargers. Reactor 1 (1 ℓ) contained a calcium sulphide slurry from which sulphide was to be stripped. Reactors 2 and 3 (1 ℓ) contained SO_2-rich potassium citrate buffer solution/ Fe (III) solution into which H_2S gas was absorbed and sulphur formed.

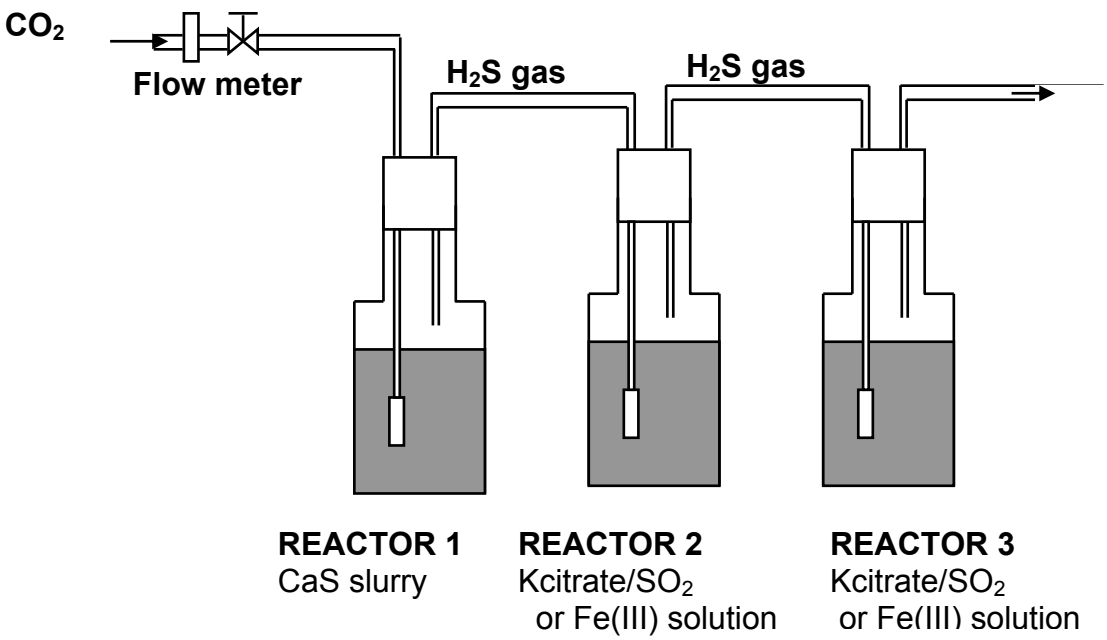

Figure 5.3 Schematic diagram of H_2S-stripping and absorption process.

5.3.2.3 Solubility of H_2S in Potassium Citrate Buffer

The experimental setup shown in Figure 5.4 was used for H_2S solubility studies. Two 1 ℓ flasks were connected in series and equipped with glass spargers.

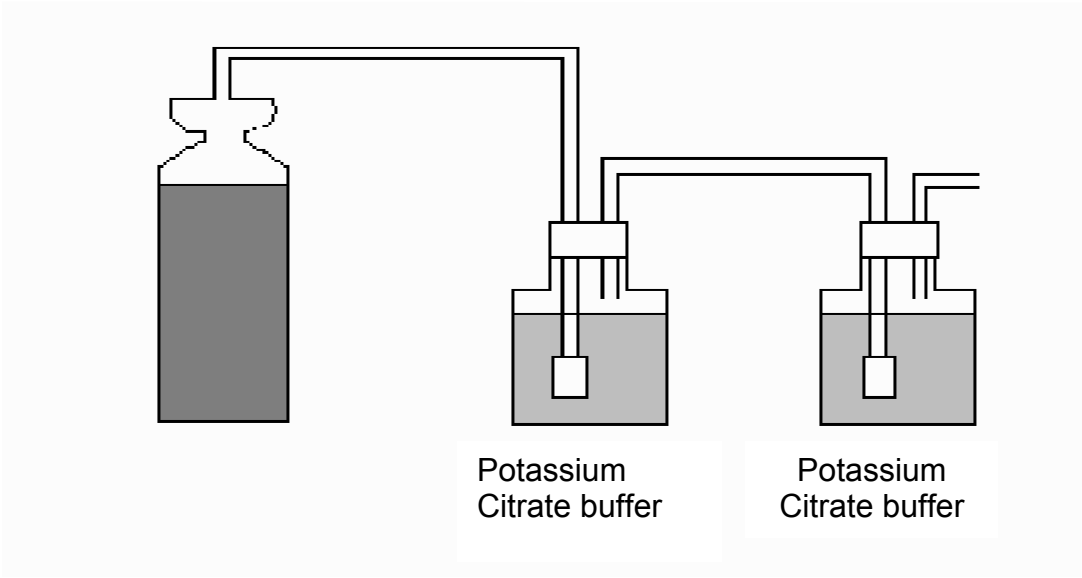

Figure 5.4 Schematic diagram of experimental setup for determining H_2S solubility in potassium citrate buffer solution

5.3.3 Experimental procedure

5.3.3.1 Sulphide stripping using a pressurized reactor

The calcium sulphide product (250 g), obtained from the decomposition of gypsum, was dissolved in water (5 ℓ) and placed in the pressurized reactor. The CO_2 was fed into the reactor. The gas was allowed to flow at pressure through the hollow shaft, finned, mechanical stirrer and mixed with the slurry. The reactor was then pressurized to the desired experimental pressure with CO_2 fed from the cylinder. The stirrer was started and the off-gas valve was opened to the flow-rate specific to each experiment.
At the experimental pressure and stirring rate, the gas in the headspace above the slurry was also re-introduced into the slurry for further reaction.

The effect of the following parameters on the stripping of sulphide using CO_2 was investigated:

- CO_2 flow-rate (2200 mℓ/min and 3300 mℓ/min)
- Temperature of CaS (25 °C and 60 °C)
- CO_2 pressure (atmospheric pressure, 100 kPa and 200 kPa)

- Hydrodynamics (500 rpm and 1000 rpm)

5.3.3.2 Sulphur production

Iron (III) process

The sulphide product from the furnace was dissolved in water and placed in the first reactor. The second and third reactors contained an iron (III) solution (Figure 5.3). The CO_2 used to strip the sulphide gas was introduced into the sulphide solution via a flow meter. The stripped H_2S gas was trapped in the iron (III) solution and converted to sulphur. Samples were taken from the sulphide reactor and iron (III) reactors at different time intervals and analysed for sulphide and iron (II) concentrations, respectively. The relationship between the following parameters, during the stripping process and sulphur formation, were investigated as a function of time:

- The accumulated amount of CO_2 dosed in the reactor for sulphide stripping.
- The amount of sulphide stripped with CO_2.
- The amount of sulphur produced, calculated from the concentration of iron (II).

The residual contents of the iron (III) reactor were analysed using XRD to determine whether compounds other than sulphur had formed.

PIPco process

The process was divided into two stages:

- ***SO_2 absorption***

Pure SO_2 gas was passed through a potassium citrate buffer. The effect of the following parameters on the absorption of SO_2 gas by potassium citrate buffer was studied:

- pH of the citrate solution.
- Potassium citrate concentration (0.5 M, 1 M and 2 M).

- Temperature of potassium citrate solution rich in SO_2 (25 °C-75 °C).

The solubility of H_2S in the potassium citrate buffer solution was also determined by absorbing H_2S gas in a 2 M potassium citrate solution at pH 6.8. H_2S gas was introduced at 600 mℓ/min for 100 min, into Reactor 1 (Figure 5.4) which contained the potassium citrate buffer solution. H_2S gas not absorbed in Reactor 1 was allowed to pass into Reactor 2. The sulphide concentrations in the liquid from both reactors were determined at 20 min intervals. The concentration of H_2S absorbed was then plotted as a function of amount of H_2S fed.

- ***Sulphur production***

The calcium sulphide product (200 g) from the thermal studies was dissolved in water and placed in the first reactor (Figure 5.3). The potassium citrate buffer solution dosed with SO_2 was placed in the second and third reactor. The CO_2 used to strip the H_2S gas was introduced into the sulphide solution via a flow meter. The stripped H_2S gas was trapped in 2 M potassium citrate buffer solution rich in SO_2. The reaction between the two gases resulted in the formation of sulphur that was analysed for purity using the LECO Combustion Techniques (paragraph 5.3.4).
The influence of CO_2 flow-rate (520 mℓ/min and 1 112 mℓ/min) on the recovery of sulphur was investigated.

5.3.4 Analytical Procedure

The pH determinations (Metrohm 691) were carried out manually. Iron (II) and sulphide analyses were carried out manually according to standard procedures (APHA, 1985).

5.3.4.1 Sulphide titration method

A sample volume (10-50 mℓ) was placed in a beaker, 10 mℓ of 0.05 M iodine, 6 drops of 50% HCl and 6 drops of starch were added to the sample. The mixture was titrated with sodium thiosulphate to a clear endpoint. The titration value obtained was substituted into the following equation to obtain the concentration of sulphide stripped:

mg/ℓ S^{2-} = 16 x ((volume I_2 x [I_2]) – (titration volume x [$Na_2S_2O_7$])) x 1 000/volume of sample (76)

5.3.4.2 Iron (II) titration method

A filtered sample volume (10-25 mℓ) was taken. 1 N H_2SO_4 (10 mℓ) and Zimmerman Reinhardt reagent (10 mℓ) were added. The mixture was titrated with 0.1 N $KMnO_4$ until the first indication of a pink colour appeared. The concentration of iron (II) was calculated as follows:

Iron(II) (mg/ℓ Fe) = 55.85 g/mol x 0.1 N x Titration volume x 1 000 / sample volume (77)

5.3.4.3 SO_3^{2-} and $S_2O_3^{2-}$ titration

The titration procedure to determine the concentration of sulphite (SO_3^{2-}) and thiosulphate ($S_2O_3^{2-}$) was developed by Pfizer and is accurate to ± 0.1 mol/ℓ (Gryka, 2005). The following method was used to analyse for SO_3^{2-} and $S_2O_3^{2-}$:

Combined SO_3^{2-} and $S_2O_3^{2-}$ titration: Sample (0.5 mℓ) was pipetted into a beaker containing water (50 mℓ) and starch indicator (1 mℓ). The solution was titrated with 0.05 M iodine solution to a yellow end point. Beginning and end titration readings were recorded (Gryka, 2005).

$S_2O_3^{2-}$ titration: Sample (0.5 mℓ) was pipetted into a beaker containing water (50 mℓ), starch indicator (1 mℓ). and formaldehyde (50 mℓ). The solution was titrated with 0.05 M iodine solution to a yellow end point. Beginning and end titration readings were recorded (Gryka, 2005).

$$SO_3^{2-} + I_2 + H_2O \rightarrow SO_4^{2-} + 2I^- + 2H^+ \quad (78)$$

$$2S_2O_3^{2-} + I_2 \rightarrow S_4O_6^{2-} + 2I^- \quad (79)$$

The following calculations were done: 0.05 M iodine was used to oxidize SO_3^{2-} to SO_4^{2-} (Reaction 78) and $S_2O_3^{2-}$ to $S_4O_6^{2-}$ (Reaction 79) to give a combined titration value A. The concentration of $S_2O_3^{2-}$ was determined by adding formaldehyde to precipitate SO_3^{2-} to give a titration value B. The difference between A and B (C) is equivalent to the SO_3^{2-} concentration.

$S_2O_3^{2-}$ is calculated from

$$(V * 2M)_{S_2O_3^{2-}} = (B * M)_{I_2} \quad (80)$$

$$M_{S_2O_3^{2-}} = \frac{(B * M)_{I_2}}{2V_{S_2O_3^{2-}}} \quad (81)$$

where V – volume of solution

B – I_2 titration volume

M – concentration in moles/ℓ

and SO_3^{2-} from

$$M_{SO_3^{2-}} = \frac{(C * M)I_2}{V_{SO_3^{2-}}} \quad (82)$$

5.3.4.4 Preparation of 2 M Potassium Citrate Buffer Solution

- **5 ℓ of 2M potassium citrate buffer solution:**

192 g/mol x 2 M x 5 ℓ = 1 920 g or 1.920 kg anhydrous citric acid

- **45 % KOH to raise the pH of the citrate solution**

56 g/mol x 2.8 mol/mol of acid x 2 M x 5 ℓ = 1.568 kg pure KOH

Citric acid is trivalent. To achieve the target pH approximately 2.8 mol (as determined experimentally) of KOH per mole of citric acid are required (Gryka, 2005).

5.3.4.5 LECO Combustion Techniques

A CS200 LECO Combustion Analyser was used for sulphur purity analysis. The instrument was calibrated using a certified reference material, and the analysis verified by analysing a different reference material of similar sulphur concentration to the sample and the calibration standard.

A portion of sample is weighed into a ceramic crucible, and an appropriate flux/accelerator mix is added (a combination of copper and tungsten). The crucible is placed in the instrument, where it is moved into the induction furnace. The crucible is heated, and the sample/flux mixture melted. Any sulphur in the sample is released and converted to SO_2. The SO_2 is carried in a stream of high-purity oxygen to the detector. The SO_2 is detected quantitatively by an infrared detector, and converted to equivalent sulphur concentration.

CHAPTER 6

RESULTS AND DISCUSSION

6.1 THERMAL STUDIES

6.1.1 Tube and muffle furnace

Table 6.1 shows the effect of various reaction parameters on the CaS yield during the thermal conversion of gypsum to CaS.

Effect of time. Experiment 1 (Table 6.1) showed that good conversion yields (> 96%) were achieved at a reaction time of 20 min. At a reaction time of 5 min, the yield was only 45%.

Effect of temperature. Experiment 2 (Table 6.1) indicated a marked improvement in the yield of the reduced mass as temperature was raised from 900 °C to 1 100 °C. The results showed further that for a carbon: gypsum mole ratio of 3:1 and a reaction time of 20 min, the conversion percentage increased from 15% at 900 °C to 96% at 1 100 °C . This could be due to the high activation energy required for the reduction of calcium sulphate to calcium sulphide. Saeed (1983) showed that the reaction between carbon and $CaSO_4$ to CaS takes place between 750 °C and 1 100 °C.

Effect of carbon: gypsum mole ratio. Experiment 3 (Table 6.1) showed that when no carbon was added, no CaS was formed. The addition of carbon to gypsum at a 1:1 mole ratio showed that only 20% of gypsum was converted to CaS. The conversion results further showed that CaO formation is favoured by a carbon: gypsum mole ratio of 1:1. Gypsum to CaO conversion of 38% was obtained. However, increasing the ratio of carbon to 2 and 3 moles to a given 1 mole of gypsum showed high conversions of gypsum to calcium sulphide (90 and 96%, respectively). The above results indicated that a reducing agent is needed for the thermal reduction of gypsum to CaS. The

high percentage conversion for a 1:2 molar ratio of gypsum to carbon corresponds to the stoichiometric amounts for the reaction of gypsum and carbon as indicated by reaction 83 (Reddy, *et al.,* 1967)

$$CaSO_4(s) + 2C(s) \rightarrow CaS(s) + 2CO_2(s) \quad (83)$$

Effect of particle size. Experiment 4 (Table 6.1) showed that the formation of calcium sulphide, is dependent upon the particle size of gypsum. When the gypsum particle size was 380 µm, the gypsum to CaS conversion was 80%. Increasing the particle size to 1 250 µm resulted in a decrease in the conversion. The improved yield of CaS afforded by 380 µm gypsum can be ascribed to the higher surface areas offered by the smaller particle size.

Effect of different reducing agents. Experiment 5 (Table 6.1) showed that the use of activated carbon as a reducing agent did not show a significantly increased yield of CaS when compared to coal. The use of activated carbon yielded 85% conversion, while coal yielded 81% conversion. The improved yield using Duff coal could be due to the volatiles contained in the coal. From these findings, it is recommended that coal be used as the reducing agent for a full scale plant. Duff coal is cheaper and readily available as compared to activated carbon.

Effect of different gypsum compounds. Experiment 6 (Table 6.1) showed that 91% of gypsum was converted to CaS when pure gypsum was used. The lower conversion percentages (76% and 81%) obtained when Anglo gypsum and Foskor gypsum were reduced to CaS can be ascribed to the impurities contained in the two gypsum compounds.

Effect of furnace type. Experiment 7 (Table 6.1) showed that the tube furnace (76%) is more efficient in converting gypsum to CaS than the muffle furnace (70%). The presence of oxygen in the muffle furnace resulted in the formation of several oxygen containing compounds such as $MgAl_2O_4$ and $Ca_2Al_2SiO_7$. However the tube furnace purged with nitrogen does not favour production of oxygen containing compounds.

Table 6.1 XRD analysis results for the thermal reduction of gypsum to CaS

Exp No.	Parameter	Value	Type of furnace	Type of gypsum	$CaSO_4$ %	CaS %	CaO %	MgO %	$Ca_2Al_2SiO_7$	$MgAl_2O_4$	$Ca_5(PO_4)_3OH$
1	Time (min)	5	Tube	Pure	49	45	7	0	0	0	0
		20			0	96	4	0	0	0	0
		60			0	93	5	0	0	0	0
2	Temperature (°C)	900	Tube	Pure	84	15	1	0	0	0	0
		1000			8	88	4	0	0	0	0
		1100			0	96	4	0	0	0	0
3	$C/CaSO_4$ mole ratio	0	Tube	Pure	100	0	0	0	0	0	0
		0.25			93	0	7	0	0	0	0
		0.5			74	0	25	0	0	0	0
		1			48	13	38	0	0	0	0
		2			2	90	8	0	0	0	0
		3			0	96	4	0	0	0	0
4	Particle size of Gypsum (µm)	380	Tube	Foskor	0	80	15	0	0	0	0
		630			22	56	18	0	0	0	0
		1250			86	1	12	0	0	0	0
5	Reducing agent	Coal	Tube	Foskor	8	81	5	0	0	0	3
		Activated carbon			7	85	4	0	0	0	2
6	Gypsum compounds	Pure	Tube	Pure	4	91	4	0	0	0	0
		Anglo		Anglo	8	76	7	7	0	0	0
		Foskor		Foskor	7	81	6	0	0	0	2
7	Furnace type	Tube	Tube	Anglo	8	76	6	8	0	0	0
		Muffle	Muffle		0	70	2	6	5	3	0

The following parameters were kept constant (in the above experiments) unless otherwise stated: temperature = 1100 °C, time = 20 min, mole ratio (carbon:gypsum) = 3: 1, gypsum amount = 5g and activated carbon was used as a reducing agent for experiment 1 to 4. For experiment 6 and 7, duff coal was used as a reducing agent.

6.1.2 Thermogravimetric analysis

The following thermogravimetric analysis were conducted when activated carbon/duff coal and pure/Anglo/Foskor gypsum were heated in nitrogen using a heating rate of 10 °C/min and a carbon/coal to gypsum ratio of 3:1 (unless otherwise stated).

6.1.2.1 Temperature study for the reaction between activated carbon and pure gypsum

Figure 6.1 shows the resultantthermogravimetric curve obtained when activated carbon and pure gypsum were heated to 1260 °C at a rate of 10 °C/min.

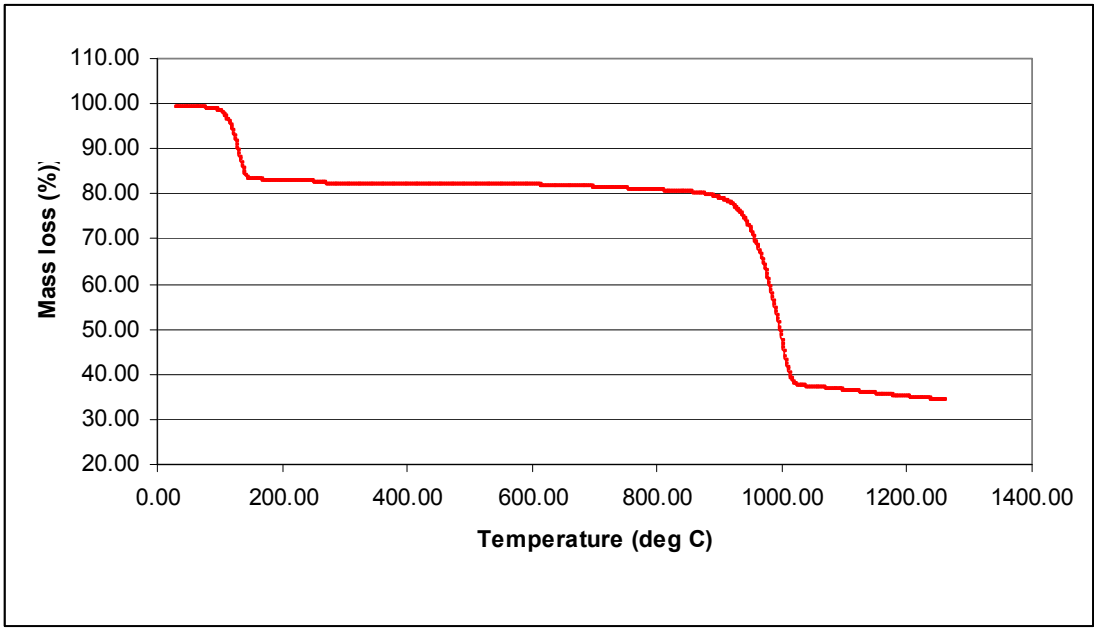

Figure 6.1 Thermogravimetric curve for the reaction between activated carbon and pure $CaSO_4.2H_2O$ at a heating rate of 10 °C/min

The effect recorded in the temperature range 80-180 °C was attributed to the loss of water of crystallisation from $CaSO_4.2H_2O$ to form $CaSO_4$ (reaction 84), (Popescu *et al.,* 1985).

$$CaSO_4.2H_2O\ (s) \rightarrow CaSO_4\ (s) + 2H_2O\ (g) \qquad (84)$$

The small mass loss between 600 °C and 850 °C was ascribed to the oxidation of carbon to carbon dioxide or carbon monoxide (reactions 85 and 86).

$$C\,(s) + O_2\,(g) \rightarrow CO_2\,(g) \quad (85)$$

$$2C\,(s) + O_2\,(g) \rightarrow 2CO\,(g) \quad (86)$$

The mass loss between 900 °C and 1 050 °C was due to the reduction of $CaSO_4$ to CaS with carbon (reaction 87). This finding confirmed the XRD results in Section 6.1 (Effect of temperature) which showed the presence of CaS between 900 °C and 1100 °C.

$$CaSO_4\,(s) + 2C\,(s) \rightarrow CaS\,(s) + 2CO_2\,(g) \quad (87)$$

Van der Merwe *et al*., (1999) showed that the descending thermogravimetric curve above 1 000 °C was due to the decomposition of the $CaSO_4$ to CaO (reaction 88)

$$CaSO_4\,(s) \rightarrow CaO\,(s) + SO_3\,(g) \quad (88)$$

6.1.2.2 Effect of carbon to gypsum mole ratio

Table 6.2 Thermogravimetric results for different mole ratios between activated carbon and pure $CaSO_4.2H_2O$

Mole ratio between carbon and gypsum (Carbon:Gypsum)	T_{min} (ºC)	T_{max} (ºC)	% mass loss	Total % mass loss
0.25:1	25	200	20.5	22.7
	200	800	2.1	
	800	1100	0.12	
0.5:1	25	200	20.6	23.3
	200	800	2.5	
	800	1100	0.17	
1:1	25	200	18.7	43.0
	200	800	5.7	
	800	1100	18.6	
3:1	25	200	17.9	60
	200	800	5.6	
	800	1100	36.2	

The results in Table 6.2 show the effect of different mole ratios of carbon to pure $CaSO_4.2H_2O$ at a heating rate of 10 °C/min. The amount of carbon was varied from 0.09 g to 1.04 g (0.25 mole to 3 mole) while that of gypsum was kept constant at 5 g. From the results in Table 6.2, it was seen that when the ratio between carbon and gypsum was 0.25:1, the mass loss was 23%. However, increasing the ratio of carbon to gypsum to 3:1 resulted in an increase in gypsum mass loss (60%). The finding emphasised the importance of adding a sufficient excess of reducing agent to effect the decomposition of calcium sulphate to CaS.

6.1.2.3 Effect of gypsum compounds and reducing agents

Table 6.3, Experiment 1 shows thermogravimetric results obtained for the comparison between three gypsum compounds from different sources using activated carbon as a reducing agent. The results showed that lower mass losses were obtained for Anglo and Foskor gypsum. This finding can also be ascribed to the constituent impurities as explained in Section 6.1.1. The mass loss of 44.8% in the case of pure gypsum, compared well with the theoretical mass loss for the reaction of pure $CaSO_4$ with carbon which is 44.9%.

From Experiment 2, it was seen that the use of coal as reducing agent results in lower mass losses with the three gypsum types. The carbon content of the Duff coal is 68.7% compared to the activated carbon which is 98.7%. This did not lower the conversion as much as expected. However, comparing the cost efficiency, the use of coal as a reducing agent in a full scale plant is recommended as discussed in Section 6.1

Table 6.3 Thermogravimetric results for the reaction between different gypsum compounds and reducing agents

Experiment number	Gypsum Source	Reducing agent	T_{min} (°C)	T_{max} (°C)	% mass loss
1	Pure Foskor Anglo	Activated carbon	650	1100	44.8 41.8 38.7
2	Pure Foskor Anglo	Duff coal	650	1100	38.5 32.9 30.5

6.1.3 Kinetic analysis

The kinetic analysis done on the thermogravimetric data obtained for the reaction between carbon monoxide and pure gypsum as well as the reaction between carbon and gypsum from three different sources (pure, Anglo and Foskor) is described in this section. Heating rates between 1 °C/min and 10 °C/min were utilised to calculate the activation energy values at different degrees of conversion (α) using the isoconversional method. The method provides a model free approximation of the activation energy, by using multiple scan analysis and is described by Ozawa (1965) and Flynn and Wall (1966).

The graphs represent the results of (1-α) (α is the degree of conversion) plotted against temperature for different heating rates, logarithm of heating rate vs reciprocal absolute temperature (log β vs. 1/T) at different degrees of conversion and the dependency of activation energy on the degree of conversion for each reaction mixture.

6.1.3.1 Reaction between carbon monoxide and pure gypsum

Six different heating rates between 1 °C/min and 10 °C/min were used to get the model free estimation of the activation energy of the reaction between carbon monoxide and pure gypsum (Figures 6.2-6.4). Figure 6.2 depicts the graph of (1 - α) versus temperature for different heating rates.

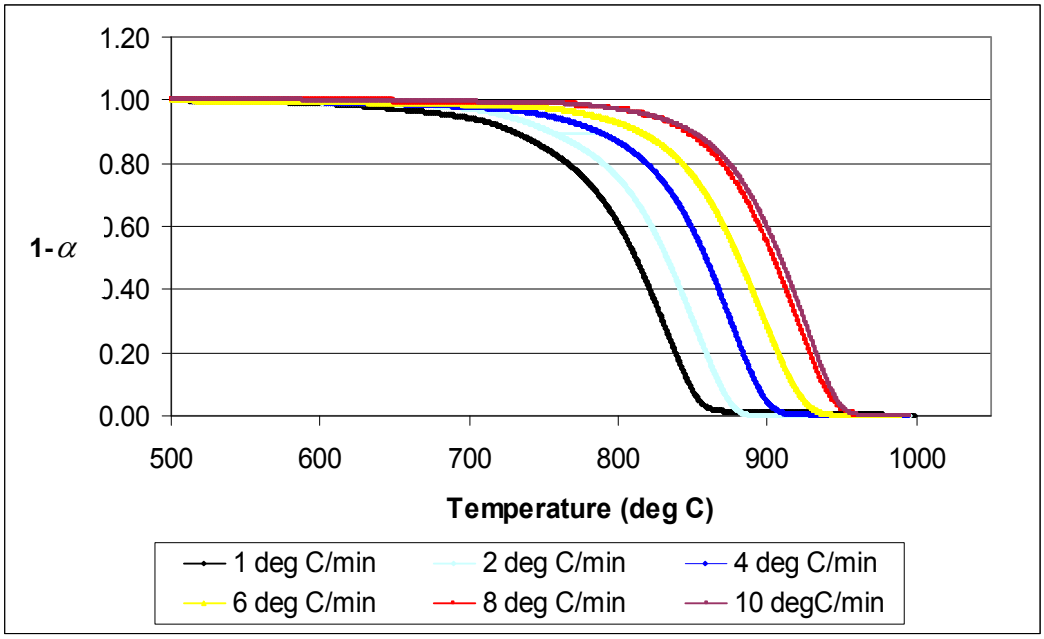

Figure 6.2 (1-α) versus temperature for six heating rates for the reaction between carbon monoxide and pure gypsum

The corresponding temperatures at a constant α at several heating rates were determined from degree of conversion versus temperature thermograms (Figure 6.2). The procedure was repeated at other values of the degree of conversion, thus testing the constancy of activation energy with respect to the degree of conversion and temperature. The graphs in Figure 6.3 show the plots made for logarithm of heating rate vs. reciprocal absolute temperature.

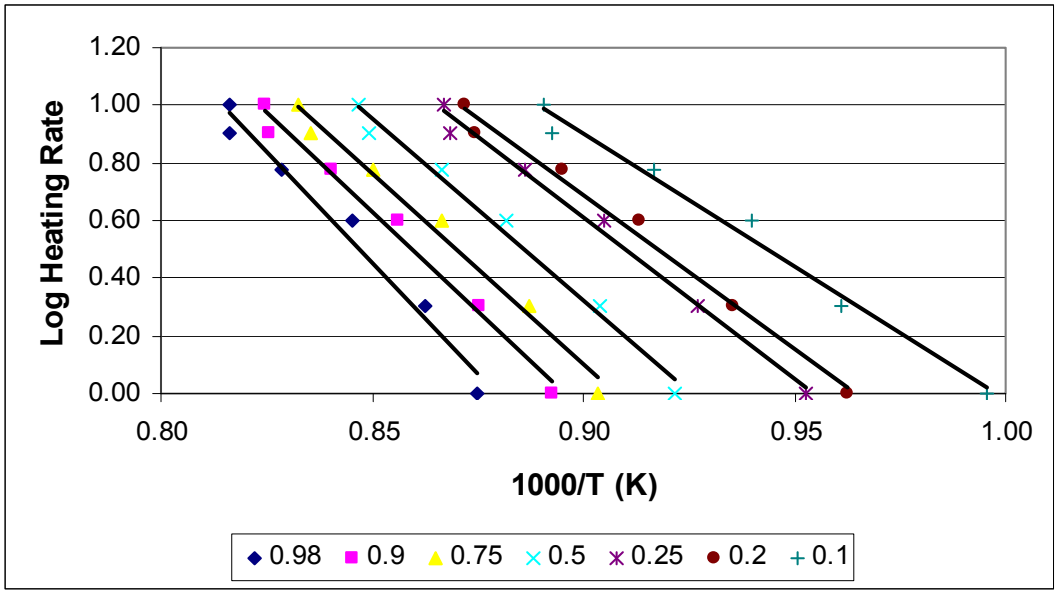

Figure 6.3 Logarithm of heating rate vs. reciprocal absolute temperature for the reaction between carbon monoxide and pure gypsum

For α equal to a constant, the plots of log β versus 1/T (Figure 6.3) were straight lines whose slopes give the activation energy at different degrees of conversion calculated from Equation 89. Figure 6.4 shows the dependency of activation energy on the degree of conversion.

$$E = -4.35 \frac{d \log \beta}{d \frac{1}{T}} \qquad (89)$$

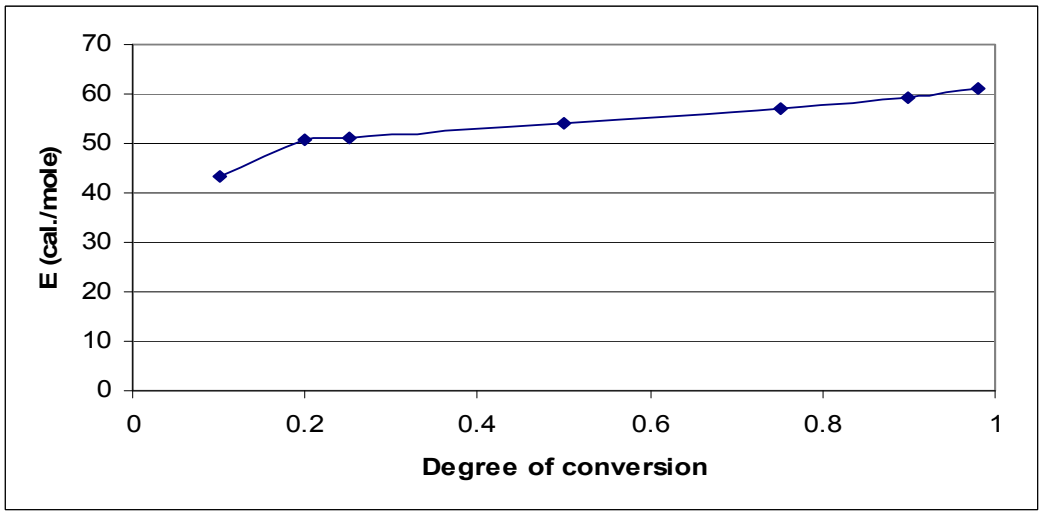

Figure 6.4 Dependency of the activation energy on the degree of conversion for the reaction between carbon monoxide and pure gypsum

6.1.3.2 Reaction between activated carbon and pure gypsum

Figures 6.5-6.7 show the temperature plotted against (1-α) for different heating rates (2, 4, 6, 8 and 10 °C/min); logarithm of heating rate vs reciprocal absolute temperature (log β vs. 1/T) at different degree of conversion, and the dependency of activation energy on the degree of conversion for the reaction between activated carbon and pure gypsum, respectively. The same procedures as indicated in 6.1.3.1 were followed.

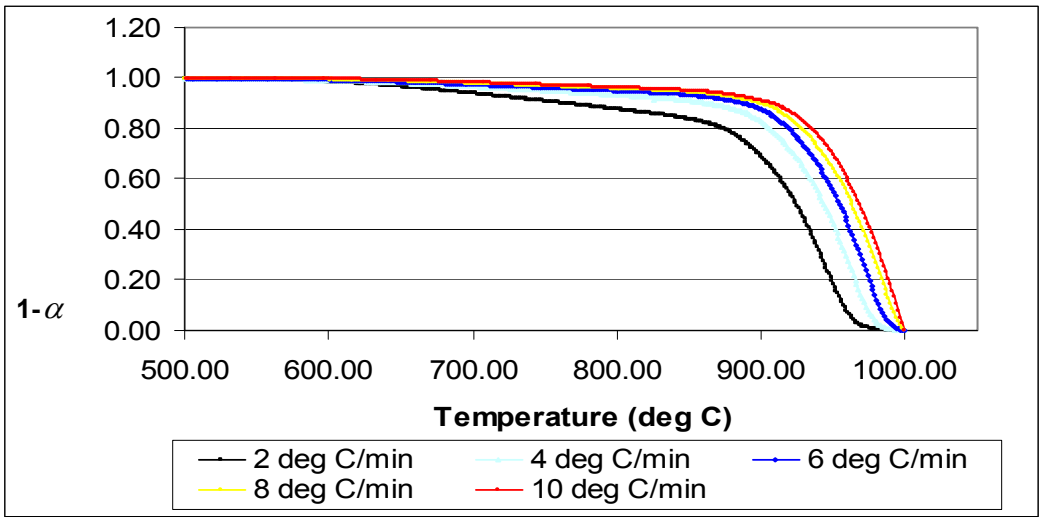

Figure 6.5 (1-α) versus temperature for five heating rates for the reaction between activated carbon and pure gypsum

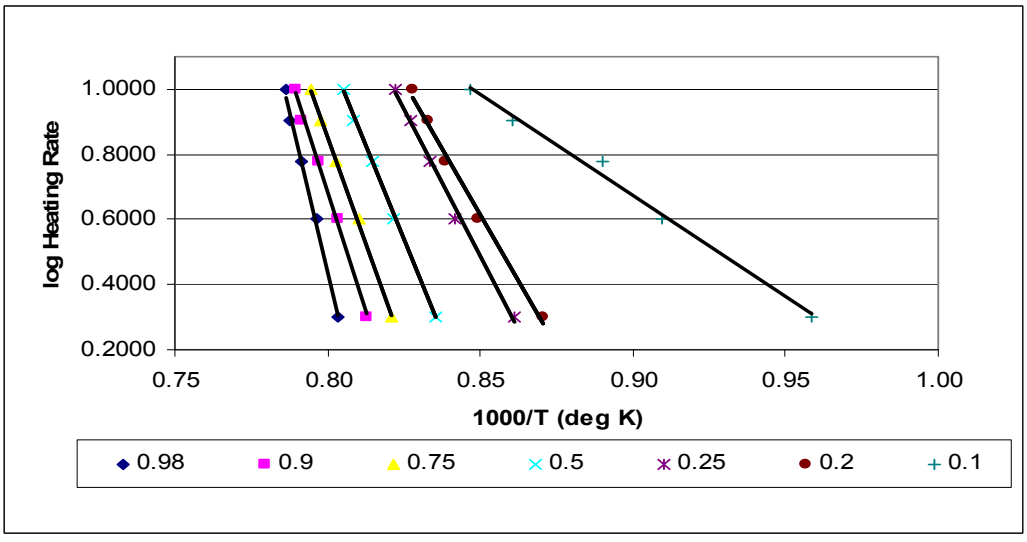

Figure 6.6 Logarithm of heating rate vs. reciprocal absolute temperature for the reaction between activated carbon and pure gypsum

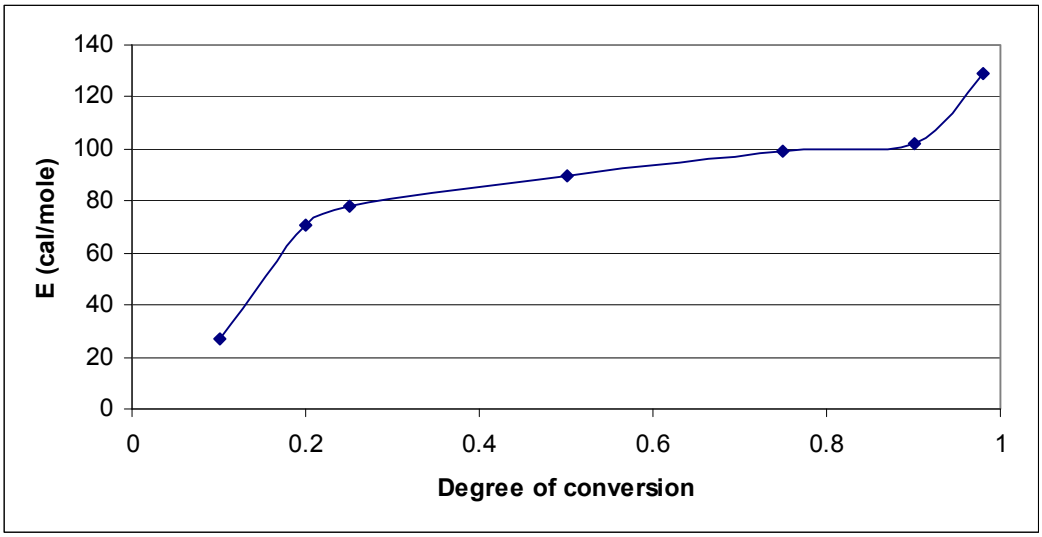

Figure 6.7 Dependency of the activation energy on the degree of conversion for the reaction between activated carbon and pure gypsum

6.1.3.3 Reaction between activated carbon and Foskor gypsum

The kinetic analysis done on the results obtained from the reaction between activated carbon and Foskor gypsum are shown in Figures 6.8-6.10.

The figures represent the temperature plotted against the (1-α) for different heating rates (2, 4, 6, 8 and 10 °C/min); logarithm of heating rate vs reciprocal absolute temperature (log β vs. 1/T) at different degrees of conversion, and the dependency of activation energy on the degree of conversion for the reaction between activated carbon and pure gypsum. The same procedures as indicated in 6.1.3.1 were followed.

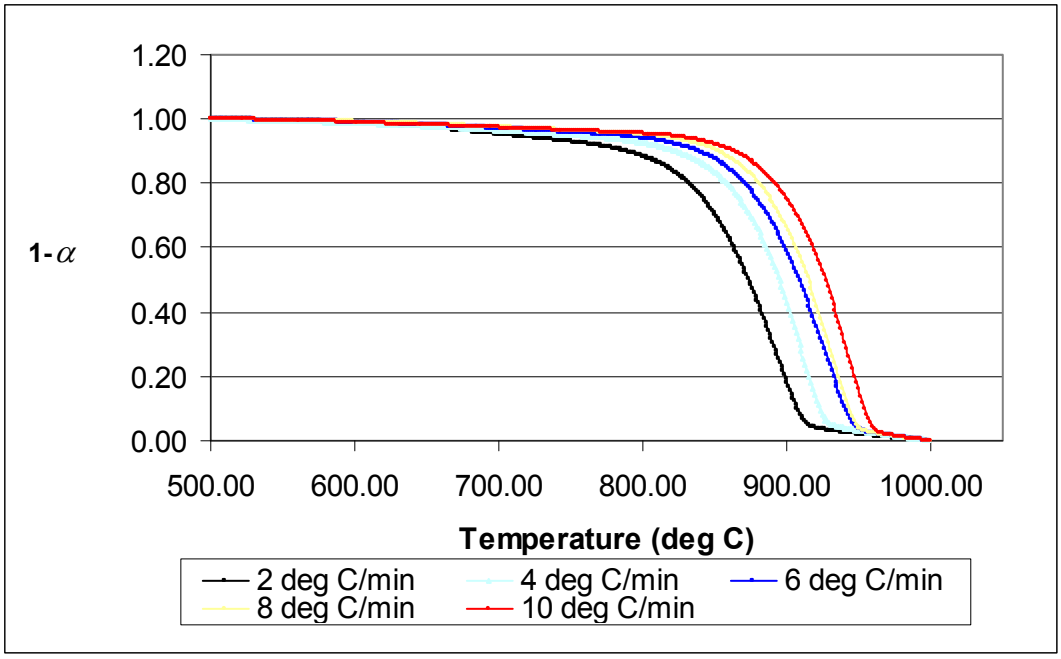

Figure 6.8 **(1-α) versus temperature for five heating rates for the reaction between activated carbon and Foskor gypsum**

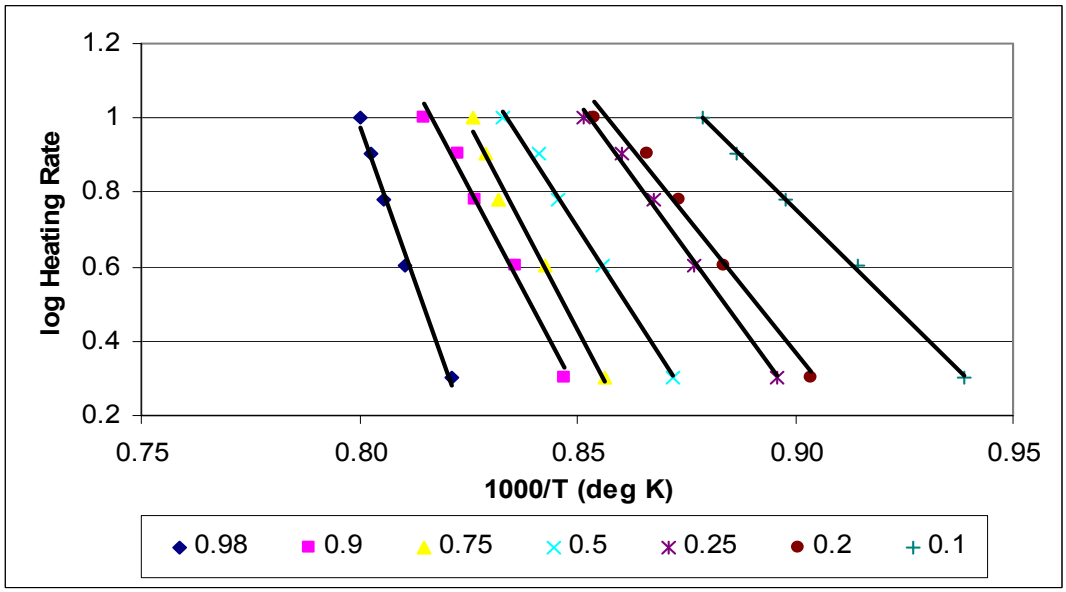

Figure 6.9 **Logarithm of heating rate versus reciprocal absolute temperature for the reaction between activated carbon and Foskor gypsum**

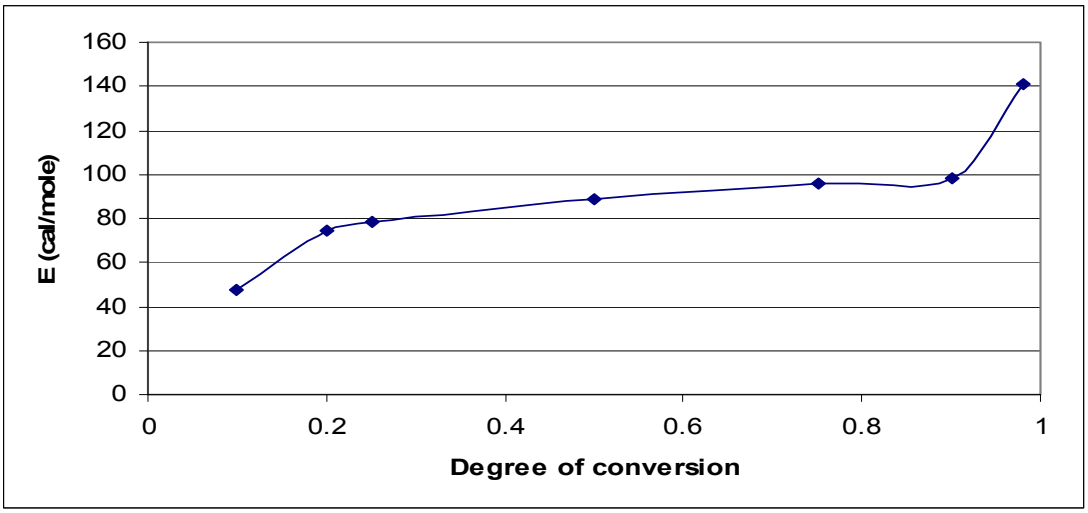

Figure 6.10 Dependency of the activation energy on the degree of conversion for the reaction between activated carbon and Foskor gypsum

6.1.3.4 Reaction between activated carbon and Anglo gypsum

Five heating rates (2, 4, 6, 8 and 10 °C/min) were utilized to obtain the activation energies for the reaction between activated carbon and Anglo gypsum. Figures 6.11-6.13 indicate temperature plotted against the (1 - α) for different heating rates (2, 4, 6, 8 and 10 °C/min); logarithm of heating rate vs reciprocal absolute temperature (log β vs. 1/T) at different degree of conversion, and the dependency of activation energy on the degree of conversion for the reaction between activated carbon and pure gypsum, respectively. The same procedures as indicated in 6.1.3.1 were followed.

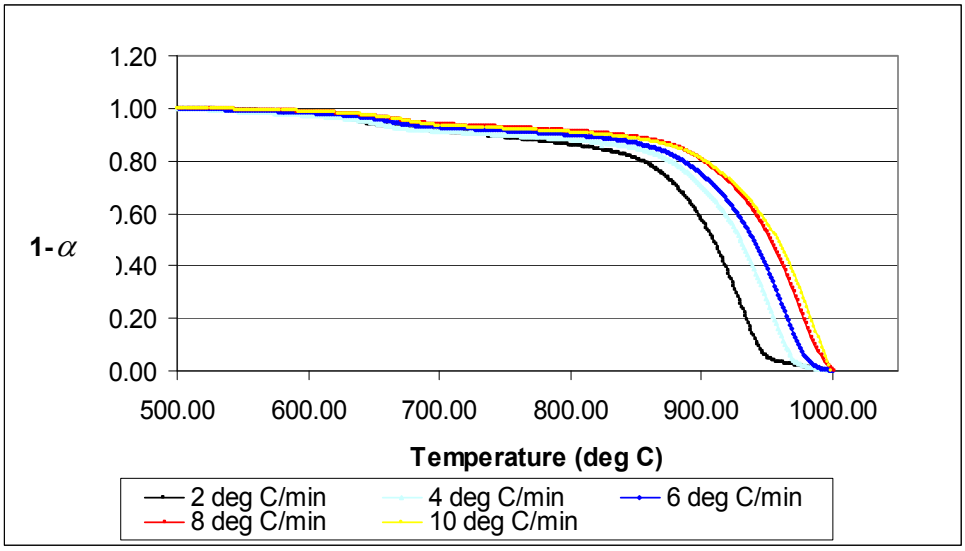

Figure 6.11 (1-α) versus temperature for six heating rates for the reaction between activated carbon and Anglo gypsum

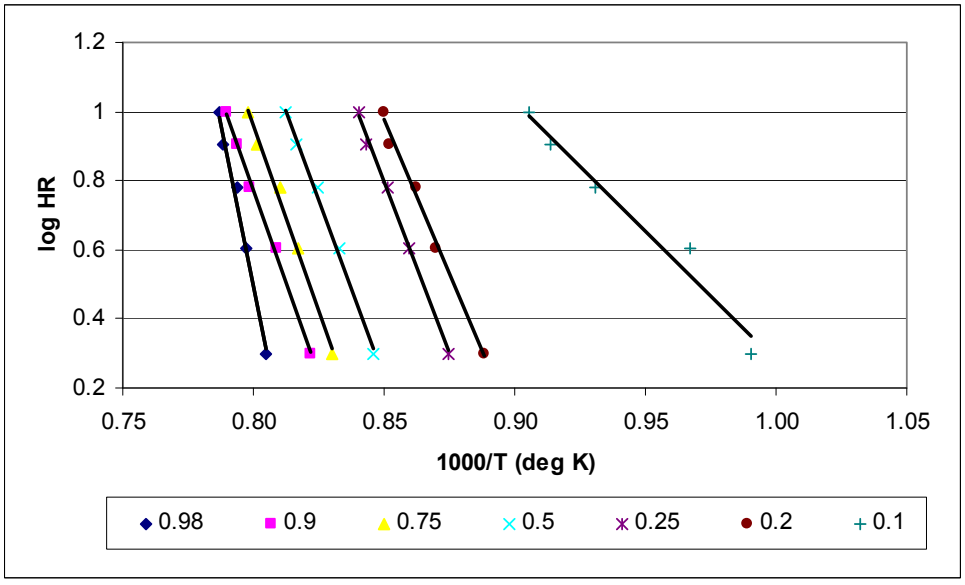

Figure 6.12 Logarithm of heating rate versus reciprocal absolute temperature for the reaction between activated carbon and Anglo gypsum

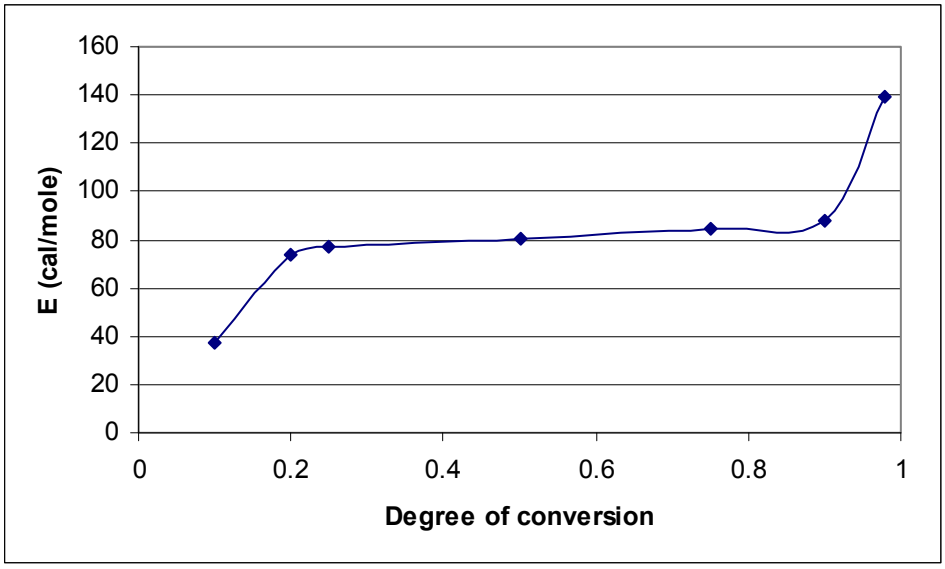

Figure 6.13 Dependency of the activation energy on the degree of conversion for the reaction between activated carbon and Anglo gypsum

Interpretation of the kinetic data.

Figures 6.2, 6.5, 6.8 and 6.11, representing the results for the degree of conversion plotted against temperature for the three gypsum types (pure, Anglo and Foskor) and the two reducing agents (activated carbon and Duff coal) at different heating rates showed that an increase in the heating rates from 1 to 10 °C/min, gave smooth curves.

Dowdy (1987) indicated that if the calculated activation energy for a certain reaction is the same for different degrees of conversion, it can be concluded that the reaction is a single step reaction. However, if the activation energy changes for different degrees of conversion, then the reaction is complex.

Applying Dowdy's conclusions about change in activation energy in Figures 6.4, 6.7, 6.10 and 6.13, representing the dependency of activation energy on the degree of conversion, it was concluded that the process under study, the thermal decomposition of gypsum in the presence of carbon/carbon monoxide, is complex.

Vyazovkin and Lesnikovich (1990) proposed a method for detailing the types of complex processes. They indicated that decreasing dependencies of activation energy on the degree of conversion show complex processes with a change in the limiting stage, e.g. processes containing a reversible intermediate stage or those with a change over from a kinetic to a diffusion controlled regime. Increasing dependencies of activation energy on the degree of conversion are characteristics of processes involving several parallel, competing reactions.

They further showed that by analysing the shape of the activation energy versus the degree of conversion curve, it may be possible to distinguish between complex processes incorporating parallel competing and parallel independent reactions. With parallel independent reactions a plateau shape is observed at the initial and final stages of conversion. Therefore, an S-shape characteristic curve is observed with parallel independent reactions (Vyazovkin *et al.*, 1992). In the case of parallel competing reactions, no S-shape characteristic curves are observed.

The above characteristics for detailing the types of complex processes were applied to the results obtained for the reaction between carbon monoxide/activated carbon and the different gypsum types (Figure 6.4, 6.7, 6.10 and 6.13). It was concluded that a complex of parallel competing reactions take place in the present study. This conclusion was supported by the following findings:

1) An increasing dependency of activation energy on the degree of conversion was observed from the four different Figures (6.4, 6.7, 6.10 and 6.13)
2) The increase in activation energy at the initial stage of the transformation (up to α=0.2) did not show a plateau and makes it possible to distinguish parallel competing reactions from a process incorporating parallel independent reactions.

Between the conversion degrees of 0.2 and 0.75, the absence of the activation energy dependency on the degree of conversion (plateau) was observed. The plateau shape indicates that there is no change in the limiting step. Possible reasons for no change in the dependency of activation energy on the degree of conversion could be due to different influences of the diffusion of gaseous products.

The figures further showed that the activation energies for the reaction between Anglo and Foskor gypsum with activated carbon were higher as compared to the activation energies for pure gypsum. This can possibly be ascribed to the impurities in Foskor gypsum and Anglo gypsum, which cause interference owing to side reactions.

Since the solid–solid reactions ($CaSO_4$ and C, reaction 90) are inherently slow as compared to gas - solid reactions ($CaSO_4$ and CO, reaction 93), it was proposed that reaction 90 occurs via intermediate reaction products, CO and CO_2 (reactions 91, 92 and 93). Figure 6.14 shows how $\Delta G°$ (Gibbs free energy, which is the measure of the thermodynamic driving force that makes a reaction occur) changes with temperature, at atmospheric pressure, for reactions 91 and 92, (Gaskell, 1993).

$$CaSO_4\,(s) + 2C\,(s) \rightarrow CaS\,(s) + 2CO_2\,(g) \quad (90)$$

$$C\,(s) + O_2\,(g) \rightarrow CO_2\,(g) \quad (91)$$

$$2C\,(s) + O_2\,(g) \rightarrow 2CO\,(g) \quad (92)$$

$$2CO\,(g) + O_2\,(g) \rightarrow 2CO_2\,(g) \quad (93)$$

$$\text{Overall reaction: } CaSO_4\,(s) + 4CO\,(g) \rightarrow CaS\,(s) + CO_2\,(g) \quad (94)$$

Figure 6.14 showed that of the two possible reactions (reactions 91 and 92) between carbon and oxygen, the one which actually occurs at a given temperature is the one which has the more negative $\Delta G°$. From the Figure

6.14 it was noted that at lower temperatures (<700°C) the equilibrium is on the exothermic carbon dioxide side and at higher temperatures the endothermic formation of carbon monoxide is the dominant product. Figure 6.14 further showed that the formation of CO_2 by oxidation of carbon is constant and independent of temperature, while the formation of CO is a decreasing line.

In the region of 700°C, the two reactions (91 and 92) have approximately equal $\Delta G°$ values (the two lines intersect). This means that the products of combustion will be a mixture of CO and CO_2.

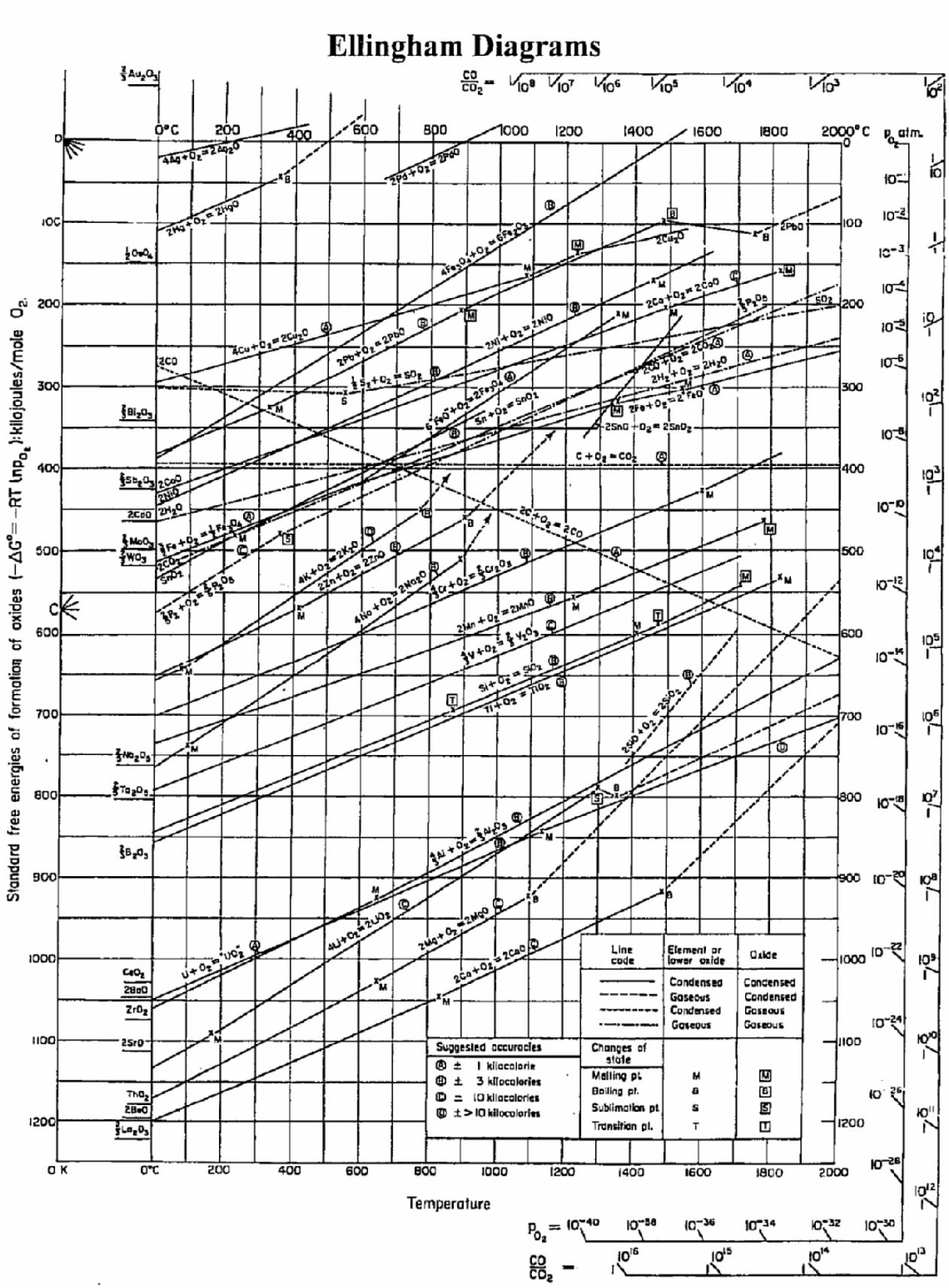

Figure 6.14 Scan of Ellingham diagram (Gaskell, 1993)

6.1.4 Isothermal studies

The isothermal experiments for the reaction between activated carbon and pure gypsum were conducted at the following temperatures: 800 °C, 850 °C, 900 °C, 925 °C, 950 °C, 975 °C and 1 000 °C . Figure 6.15 depicts the curves obtained for degree of conversion plotted against time at different temperatures. Different kinetic equations (as described in section 2.4.3) were used to distinguish the reaction mechanisms under isothermal conditions. Kinetic equations exist between the reacted fraction (α) and the time (t) for heterogenous reaction under isothermal conditions. For this study, the kinetic equations applicable when the rate-limiting process is diffusion and when it is a reaction at the phase boundary between the reactant and the reaction product were used, for example:

$$1-(1-\alpha)^{1/3} = kt \quad (95)$$

$$1-(1-\alpha)^{1/2} = kt \quad (96)$$

$$\left[1-(1-\alpha^{1/3})\right]^2 = kt \quad (97)$$

When the data were fitted in the above kinetic equations, a non-linear shape of the Arrhenius curve was obtained. This confirmed that the thermal decomposition of gypsum in the presence of carbon is not a single-stage reaction but rather a complex process.

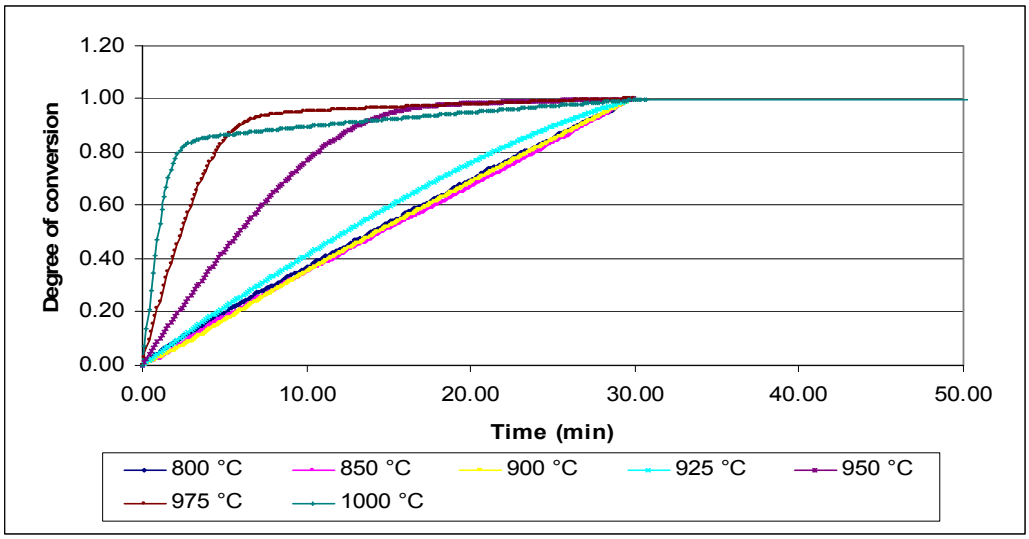

Figure 6.15 Plot of degree of conversion versus time for the reaction between activated carbon and pure gypsum under different isothermal conditions

Table 6.4 shows the mass losses obtained from thermogravimetric analysis of the reaction between activated carbon and pure gypsum at different temperatures. The results indicated that when the sample was heated at 800 °C, 21.1% mass was lost. However, increasing the temperature to 1 000 °C resulted in an increase in the mass loss to 64.8%. This result showed that the reaction between carbon and gypsum is temperature dependent and is favoured at high temperature.

Table 6.4 Thermogravimetric results for the reaction between activated carbon and pure gypsum under different isothermal conditions

Temperature ºC	T_{min} ºC	T_{max} ºC	Total mass loss (%)
800	25	800	21.1
850	25	850	23.4
900	25	900	42.6
925	25	925	59.1
950	25	950	63.5
975	25	975	63.8
1000	25	1000	64.8

6.2 SOLUBILITY OF CaS

Figures 6.16 and 6.17 show the results when the effects of stirring and temperature on the solubility of CaS were investigated. Initial sulphide concentrations for stirring and temperature studies were 270 mg/ℓ and 144 mg/ℓ, respectively. Sulphide dissolved in solution was measured as a function of time and temperature.

From Figure 6.16 it was noted that, the solubility of CaS increases from 270 mg/ℓ to 390 mg/ℓ with time 90 to 60 min. The increase in the solubility of CaS may be due to the oxygen available during stirring. Garcia- Calzada *et al.,* (2000) showed that oxygen accelerates CaS solubility due to the oxidation of HS^- to SO_3^{2-} and SO_4^{2-}

However, increasing the time from 60 min to 180 min did not show much change in the dissolved sulphide. The sulphide measured was approximately 390 mg/ℓ. The findings confirmed the low solubility of CaS.

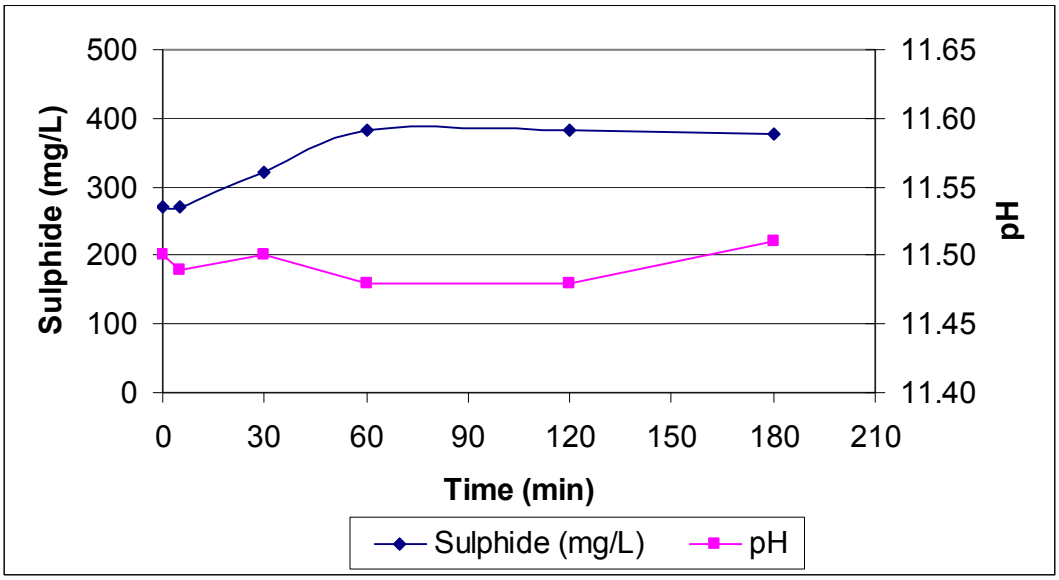

Figure 6.16 Effect of stirring on CaS solubility

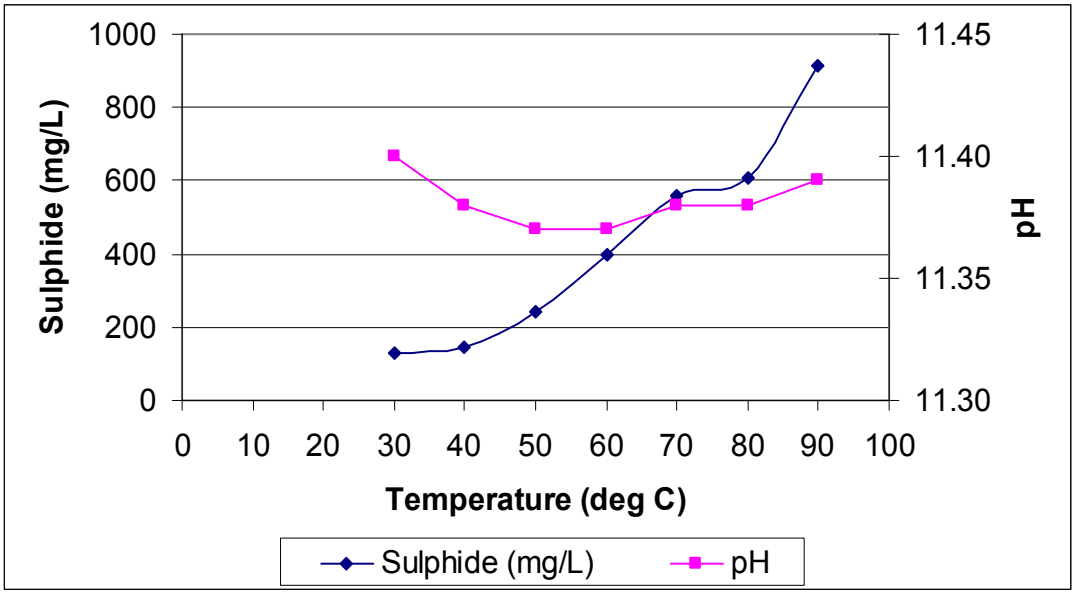

Figure 6.17 Effect of temperature on the CaS solubility

Figure 6.17 shows the effect of temperature on the solubility of CaS. The results show that increasing the temperature of CaS slurry resulted in an increase in the solubility of CaS. The graph further showed that at low temperature (30 °C-40 °C), the sulphide quickly dissolves to saturation. When the temperature was increased from 40 °C to 90 °C, the solubility of CaS increased from 144 mg/ℓ to 915 mg/ℓ.

The pH graphs from the above two figures (Figures 6.16 and 6.17) showed that when CaS was slurried in water, the pH value of the slurry was above 11. The higher pH value is due to the formation of $(CaOH)^{+}_{(aq)}$ (reaction 98) which is very basic. And for as long as there is no CO_2 gas available to strip the sulphide from CaS slurry, the pH will stay high. Garcia- Calzada (2000) further showed that at pH > 10, the sulphide is present as $HS^{-}_{(aq)}$. At pH < 10, sulphide is present as H_2S gas.

$$CaS\ (s) + H_2O\ (aq) \rightarrow (CaOH)^{+}\ (aq) + HS^{-}(aq) \qquad (98)$$

6.3 REACTION MECHANISM FOR SULPHIDE STRIPPING

The following study was conducted with the aim to investigate the reaction mechanism for the sulphide stripping from CaS slurry with CO_2 gas.

6.3.1 Behaviour of sulphide, calcium, alkalinity and pH during the sulphide stripping process

Figure 6.18 shows the time dependent behaviour of sulphide, calcium, alkalinity, CO_2 fed and pH during the sulphide stripping process. The initial CaS concentration was 1 083 mmol/ℓ and the CO_2 flow-rate, 520 mℓ /min.

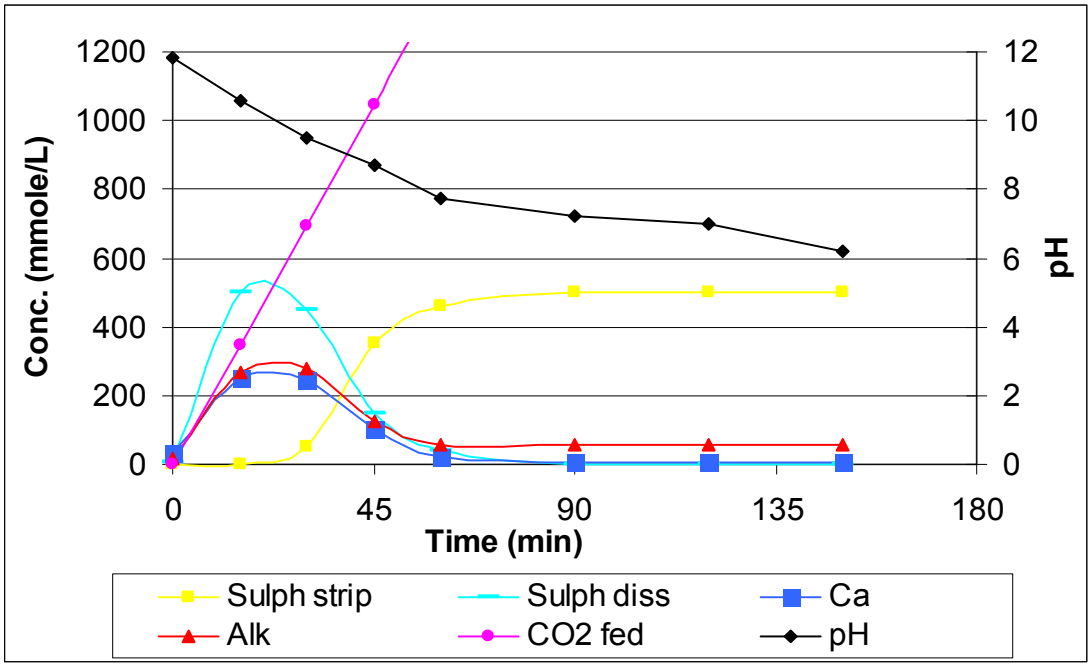

Figure 6.18 Behaviour of calcium, pH and sulphide during the sulphide stripping process with CO_2

The influence of the following parameters on the stripping process was noted from their representative graphs in Figure 6.18:

- ***Sulphide dissolved and stripped***

The graphs showed that during the first 30 min of the experiment, as CO_2 was passed through the CaS slurry, CaS dissolves to form $Ca(HS)_2$ (proposed intermediate, reaction 99). As more CO_2 (after 30 min) was added, the sulphide in the form of $Ca(HS)_2$ is decomposed and stripped off as H_2S gas (reaction 100). The graphs further showed that from the 1083 mmol/ℓ of sulphide as CaS that was initially slurried, only 510 mmol/ℓ sulphide dissolved

and stripped with CO_2. An investigation was carried out to explain why only 510 mmol/ℓ of sulphide dissolved and stripped. The results will be discussed in the following section.

$$2CaS\ (s) + CO_2\ (g) + H_2O\ (aq) \rightarrow CaCO_3\ (s) + Ca(HS)_2\ (aq) \quad (99)$$

$$Ca(HS)_2\ (aq) + CO_2\ (g) + H_2O\ (aq) \rightarrow CaCO_3\ (s) + 2H_2S\ (g) \quad (100)$$

- ***Calcium and Alkalinity***

The calcium graph showed that 250 mmol/ℓ of calcium was in solution and the alkalinity (an indication of the CO_3^{2-} concentration) was 270 mmol/ℓ. The concentrations of the two components (calcium and carbonate, reaction 101) were almost half the value of sulphide (as $Ca(HS)_2$) in solution (510 mmol/ℓ). From reaction 99, $Ca(HS)_2$ is equivalent to 2 mol sulphide as CaS but 1 mol $CaCO_3$ (reaction 99). The above finding indicates the formation of $Ca(HS)_2$. Furthermore, the low Ca concentration shows that $CaCO_3$ precipitates out due to its low solubility at pH values of 7.5 and higher.

$$Ca^{2+} + CO_3^{2-} \rightarrow CaCO_3\ (s) \quad (101)$$

- ***pH***

The pH graph indicates that when CO_2 is passed through a CaS slurry, the pH drops from 11.8 to 6.2. It was further concluded that above pH 10, sulphide is in solution as $Ca(HS)_2$ and below pH 10 it is present as H_2S gas (reaction 99 and 100, respectively) .

6.3.2 Analysis of the dissolved and suspended sulphide

Figure 6.19 depicts the experiment conducted with the aim to explain why only half of the initial sulphide slurried was measured (as dissolved and stripped) during the stripping process in the previous experiment (Figure. 6.18). The investigation was carried out using CaS slurry with an initial concentration of 1 200 mmol/ℓ and CO_2 at a flow rate of 520 mℓ/min. During the experiments, samples were taken and analysed. The sulphide analysis was done on the clear solution (filtrate) and on the mixed solution (filtrate and solids).

The results of analysing the two solutions showed that when sulphide was measured in the clear solution, only 650 mmol/ℓ sulphide concentration was present as dissolved sulphide. However, when sulphide was analysed from the mixture, 1 175 mmol/ℓ of sulphide was in suspension. The graph further showed that from the initial CaS concentration of 1 200 mmoe/ℓ, 1 175 mmol/ℓ of sulphide was stripped off with CO_2 gas. The difference of 25 mmol/ℓ sulphide may have escaped during the experiment. The finding indicated that during the stripping of sulphide from CaS slurry with CO_2, sulphide exists in solution as $Ca(HS)_2$ (aq) and is also present as solid $Ca(HS)_2$ (s). This demonstrates the low solubility of $Ca((HS)_2$.

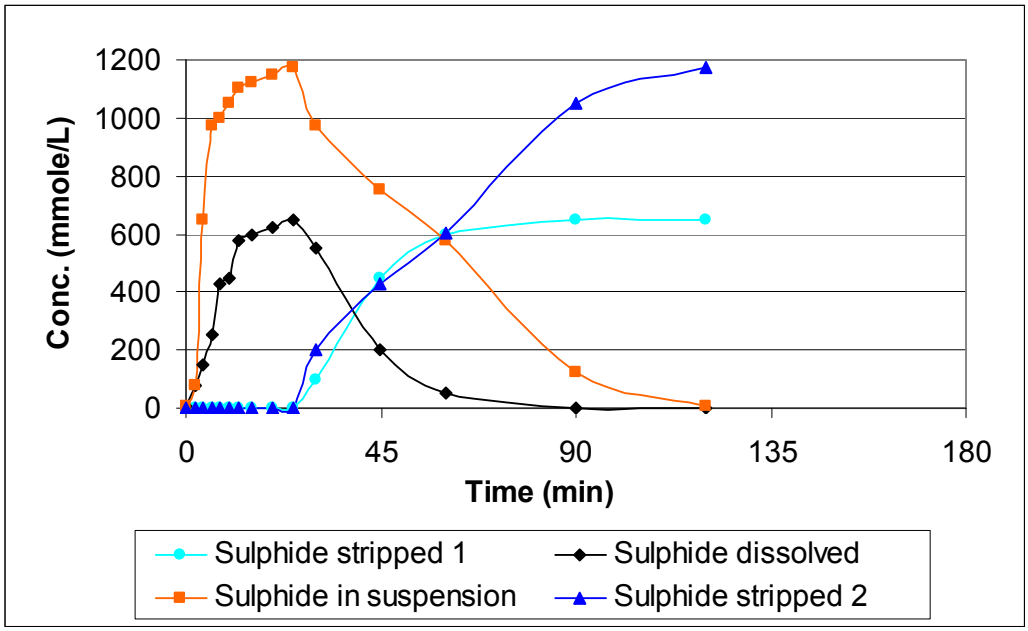

Figure 6.19 Analysis of the dissolved and suspended sulphide

6.4 SULPHIDE STRIPPING USING A PRESSURISED UNIT

Table 6.5 and Figures 6.20-6.23 illustrate the effect of various parameters (CO_2 flow-rate, temperature, pressure and hydrodynamics) on the rate of sulphide stripped, during the stripping of sulphide (as CaS) with CO_2. The experiments were carried out in a pressurised unit.

Table 6.5 Experimental conditions for the data reported in Figures 6.20-6.23

Parameters	Pressure (kPa)	Temp (°C)	Flow (ℓ/min)	Stirring Rate (r/min)
CO_2 flow	100	25	**2.22 (40%)**	1 000
	100	25	**3.34 (60%)**	1 000
Pressure	**100**	25	3.34	1 000
	200	25	3.34	1 000
Temperature	100	**25**	3.34	1 000
	100	**60**	3.34	1 000
Mixing intensity (r/min)	100	25	2.22	**500**
	100	25	2.22	**1 000**

The effect of the various parameters is discussed below.

Flow rate. The rate of sulphide stripped increased with increasing CO_2 flow-rates (Figure 6.20). The results showed that at high flow-rate (3.34 ℓ/min), more CO_2 gas entered the reactor to react with the CaS and as a result more sulphide (295 mmol) was being stripped. At low flow-rate (2.24 ℓ/min), it can be assumed that there was a sub-stoichiometric concentration of CO_2, and hence the amount of sulphide stripped was less (235 mmol).

Temperature. The rate of sulphide stripped increased with increased temperature (Figure 6.21). At 60 °C, 449 mmol/ℓ sulphide was stripped and at 25 °C only 297 mmol/ℓ. The results indicated that at higher temperature, more CaS was converted to $Ca(SH)_2$ and hence more sulphide was stripped off with CO_2. At lower temperature less CaS was converted and less sulphide was stripped.

Stirring rate. The rate of sulphide stripping increased with increased stirring rate (Fig. 6.22). When the stirring rate was 500 rpm, the amount of sulphide stripped was 245 mmol/ℓ. Stirring the CaS slurry at 1 000 rpm, the sulphide stripped increased to 565 mmol/ℓ. A function of the reactor design was such that when the stirring rate was increased it allowed for more of the gas in the headspace above the liquid to be sucked into a stirring vortex formed around the mixer shaft and contacted with the liquid. Through an increased stirring rate, there is improved mixing/contacting between the stripping gas (CO_2) and the dissolved sulphide as $Ca(HS)_2$, resulting in a faster rate of reaction.

Pressure. The rate of sulphide stripping increased with a decrease in pressure (Figure 6.23). When the pressure of CO_2 was 100 kPa, the sulphide stripped was 297 mmol/ℓ. However, when the pressure was increased to 200 kPa, the sulphide stripped decreased to 167 mmol/ℓ. This finding was attributed to the solubilities of CO_2 and H_2S that increased with increased pressure thereby decreasing the amount of CO_2 available for stripping the sulphide.

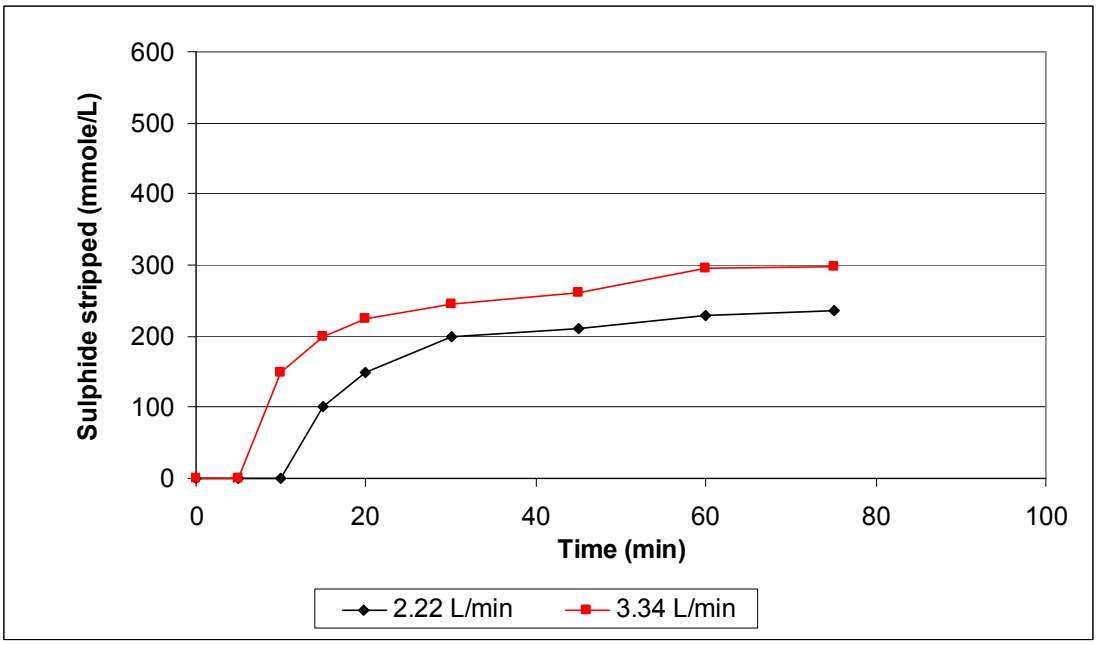

Figure 6.20 Effect of CO_2 flow rate on the sulphide stripping

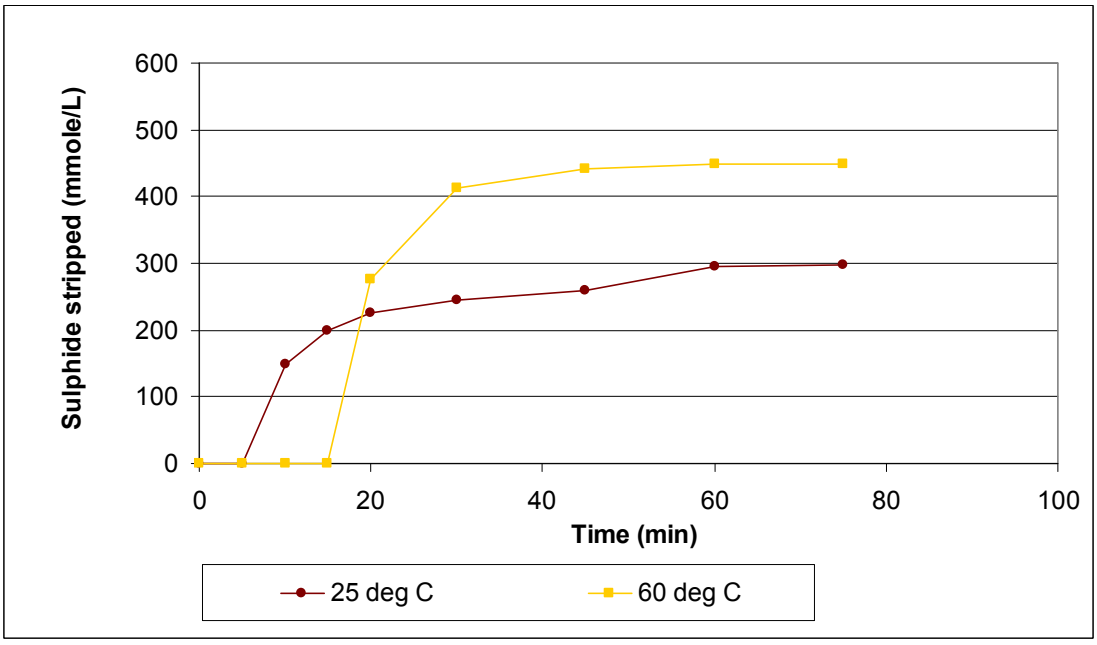

Figure 6.21 Effect of temperature on the sulphide stripping

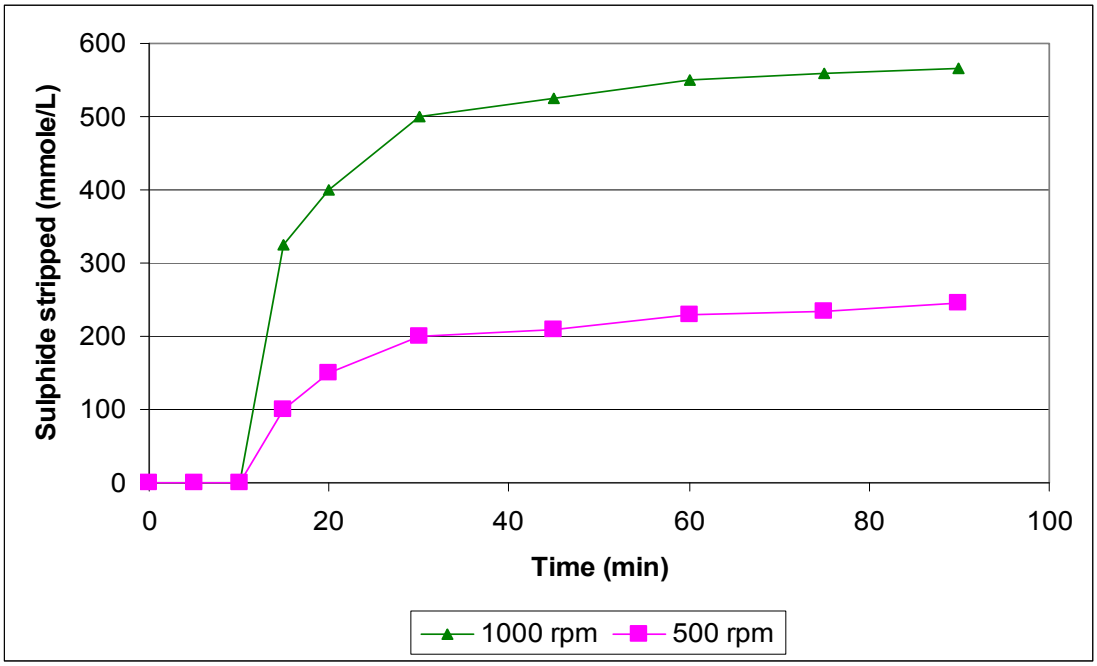

Figure 6.22 Effect of hydrodynamics on the sulphide stripping

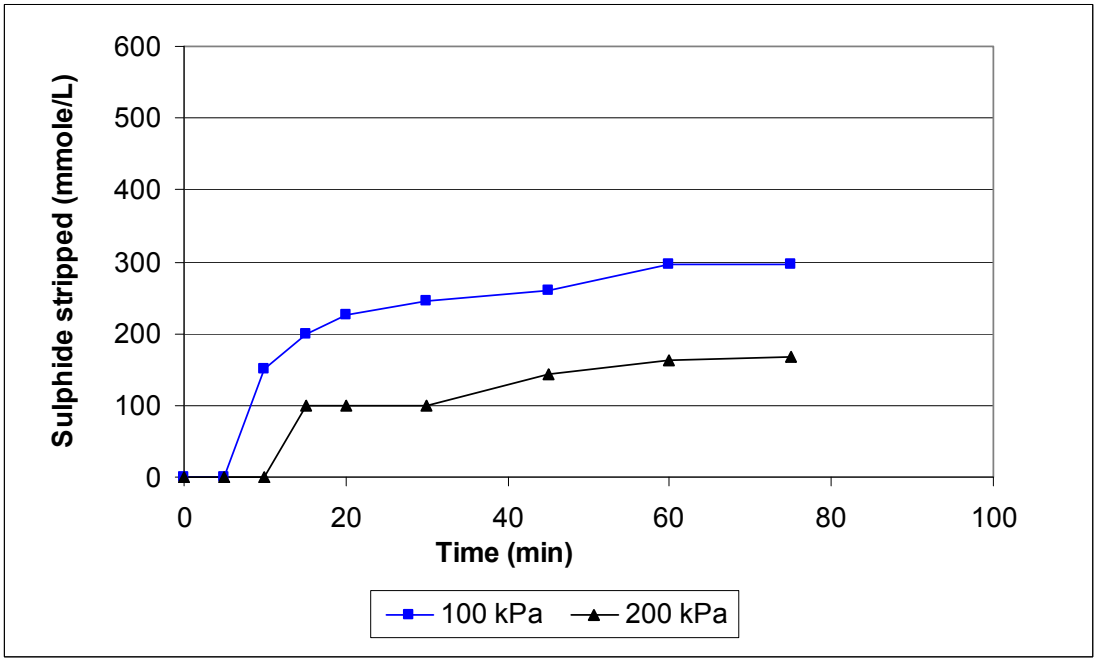

Figure 6.23 Effect of pressure on the sulphide stripping

6.5 H_2S GAS ABSORPTION AND SULPHUR FORMATION

This study was done to obtain an effective method for H_2S gas absorption and sulphur recovery. The two methods tested were the iron (III) process and the PIPco process.

6.5.1 Iron (III) process

This method involves the absorption of H_2S gas into an iron (III) solution (reaction 102). Figure 6.24 shows the time dependent behaviour of sulphide stripped load, pH, sulphur formed load and the CO_2 dosed load during the iron (III)-process.

$$H_2S\ (g) + 2Fe^{3+}\ (aq) \rightarrow S\ (s) + 2Fe^{2+}\ (aq) + 2H^{+}\ (aq) \qquad (102)$$

Similar conclusions were drawn from the behaviour of pH and sulphide as indicated in Section 6.3. For example, the pH decreases when sulphide is stripped with CO_2 and CaS dissolves as $Ca(HS)_2$ (aq). The sulphur curve showed that at 20 min reaction time, 113 mmol/ℓ of sulphide was stripped with CO_2 gas but only 8 mmol/ℓ of sulphur was formed in the iron (III) solution. This difference between the sulphide and sulphur formed can be explained in terms of a proposed, intermediate FeS complex that forms in the presence of iron (III) and H_2S gas. During the initial period (45-90 min) the sulphide stripped increased from 129 mmol/ℓ to 133 mmol/ℓ but the sulphur amount only increased from 36 mmol/ℓ to 51 mmol/ℓ. From the XRF results, it was found that 51% of the stripped H_2S was converted to elemental sulphur. The sulphur obtained from this study was brown. The investigation was stopped because more steps are required to purify the product.

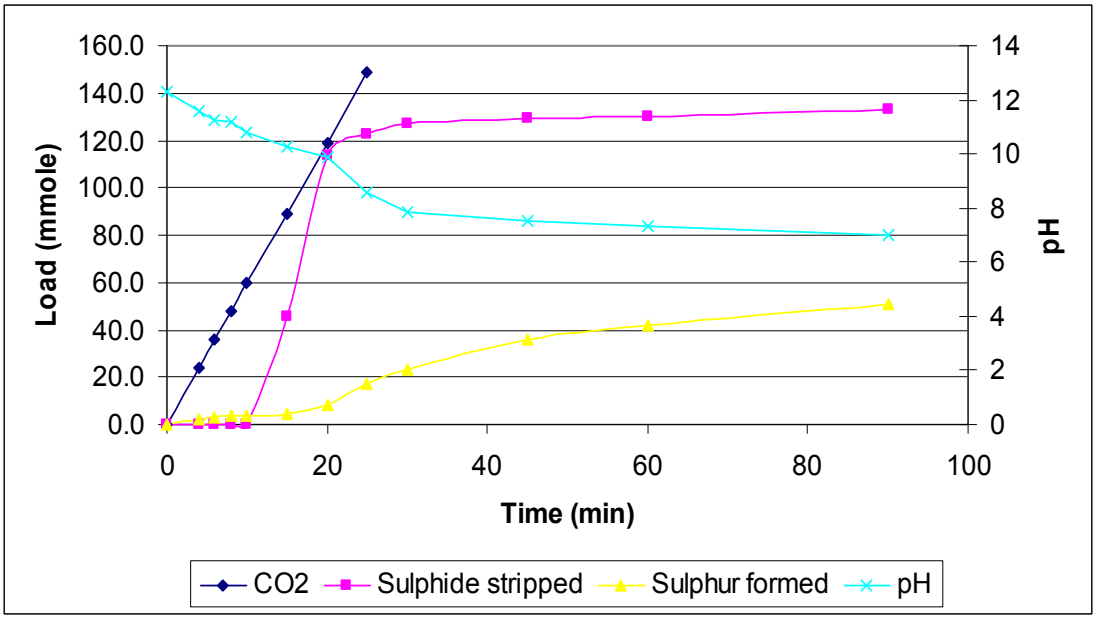

Figure 6.24 Behaviour of sulphide stripped, pH, sulphur formed and the CO_2 dosed during the iron (III)-process.

6.5.2 PIPco Process

In the PIPco process, H_2S gas is converted to sulphur, by reacting it with SO_2 gas in solution (reaction 103).

$$2H_2S\ (g) + SO_2\ (g) \rightarrow 3S\ (s) + 2H_2O\ (aq) \qquad (103)$$

The experiments reported in this section were carried out to establish optimum pH values and solubilities.

6.5.2.1 Effect of pH and concentration of potassium citrate on the absorption of SO_2 gas

Figures 6.25-6.27 depict the results obtained when the influence of pH, on different potassium citrate solutions for SO_2 gas absorption, was studied. The concentration of the citrate solutions was varied from 0.5 M to 1 M to 2 M, temperature was 25 °C and the gas flow-rate was 300 mℓ /min.

The results showed that for the different concentrations of potassium citrate (2 M, 1 M and 0.5 M) the pH decreases due to the absorption of acidic SO_2 gas which is acidic. However, it was further noted that in the beginning of the process, when the pH was still above 3, the rate of absorption was high and as the pH dropped, the absorption rate also decreased. This showed that the absorption of SO_2 if favoured by a pH higher than 3. At very low pH values the gas will remain in the gaseous form and no absorption will occur in the citrate solution.

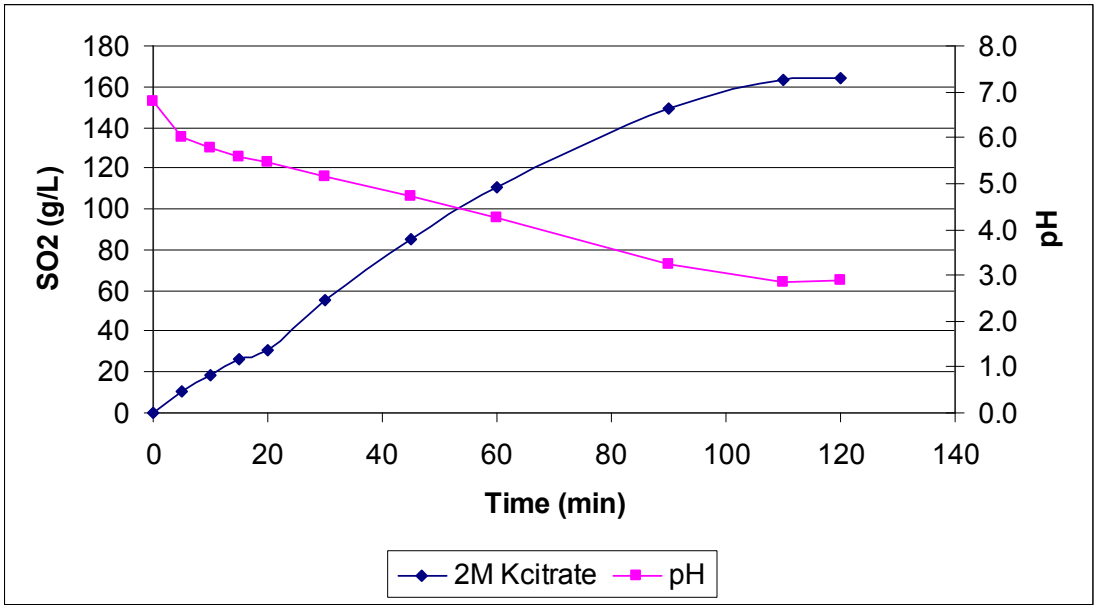

Figure 6.25 Effect of pH and 2 M of potassium citrate on the absorption of SO_2 gas

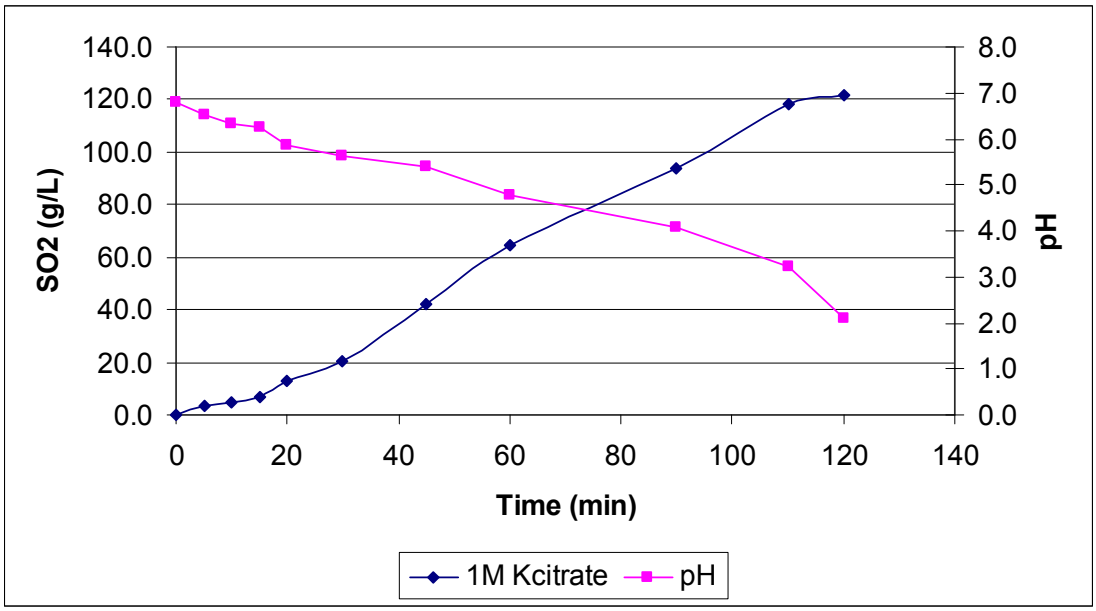

Figure 6.26 Effect of pH and 1M of potassium citrate on the absorption of SO_2 gas

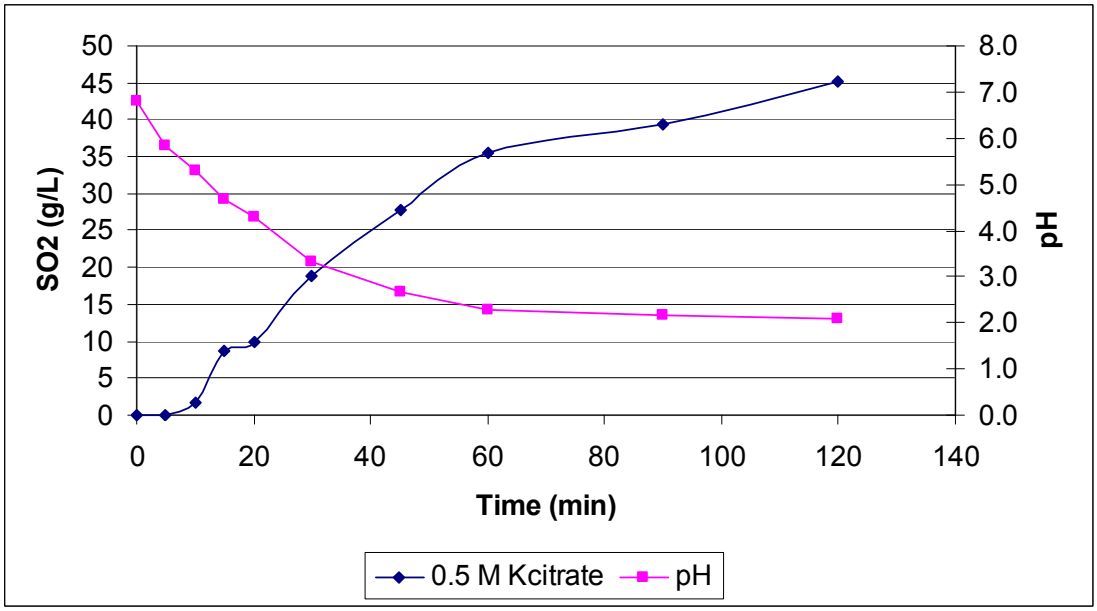

Figure 6.27 Effect of pH and 0.5M of potassium citrate on the absorption of SO_2 gas

The results depicted in Figures 6.25-6.27 further showed that with 2.0 M potassium citrate solution, the absorption of SO_2 gas was 164 g/ℓ after 120 min. However, when the potassium citrate concentration was low at 1.0 M and 0.5 M, the absorption decreased to 121 g/ℓ and 45 g/ℓ, respectively.

These findings showed that the absorption capacity is higher for solutions of higher citrate buffer concentration because of correspondingly larger buffer capacities. Therefore as more buffer capacity is available, more hydrogen ions formed in reaction 105 can bind to the citrate ions and be 'removed' by the buffer. The finding corresponded well with published capacity of 120-170 g/ℓ of SO_2 for 2 M potassium citrate solution (Gryka, 1992).

SO_2 (g) + H_2O (aq) → HSO_3^- (aq) + H^+(aq) (104)

Cit^{3-} (aq) + H^+ (aq) → $HCit^{2-}$ (aq) (105)

$HCit^{2-}$ (aq) + H^+ (aq) → H_2Cit^- (106)

6.5.2.2 Effect of temperature on the absorption of SO_2 in citrate buffer

Figure 6.28 shows the influence of temperature on the absorption of SO_2 in a 2 M potassium citrate solution at pH 6.8.

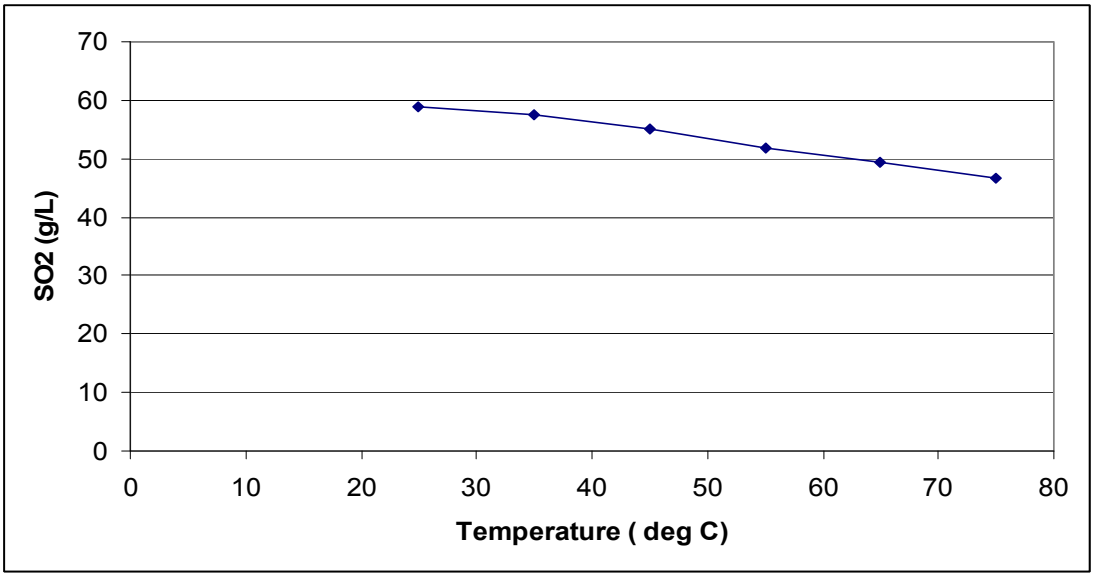

Figure 6.28 Effect of temperature on SO_2 absorption into a potassium citrate solution

The results showed that when the temperature of the potassium citrate solution was 25 °C, the SO_2 absorbed was 59 g/ℓ. When the temperature was increased from 35 °C to 75 °C, the SO_2 absorption decreased from 58 g/ℓ to

47 g/ℓ. These results showed that the solubility of SO_2 decreases with increasing temperatures. Gryka (1992) showed that the absorption of SO_2 into a potassium citrate solution should take place at a temperature as low as possible.

6.5.2.3 Solubility of H_2S in Potassium Citrate buffer solution

Figure 6.29 shows the relationship between H_2S loaded and H_2S absorbed in a 2 M potassium citrate buffer solution at ambient temperature and atmospheric pressure. Even though 800mmol/l of H_2S was fed to the system only 24 mmole/ℓ (752 mg sulphide/ℓ) was absorbed in the first citric acid solution and 17 mmole/ℓ (544 mg sulphide/ℓ) in the second. Therefore, at atmospheric pressure and ambient temperature, the solubility of H_2S in potassium citrate buffer solution is very low, only between 2% to 3%.

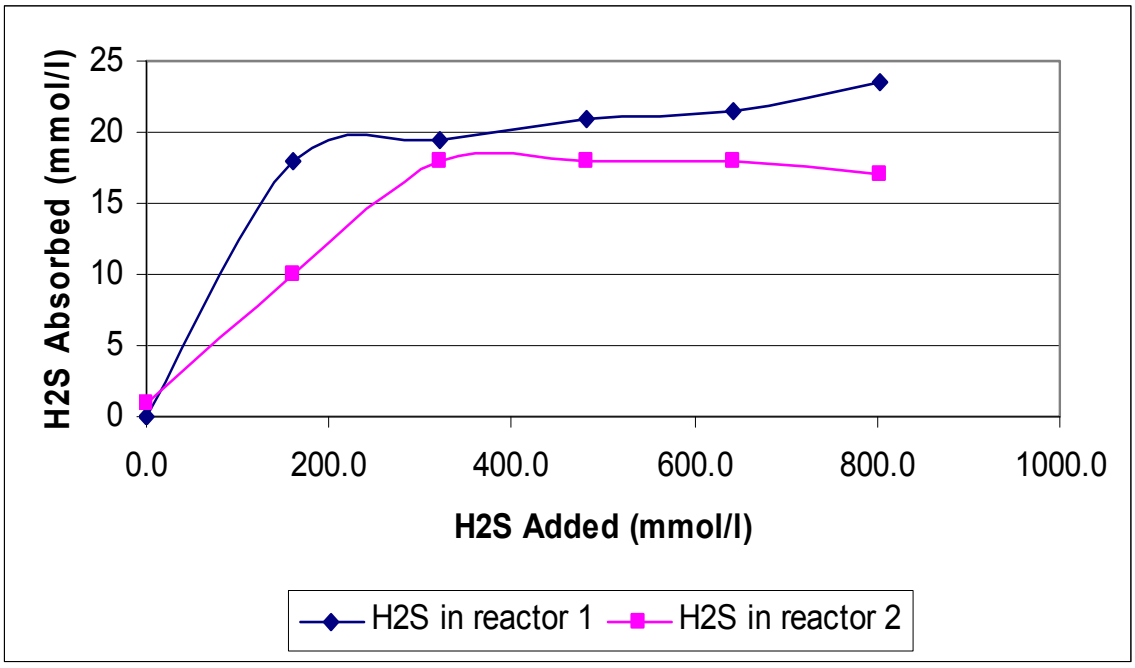

Figure 6.29 Solubility of H_2S gas in potassium citrate buffer solution

6.5.2.4 Sulphur production via the PIPco process

The purpose of this section is to determine the effect of CO_2 flow rate on the formation of intermediate compounds during sulphur production via the PIPco process.

Figures 6.30-6.33 and Tables 6.6 and 6.7 show the results, as well as the experimental conditions, when sulphide was stripped with CO_2 from a CaS slurry, followed by absorption of the stripped H_2S gas in a SO_2-rich potassium citrate solution for sulphur formation. The effect of CO_2 flow rate was investigated by experiments at 520 mℓ/min and at 1112 mℓ/min.

Figure 6.30 shows the relationship between the concentrations of the various species versus time when CO_2 was passed through at a flow-rate of 520 mℓ/min. The initial CaS concentration in the slurry was 2 167 mmol/ℓ and the pH was 12.2. The sulphide level in solution was 3.0 mmol/ℓ before the addition of CO_2.

During CO_2 addition the pH dropped from 12.2 to 8.2. The sulphide concentration in the slurry reactor dissolved until it reached a maximum concentration of 1 375 mmol/ℓ due to the formation of $Ca(HS)_2$. With further CO_2 addition, the pH dropped further to 6.9 and sulphide was stripped completely. The stripped H_2S reacted with the SO_3^2 in citrate reactors. The SO_3^{2-}concentration in Reactor 1 dropped sharply, while in Reactor 2 it dropped slowly. The rapid drop in Reactor 1 was ascribed to the formation of sulphur and possibly to some of the SO_2 being stripped with CO_2. The slow drop in the SO_3^{2-}-concentration in Reactor 2 was ascribed to SO_2-stripping with CO_2.

From Figure 6.31, which shows the relationship between load (accumulated amount) removed or formed of the various parameters as a function of time, it was noted that:

- 2 167 mmol CaS was initially slurried.
- 1 375 mmol of the $Ca(HS)_2$ formed was in solution and the balance was present as a solid as the solubility of $Ca(HS)_2$ was exceeded (Section 6.3.2).

- 2 180 mmol SO_3^{2-} was removed, which is more than the concentration of CaS that was slurried. This showed that a portion of the SO_2 was stripped with CO_2. This observation explains why the PIPco process needs to be operated under excess H_2S-conditions.

The experiment described above for 520 mℓ/min CO_2 was repeated for a CO_2 flow rate of 1 112 mℓ/min (Figures 6.32 and 6.33 and Table 6.7). Similar conclusions were drawn except for the behaviour of SO_3^{2-} in the SO_2/citrate reactor. The following similar observations were made:

- 2 167 mmol CaS was initially slurried.
- 1 300 mmol dissolved in solution as $Ca(HS)_2$, and the balance was in solid form as $Ca(HS)_2$.
- 2 310 mmol SO_3^{2-} was removed which is more than expected from the amount of CaS that was slurried. This shows that a portion of the SO_2 was stripped with CO_2.

The following differences were observed between the two CO_2 flow-rates studies: The increase in SO_3^{2-}-concentration during the initial period (Figure 6.32) was ascribed to the formation of an intermediate compound when H_2S was reacted with the SO_2/citrate solution. This compound is oxidised to sulphate from a much lower valence (valence of S species) when reacted with iodine, compared to SO_3^{2-}, which has a valence of +4. The intermediate could be $S_3O_4^{2-}$, with a valence of +2. Reaction 107 shows the reaction of $S_3O_4^{2-}$ with iodine. This was determined by way of elimination of the reactions with iodine of the various sulphur species.

- $S_2O_3^{2-}$ is oxidised to $S_4O_6^{2-}$ (reaction 79) and the latter will not be further oxidised with iodine
- SO_3^{2-} is oxidised to SO_4^{2-} (reaction 78)
- Thus, $S_3O_4^{2-}$ is the only remaining sulphur species and can only be oxidized to SO_4^{2-}. I

$$S_3O_4^{2-}(aq) + 6I_2(aq) + 8H_2O(aq) \rightarrow 3SO_4^{2-}(aq) + 12I_2(aq) + 16H^+(aq) \quad (107)$$

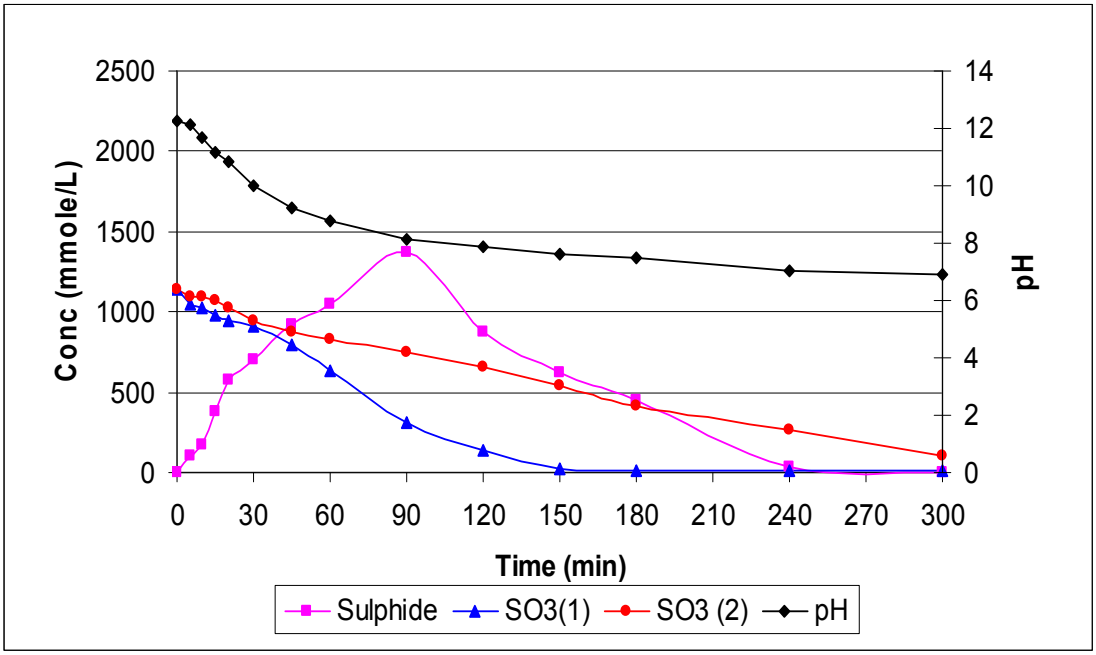

Figure 6.30 Sulphide stripping with CO_2 gas at a flow rate of 520 mℓ/min (concentrations versus time).

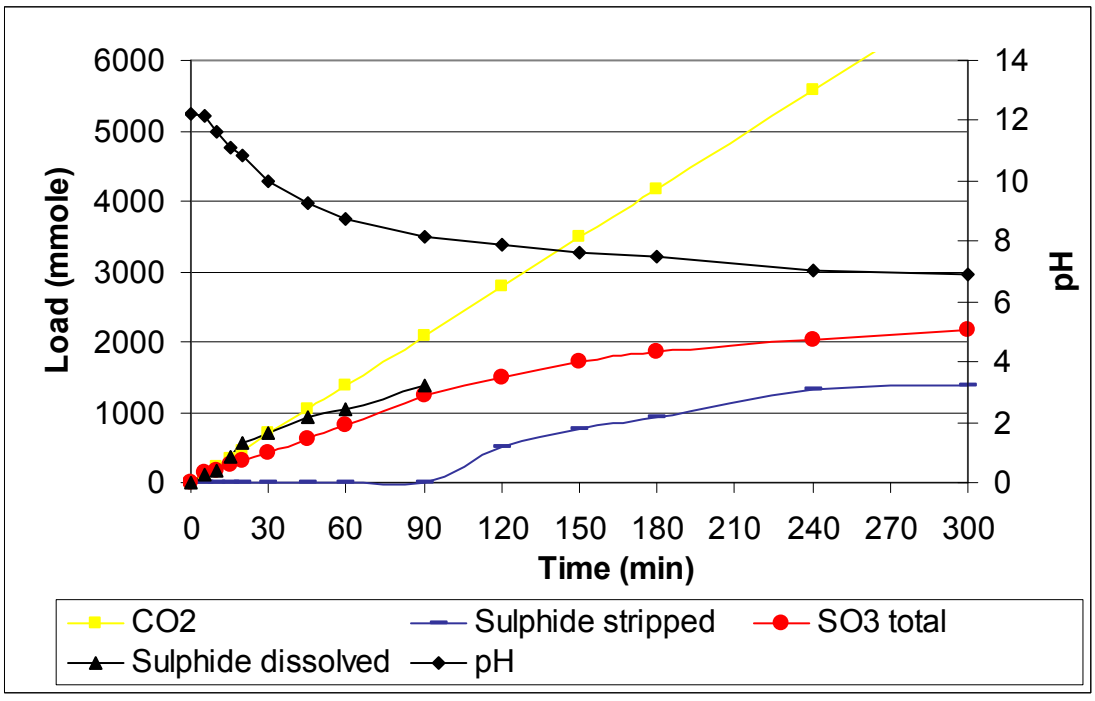

Figure 6.31 Sulphide stripping with CO_2 gas at a flow rate of 520 mℓ/min (load versus time).

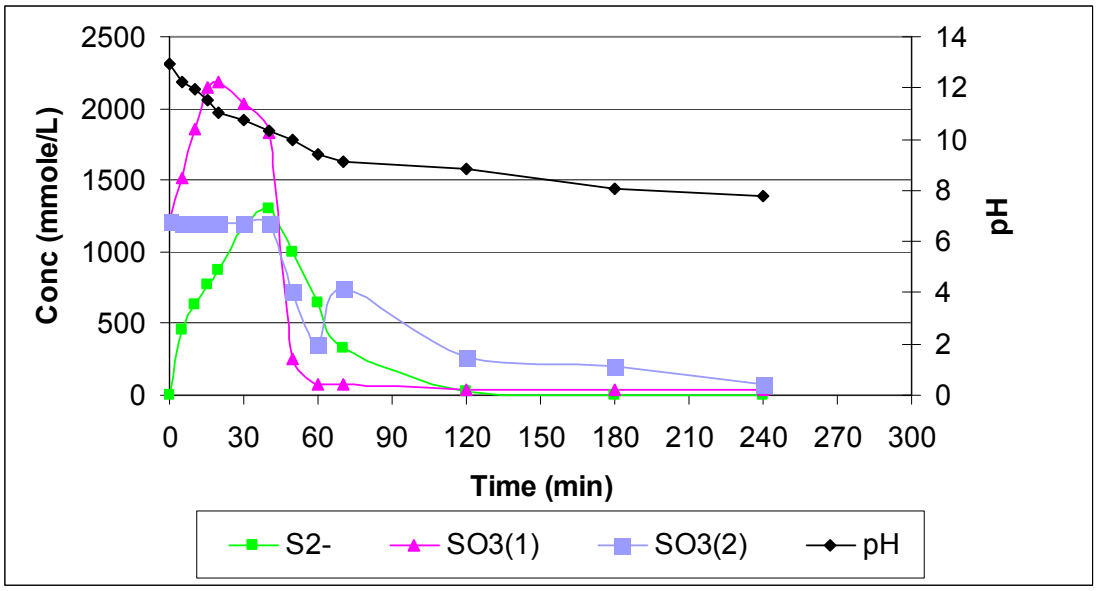

Figure 6.32 Sulphide stripping with CO_2 gas at a flow rate of 1112 mℓ/min (concentrations versus time).

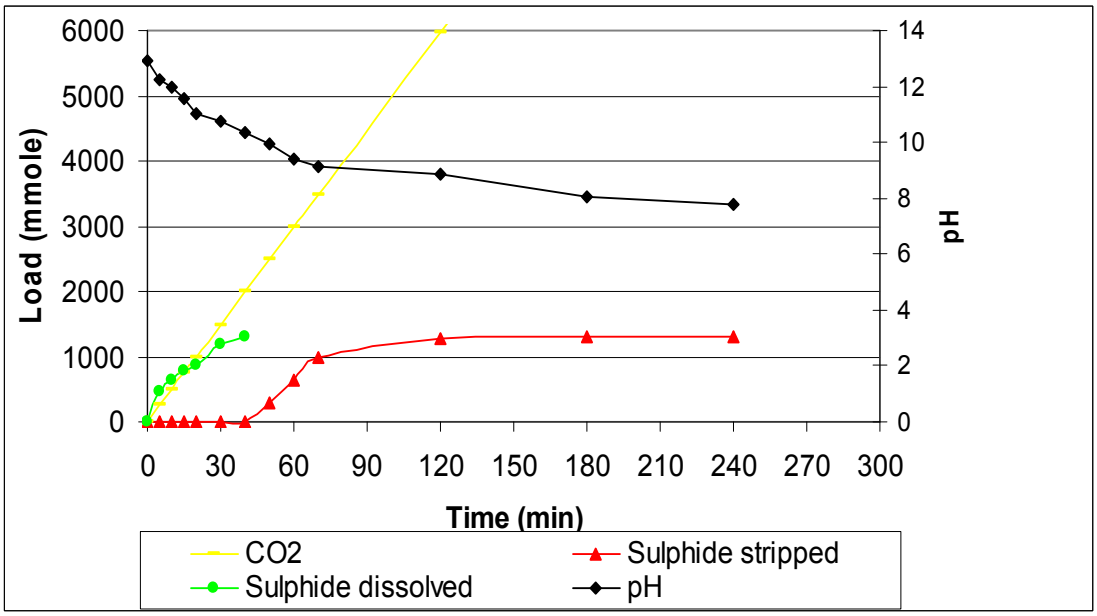

Figure 6.33 Sulphide stripping with CO_2 gas at a flow rate of 1112 mℓ/min (load versus time).

Table 6.6 Sulphide stripping with CO_2 gas at a flow rate of 520 mℓ/min

Parameter	CaS reactor		SO_2/Citrate 1		SO_2/Citrate 2	
Time (min)	0	300	0	300	0	300
Citric acid (g/ℓ)			768		768	
KOH (g/ℓ)			673		673	
CO_2 (mL/min)	520					
CaS (mmole/ℓ)	2167					
Sulphide (mmole/ℓ)	2167	64				
SO_3^{2-} (mmole/ℓ)			1145	10	1145	100
pH	12.2	6.9				

Table 6.7 Sulphide stripping with CO_2 gas at a flow rate of 1112 mℓ/min

Parameter	CaS reactor		SO_2/Citrate 1		SO_2/Citrrate 2	
Time (min)	0	240	0	240	0	240
Citric acid (g/ℓ)			768		768	
KOH (g/ℓ)			673		673	
CO_2 (mℓ/min)	1112					
CaS (mmole/ℓ)	2167					
Sulphide (mmole/ℓ)	2167	16				
SO_3^{2-} (mmole/ℓ)			1215	40	1215	80
pH	12.9	7.8				

6.5.2.5 Purity of sulphur recovered

The LECO Combustion Techniques used to assay the purity of sulphur showed that sulphur with purity between 96 and 99% was recovered.

To identify the other elements formed during the recovery of sulphur, XRF analyses were conducted on the sulphur samples. The results are indicated in Table 6.8.

Table 6.8 Results of XRF analysis of recovered sulphur

Elements	Conc. Impurities
K	820 ppm
Fe	91 ppm
Ca	184 ppm
Mg	170 ppm
Si	20 ppm
Co	40 ppm
Cr	60 ppm
Ni	56 ppm

6.5.2.6 Economic feasibility

The recovery of sulphur and $CaCO_3$ from gypsum based on laboratory and pilot studies (pilot results not included in this study), seems to be economically feasible. From 1 ton of gypsum it was calculated that 0.18 ton of sulphur (Value = R180) and 0.58 t of $CaCO_3$ (Value = R145) can be recovered. The prices of sulphur and $CaCO_3$ were taken at R500/t and R250/t, respectively. This compares favourable with the cost of the main raw material, coal. At a coal to gypsum ratio of 0.3, and a coal cost of R400/t, the cost of the coal amounts to R120/t of gypsum. This is significantly less than the combined value of R296 of sulphur and $CaCO_3$. This value would be even higher if chemically pure $CaCO_3$ is recovered. The price of chemically pure $CaCO_3$ amounts to R3 000/t compared to the R250/t for waste or mined $CaCO_3$.

CHAPTER 7

CONCLUSIONS

7.1 THERMAL STUDIES

The thermal conversion of gypsum to CaS in a tube furnace and nitrogen atmosphere takes place between 900 °C-1 100 °C:

$$CaSO_4\ (s) + 2C\ (s) \rightarrow CaS\ (s) + 2CO_2\ (g) \qquad (108)$$

96% conversion gypsum to CaS was obtained when a reducing agent, carbon, was used. Controlling the amount of carbon added, relative to the amount of gypsum, higher reduction yields were achieved when the molar ratio of gypsum to carbon was 1:2 and 1:3. 380 µm particle size of gypsum yielded 80% reduction percentages due to the higher reactant surface areas for smaller particles.

The reaction time between gypsum and carbon was also found to be shorter. The optimum time found was 20 min. The impurities present in Anglo and Foskor gypsum seemed to lower the CaS yields as compared to pure gypsum. Regardless of the grade of Duff coal, which is low, 81% CaS yields were obtained when Duff coal was used as a reducing agent. Due to the high cost of activated carbon, Duff coal was recommended for use on a full-scale plant.

Depending on the presence of oxygen in the muffle furnace, the CaS obtained after heating the gypsum at 1 100 °C was contaminated by oxygen-containing compounds. The tube furnace which had been purged with nitrogen yielded none of these contaminants. The thermal decomposition of gypsum to CaS should therefore be carried out in an oxygen-deficient environment.

Thermogravimetric results showed that the loss of water of crystallisation from pure gypsum ($CaSO_4.2H_2O$) takes place in the temperature range 80 °C-180 °C. The small mass loss occurring between 650 °C-800 °C was attributed to the oxidation of carbon. The mass loss between 900 °C-1 050 °C confirmed the formation of CaS.

Kinetic analysis showed that complex reactions occurred between activated carbon/carbon monoxide and the three gypsum types (pure, Anglo and Foskor gypsum). This conclusion was made from the fact that the activation energies changed for different degrees of conversion. The increasing dependencies of activation energy on the degree of conversion were evidence for a complex reaction involving parallel reactions. The increase in activation energy at the initial stage (α < 0.2) of transformation shows parallel competing reactions.

Between the conversion degree of 0.2-0.75, a relative constant dependency of the activation energy on the degree of conversion showed that there is no change in the rate limiting step. This observation was claimed on different influence of diffusion of gaseous products. The presence of impurities in the Foskor and Anglo gypsums caused interferences owing to side reactions.

Solid–solid reactions are slow as compared to solid–gas reactions as evidenced by their higher activation energies. It was concluded that the reaction between activated carbon and gypsum could occur via the reaction product CO and CO_2 depending on the temperature. Below 700 °C, CO_2 is the dominant product while above 700 °C, CO is dominant.

The thermogravimetric data obtained during isothermal studies confirmed that the reaction between activated carbon and pure gypsum is complex because the data failed to give straight line graphs when fitted to different kinetic equations.

7.2 SOLUBILITY OF CaS

The solubility of CaS increased from 270 to 390 mg/ℓ with time 90 to 60 min, through stirring. Increasing the temperature from 30 °C-90 °C also increased the solubility of CaS from 130 mg/ℓ to 915 mg/ℓ. The high pH (pH>11) of a CaS slurry is due to the formation of $(CaOH)^{+}_{(aq)}$ which is very basic. At this high pH, sulphide is present as $HS^{-}_{(aq)}$.

7.3 REACTION MECHANISM FOR SULPHIDE STRIPPING

During the stripping of sulphide (as CaS) with CO_2 gas at 25 °C and atmospheric pressure, CaS reacts first to form an intermediate, $Ca(HS)_2$, before the sulphide is stripped off. Due to the low solubility of CaS, not all the sulphide dissolves as $Ca(HS)_{2(aq)}$ during the stripping process, a certain amount stays undissolved as $Ca(HS)_{2(s)}$. As more CO_2 is added, the sulphide which is in the form of $Ca(HS)_2$ is stripped off as H_2S gas:

$$2CaS\ (s) + CO_2\ (g) + H_2O\ (aq) \rightarrow CaCO_3\ (s) + Ca(HS)_2\ (aq,s) \qquad (109)$$

$$Ca(HS)_2\ (aq,s) + CO_2\ (g) + H_2O\ (aq) \rightarrow CaCO_3\ (s) + 2H_2S\ (g) \qquad (110)$$

The pH of the sulphide solution drops from pH 11 to 7 due to the formation of $CaCO_3$.

7.4 SULPHIDE STRIPPING USING A PRESSURISED UNIT

The rate of sulphide stripping can be increased by controlling the following parameters:

1) Flow rate

A high flow rate (3.34 ℓ/min) of CO_2 gas increased the rate of sulphide stripped to 295 mmol/ℓ compared to 235 mmol/ℓ for 2.24 ℓ/min.

2) Temperature

The increase in temperature from 25 °C to 60 °C resulted in an increase in the rate of sulphide stripping from 297 mmol/ℓ to 449 mmol/ℓ, respectively. This indicated that the solubility of CaS increases with temperature.

3) Stirring rate

The rate of sulphide stripped increased from 245 mmol/ℓ to 565 mmol/ℓ, when the stirring rate was 500 rpm and 1000 rpm, respectively. It was concluded that at a faster stirring rate, the contact between the CO_2 gas and sulphide species improves.

4) Pressure

The rate of the sulphide stripping increased with a decrease in pressure. At 100 kPa, the sulphide stripped was 297 mmol/ℓ and at 200 kPa, only 167 mmol/ℓ was stripped. The results showed that the solubility of CO_2 gas and H_2S gas increased at an increased pressure.

7.5 SULPHUR FORMATION

The two processes iron (III) and PIPco were investigated for sulphur recovery. The iron (III) method involves the absorption of H_2S gas into a iron (III) solution while in the PIPco, H_2S gas is absorbed into a potassium citrate solution rich in SO_2 gas for sulphur formation.

It was concluded that the iron (III) process yields poor quality sulphur. The sulphur recovered was brown in colour due to the presence of iron (III) and contained FeS. The purity of the sulphur was 51 %. No further work was done following this finding.

From the PIPco process, pure yellow sulphur with a purity between 96%-99% was recovered.

The following parameters are of importance in the PIPco process:

- ***pH***

The pH of the potassium citrate must be higher than 3 for better SO_2 absorption. At very low pH, the potassium citrate cannot absorb SO_2.

- ***Concentration of potassium citrate.***

The 2 M concentration of potassium citrate absorbs 164 g/ℓ of SO_2 gas within a period of 120 minutes while 1 M and 0.5 M absorbs 125 g/ℓ and 45 g/ℓ, respectively. It was concluded that the absorption capacity is higher for solutions of higher buffer concentration. The overall results showed that potassium citrate is a good absorbent for SO_2 gas.

- ***Temperature***

The results, as obtained from this study showed that optimum temperature for the absorption of SO_2 gas into the potassium citrate was 25 °C. At this temperature, 59 g/ℓ SO_2 was absorbed.

Increasing the temperature of the potassium citrate from 35 °C to 75 °C resulted in a decrease in the SO_2 gas absorption (from 58 g/ℓ to 47 g/ℓ, respectively).

It was further shown that the solubility of H_2S gas in the potassium citrate solution is very low, between 2%-3%. Therefore, during sulphur production, the H_2S gas will react with the SO_2 gas to form sulphur.

7.6 RECOMMENDATIONS

The aim of this project was to investigate, understand and optimize various stages of the sulphur recovery process on laboratory scale to the stage prior to full-scale implementation. The following recommendations are proposed for full-scale implementation:

- A rotating kiln must be used to heat gypsum to prevent lump formation.
- Gypsum must be dried to prevent lumps forming.
- Duff coal can be used as a reducing agent as well as a source of heat for the kiln because is readily available and cheap.
- To reduce the operation cost, propane can be used to pre-heat the kiln as opposed to electrical power.
- CaS from the kiln needs to be cooled before slurried to avoid boiling.
- To increase the rate of solubilisation of CaS during the stripping of sulphide, the CaS slurry should be stirred and heated at a temperature between 60 °C-90 °C
- The citrate solution must be buffered with KOH to control the pH at the optimum level for the following competing reactions:
    - Absorption of acid gasses, H_2S and SO_2, is favoured at higher pH values. At low pH values the gasses will remain in the gas form and no absorption will occur in the citric acid.
    - Sulphur formation which favour low pH occurs according to the reaction:

$$2HS^- + S_2O_3^{2-} + 4H^+ \rightarrow 4S + 3H_2O \qquad (111)$$

- Potassium citrate may be used for SO_2 absorption during sulphur production because it is a good absorbent for SO_2 gas

- The process temperature is controlled at 125 °C and the pressure at 3 bar to retain sulphur in liquid form and to prevent the water from evaporating.

7.7 PROPOSED PROCESS DESCRIPTION

The process description below is a proposed design to recover sulphur from the waste gypsum resulting from the treatment of acid mine drainage in the Key Plan water treatment plant to recover potable water for the Witbank Local Council.

1) Kiln

The main purpose of the kiln is to reduce the gypsum ($CaSO_4.2H_2O$) to CaS. The first step in the process is to dry the wet gypsum from about 25% moisture to about 10% and to blend it with Duff coal at a ratio of 26% (coal to dried gypsum). The coal acts both as a source of heat as well as a reductant in the kiln. The blended gypsum and coal mixture is stored in a “day” bin from where it is discharged into the kiln by a calibrated screw feeder. The kiln is pre-heated with propane to a temperature of 1100 °C. Combustion air is controlled to yield an off-gas CO concentration of 1.5 to 2%.

Gas analyses are carried out at regular intervals with the aid of a Testo analyzer (O_2 and CO). Hot gases from the kiln are cooled in a trombone radiation cooler to below 200 °C and filtered in the bagfilter. From the bagfilter approximately 1/3 of the gas is blown by the ID fan to the stack. Approximately 2/3 of the offgas is further cooled to about 35 °C and compressed to 5 Bar into a 2 m^3 pressure vessel.

CaS exits from the kiln at about 900 ^oC and is cooled by a water-cooled screw to below 90 °C. It is captured in a steel flask on a scale. Sampling of the kiln

feed is by grab samples from the belt every hour. Material captured in the radiation cooler and bagfilter is weighed and sampled (depending on the quantity and quality it could be discharged with the other CaS into the slaker). While one CaS flask fills the other one is cooled and discharged into the hopper feeding the slaking vessel.

2) Slaking or Slurring, Sulphide Stripping and Sulphur production

Slaking takes place when the cooled CaS is slurried with water. During slaking small quantities of sulphide (as $HS^-_{(aq)}$) are generated and therefore the slaking vessel is vented to the scrubbing circuit. Slaking takes place continuously by controlling the feedrate of CaS and water to the slaking vessel. CaS feed rate is set by adjusting the manual variable speed of the screw feeder from the hopper into the slaking vessel. As the slaking reaction is virtually instantaneous, the slaking vessel can be considered a CSTR (Continuous Stirred Tank Reactor).

After slaking, the next step is stripping of sulphide from the CaS. This is achieved by pumping the slurry into a jacketed reactor at 4 bar pressure and bubbling through.CO_2 from the kiln. The slurry is heated to 60 °C and H_2S is stripped off. The stripping reaction is controlled by controlling the pH in the stripping vessel through the feedrate of CO_2 to the vessel. Two stripping vessels are used and they are arranged such that the feed of CO_2 can be done in parallel or counter-currently. The process is followed by assaying the slurry from the second vessel. H_2S from the stripping vessel is compressed by a blower and fed to the PIPco reactor where conversion to sulphur takes place.

The unique feature of the PIPco process is that the reaction takes place in a buffered citric acid solution (pH 4-6) at 125 °C and 3-4 bar pressure. These conditions are chosen because sulphur is a liquid at that temperature and the higher pressure reduces evaporation of water.

Approximately 1/3 of the sulphur formed in the PIPco reactor is combusted with excess air at 1000 °C to SO_2. The SO_2 gas is cooled to below 50 °C in a

water/gas cooler. The cooled SO_2 is absorbed into citric acid to about 120 g/ℓ SO_2 in an absorption column. Vent gases from the absorption column are scrubbed in a milk of lime scrubber to absorb any residual SO_2 gas. The rich citrate solution is mixed with the H_2S gas and heated to 125 °C and then pumped at 3-4 bar pressure into the PIPco reactor. In the PIPco reactor the Claus reaction takes place which converts hydrogen sulphide and sulphur dioxide into elemental sulphur and water.

Liquid sulphur is periodically tapped off from the bottom of the reactor and granulated in water. It is scraped from the granulation tank and air dried and weighed. Vent gases leave the top of the reactor and lean citrate solution is cooled to below 50 °C and loaded again with SO_2 to repeat the process. The vent gases are scrubbed in a small milk of lime scrubber to capture any H_2S and SO_2 present as insoluble calcium compounds. A small percerntage of the combusted sulphur enters the circuit as SO_3 and will accumulate in the cooled citrate tank as potassium sulphate. It is removed from time to time and dried and assayed to complete the sulphur balance.

CHAPTER 8

REFERENCES

Ackman, T.E. 1982. Sludge disposal from acid mine drainage treatment. US Bureau of Mines, Report of Investigations. 8672, Pittsburgh, PA, USA

Agnello, V.N., Duval, J., Mokaila, G.E. and Ratlabala, M.E. 2003. Industrial Minerals. Department of Minerals and Energy. Government of South Africa.

Ali, S.M., Haque, I. and Ahmed, B. 1968. Reduction of indigenous gypsum with charcoal. Pak. J. Sci. Ind. Res. **11** (2): 172-174.

Anthony, J.W., Bideaux, R. A., Bladh, K. W. and Nichols, M.C. 1990. Handbook of Mineralogy. Mineral Data Publishing, Tuscon, Arizona. **1**: 471.

APHA, 1985. Standard Methods for the Examination of Water and Wastewater. 12th edition. American Public Health Association. New York, NY, USA.

Asai, S., Konishi, Y. and Yabu, T. 1990. Kinetics of absorption of hydrogen sulphide into aqueous ferric sulphate solutions. Amer. Inst. Chem. Eng. J. **36** (9): 1331- 1338.

Astarita, G., Savage, D.W. and Bisio, A. 1983. Gas treatment with Chemical solvents, John Wiley & Sons, New York, NY, USA.

Atoji, M. and Rundle, R.E. 1958. Neutron diffraction study of gypsum, $CaSO_4.2H_2O$. J.Chem.Phys. **29** (6): 1306-1311.

AWWA, 1999. Water Quality and Treatment. 5th edition, American Water Works Association, McGraw Hill Inc., New York, NY, USA.

Azaroff, L.V. 1968. Elements of X-ray crystallography. McGraw-Hill Book Company, New York. pp 610.

Ball, M.C. and Norwood L.S. 1969. Studies in the calcium sulphate-water system. J. Chem. Soc. **4**: 1633.

Bamford, C.H and Tipper, C.F.H. 1980. Comprehensive chemical kinetics. reactions in the solid state. Elsevier Scientific Publishing Company. Vol **22**.

Barnes, H.L. and Romberger, S.B. 1968. Chemical aspects of acid mine drainage. J. Water Pollut. Contr. Fed. **40** (3): 371-384.

Beckhoff, B., Kanngießer, B., Langhoff, N., Wedell, R. and Wolff, H. 2006. Handbook of Practical X-Ray Fluorescence Analysis. 1st edition, Springer. Berlin.

Bekassy-Molnar, E., Marki, E. and Majeed, J.G. 2005. Sulphur dioxide absorption in air lift tube absorbers by sodium citrate buffer solution. Chem.Eng. Process. **44** (9): 1039-1046.

Benstedt, J. 1979. Early hydration behaviour of Portland cement containing chemical by-product gypsum. Cem.Tech. **10** (10): 404-410.

Bezou, C., Nonat, A., Mutin, J.C., Norlund Christensen, A. and Lehman, M.S. 1995. Investigation of the crystal structure of γ- $CaSO_4$, $CaSO_4.0.5H_2O$ and $CaSO_4.0.6H_2O$ by powder diffraction methods. J. Solid State Chem. **117**: 165-176.

Bish, D.L. and Howard, S.A. 1988. Quantitative phase analysis using Rietveld method. J. Appl. Cryst. **21**: 86-91

Blaine, R. L. and Hahn B. K. 1998. Obtaining Kinetic Parameters by Modulated Temperature Thermogravimetry. J. Therm. Anal. **54**: 695-704

Bosch, C. 1990. Distribution and inhibition of iron-oxidising bacteria in relation to acid drainage from gold and coal mine dumps in the Southern Transvaal. MSc Thesis, University of Stellenbosch, Stellenbosch, December.

Brauer, G. 1963. Handbook of Preparative Inorganic Chemistry, New York, 2nd edition. **1**: 938.

Brown, M.E. 1988. Introduction to thermal methods, techniques and applications. Chapman & Hall, New York. pp 1-20.

Budavari, S. 1989. The Merck Index, 11th edition. Merck & Co., Inc., Rahway New Jersey, USA. pp 257.

Buhrke, V. E., Jenkins, R. and Smith, D. K. 1998. A practical guide for the preparation of specimens for XRF and XRD Analysis. 2nd edition. Wiley, New York.

Bye, G.C. 1983. Portland Cement: Composition, Production and Properties, Pergamon Press, Oxford. pp 19.

Cadena, F. and Peters, R.W. 1988. Evaluation of chemical oxidizers for hydrogen sulphide control. J. Water Pollut. Control Fed. **60:** 1259-1263.

Chamber of Mines Research Organisation. 1988. New desalination programme on stream. R&D News CM, October.

Chandler, R.H. and Isbell, R.A.C. 1976. The Claus Process. R.H. Chandler Ltd., Braintree, USA.

Charsley, E.L. and Warrington, S.B. 1992. Thermal Analysis: Techniques and Application. The Royal Society of Chemistry. pp 1-16 and pp 31-58.

Chemeffco. GYP-CIX Brochure. (undated). South Africa.

Cork, D.J., Jerger, D. E. and Maka, A. 1986. Biocatalytic production of sulphur from process waste streams. Biotechnol. Bioeng. **16**: 149-162.

Davis, B.L. 1992. Quantitative phase analysis with Reference Intensity Ratios. National Institute of Standards and Technology, Special Publication. **846**: 7-15.

Davis, B.L., Kath, R. and Spilde, M. 1990. The Reference Intensity Ratio: its measurement and significance, Powder Diffraction. **5** (2): 76-78.

Dowdy, D.R. 1987. Meaningful activation energies for complex systems. The application of Ozawa-Flynn-Wall method to multiple reactions, J. Therm. Anal. Cal. **32**: 137-147.

Doyle, C.D. (1962). Estimating isothermal life from thermogravimetric data. J. Appl. Polym. Sci. **6**: 639-646.

Du Preez, L.A., Odendaal, J.P., Maree, J.P. and Ponsonby, M. 1992. Biological removal of sulphate from industrial effluents using producer gas as energy source. Environ. Technol. **13**: 875-882.

Durham, B., Bourbigot, M. and Pankratz, T. 2001. Membrane as pre-treatment to desalination in waste reuse: operating in the municipal and industrial sectors. Desalination. **138**: 83-90.

Eloff, E., Greben H.A., Maree, J.P., Radebe, B.V. and Gomes, R.E. 2003. Biological sulphate removal using hydrogen as the energy source, Proceedings of the 8th International Mine Water Association (IMWA) Congress. Johannesburg, 20 -25 October. pp 99-108.

Erofe'ev, B.V. 1946. Generalized equation of chemical kinetics and its application in reactions involving solids. Compt. Rend. Acad. Sci. URSS (Russian journal). **52**: 511-514.

Flynn, J.H. 1983. The isoconversional method for determination of energy of activation at constant heating rates. J. Therm. Anal. **27**: 95-102.

Flynn, J.H. and Wall, L.H. 1966. A quick direct method for the determination of Activation Energy from Thermogravimetric data. J. Polym. Sci. Part B: Polymer letters. **4**: 323-328.

Follner, F., Wolter, A., Preusser, A., Indris, S., Silber, C. and Follner, H. 2002. The setting behaviour of α- and β-$CaSO_4.0.5H_2O$ as a function of crystal structure and morphology. Cryst. Res. Technol. **37** (10): 1075–1087.

Forster, S. 1988. Department of Water Affairs and Forestry. Personal Communication.

Garcia- Calzada, M., Marban, G. and Fuertes, A. 2000. Decomposition of CaS particles at ambient conditions. Chem. Eng. Sci. **55**: 1661-1674.

Garn, P.D. 1965. Thermoanalytical methods of investigation. 1st edition. Academic Press, New York. pp 606.

Garn, P.D. 1978. Kinetic parameters. J. Therm. Anal. **13**: 581-593.

Garner, W.E. 1955. Chemistry of the Solid State. Butterworth Scientific Publications, London. Chapter 8.

Gaskell, D.R. 1973. Introduction to Metallurgical Thermodynamics. McGraw-Hill. pp 442-453.

Geldenhuys, A.J., Maree, J.P., de Beer, M. and Hlabela, P. 2001. An integrated limestone/lime process for partial sulphate removal. Paper presented at the Environmentally Responsible Mining Conference, South Africa, CSIR, Pretoria, 25-28 September.

Graham, F. 1995. The Discovery of X-Rays. Scientific American. November. pp 86-91.

Gryka, G.E. 1992. System for recovering sulphur from gases especially natural gas. PIPco, Inc., Southport, CT (USA).

Gryka, G.E. 2005. Titration for HSO_3 and HS_2O_3, Personal Communication. PIPco, Inc., Southport, CT (USA).

Hand, R.J. 1997. Calcium sulphate hydrates: a review. Br. Ceram. Trans. **96** (3): 116-120.

Hill, R.J. 1991. Expanded use of the Rietveld Method in studies of phase abundance in multiphase mixtures, powder diffraction, **6** (2): 74-77.

http://www.nelliott.demon.co.uk/company/claus.html. Converting Hydrogen Sulphide by the Claus Process.

Imaizumi, T. 1986. Some Industrial Applications of Inorganic Microbial Oxidation in Japan. Biotechnol. Bioeng. Symp. **16**: 363-371.

Jander, W. 1927. Reactions in the Solid State at High Temperatures. J. Inorg. Gen. Chem. **163**: 1-30.

Johnston, F. and McAmish, L. 1973. A study of the rates of sulphur production in acid thiosulfate solutions using S-35. J. Colloid. Interf. Sci. **42**: 112-119.

Jones, G.A., Brierley, S.E., Geldenhuis, S.J.J. and Howard, J.R. 1988. Research on the contribution of mine dumps to the mineral pollution load in the Vaal Barrage. Report 136/1/89 to the Water Research Commission by Steffen, Robertson and Kirsten (Pretoria) Inc. pp 1-8.

Juby G.J.G., Schutte, C.F. and van Leeuwen, J.W. 1996. Desalination of calcium sulphate scaling mine water: design and operation of the Sparro process. Water SA. **22** (2): 161-172.

Keattch, C.J. and Dollimore, D. 1975. An Introduction to Thermogravimetry. 2nd edition. Heyden, London. pp 164.

Keller, J.L. 1956. U.S. Pat. 2,729,543. Removal of sulfur dioxide from gases containing the same. Los Angeles. California. January.

Klug, H.P. and Alexander, L.E. 1974. X-Ray Diffraction procedures: For Polycrystalline and Amorphous Materials, 2nd ed. John Wiley & Sons, New York, London. pp 992.

Kobayashi, H.A., Stenstrom, M. and Mah, R. A. 1983. Use of photosynthetic bacteria for hydrogen sulfide removal from anaerobic waste treatment effluent. Wat. Res. **17**: 579-587.

Kohl, A.L. and Riesenfeld, F.C. 1985. Gas purification. 4th edition. Gulf Publishing Company. Houston, Texas, USA.

Korosy, L., Gewanter, H.L., Chalmers, F.S. and Vasan, S. 1974. Chemistry of SO_2 absorption and conversion to sulphur by the Citrate Process. 167th American Chemical Society National Meeting. Los Angeles. 5 April.

Larraz, R. 1999. Hydrocarbon Processing. Student paper. July. pp 69-72.

Lesnikovich, A.I. and Levchik, S.V. 1983. A method of finding Invariant Values of Kinetic Parameters. J. Therm. Anal. **27**: 89-94.

Loewenthal, R.E., Wiechers H.N.S., Marais G.V.R. 1986. Softening and stabilization of municipal waters. WRC Report No. 24/86. Pretoria, RSA.

Lloyd, G.M. 1985. Phosphogypsum. Florida Institute of phosphate research. Publication no. 01-000-035.

Lubelli, B., van Hees, R. P. J. and Caspar, J. W. P. 2004. The role of sea salts in the occurrence of different damage mechanisms and decay patterns on brick masonry, Con. Build. Mat. March. **18** (2): 119-124.

Mantel, D.G. 1991. The manufacture, properties and applications of Portland Cements, Cement Additives and Blended Cements, Penrose Press, PPC, Johannesburg. pp 13.

Mantel, D.G. and Liddell, D.G. 1988. Manufacture of synthetic gypsum from limestone and sulfuric acid. World Cement. October. **19** (10): 404-410.

Maree, J.P. 1988. Sulphate removal from industrial effluents. Ph.D Thesis, University of the Orange Free State, Bloemfontein.

Maree, J.P. and Hill, E. 1989. Biological removal of sulphate from industrial effluents and concomitant production of sulphur, Water Sci. Technol. **21**: 265-276.

Maree, J.P. and Strydom, W.F. 1985. Biological sulphate removal from a packed bed reactor, Wat. Res. **19** (9): 1101-1106.

Maree, J.P., Bosman, D.J. and Jenkins, G.R. 1989. Chemical removal of sulphate, calcium and heavy metals from mining and power station effluents. Water Sewage and Effluent. September. **9** (3): 10-25.

Maree, J.P., Gerber, A. and Hill, E. 1987. An integrated process for biological treatment of sulphate containing industrial effluents. J. Water Pollut. Control Fed. **59** (12): 1069-1074.

Maree, J.P., Leibowitz, A. and Dods, D. 1990. Sulphate wastes. Rustenburg Symposium.

Maree, J.P., Theron, D., Nengovhela, N.R., Hlabela, P.S. 2005. Sulphur from smelter gases and sulphate –rich effluents. J. S. Afr. Inst.Min.Metall. **105**: 1-4.

Molony, B. and Ridge, M.J. 1968. Aust. J. Chem. **21** (4): 1063.

Murat, M., Hajjouji, A. E. and Comel, C. 1987. Investigation on some factors affecting the reactivity of synthetic orthorhombic anhydrite with water: Role of foreign cations in solution. Cem. Concr. Res. **7** (4): 633–639.

Nagl, G. 1997. Controlling H2S emission. Chem. Eng. March. **104**: 125-128.

Ozawa, T. 1965. A new method of analysing Thermogravimetric data. Bull. Chem. Soc. Japan. **38**: 1881-1886.

Pagella, C. and Faveri, D.M. 1999. H_2S gas treatment by iron bioprocess. Chem. Eng. Sci. **55** (12): 2185-2194.

Piloyan, G.O., Ryabchikov, I.D. and Novikova, O.S. 1966. Determination of activation energies of chemical reactions by Differential Thermal Analysis. Nature (London). **212**: 1229.

Popescu, M., Simion, A. and Matei, V. 1985. Study of thermal behaviour up to 1550 ºC of materials containing calcium sulphate. J. Therm. Anal. **30**: 297-303.

Pulles, W., Juby, G.J.B. and Busby, R.W. 1992. Development of the Slurry Precipitation and Recycle Reverse Osmosis (SPARRO) technology for desalinating scaling mine waters. Wat. Sci. Technol. **25** (10): 177-192.

Rameshni, M. and Santo, S. 2005. Production of Elemental Sulphur from SO_2. RSR (Ramenshi SO_2 Reduction). WorleyParsons. Arcadia, California 91007, USA.

Ratlabala, M.E. 2003. An Overview of South Africa's Mineral Based Fertilizers. Department of Minerals and Energy. Government of South Africa.

Ray, W.G., Arbo, J.C. and Gryka, G.E. 1990. Process for Recovery of Sulphur from a Gas Stream. US Patent 5,057,298, assigned to PIPco Inc., Southport, CT (USA).

Reddy, P.P., Ratinam, M., Sundaram, N. and Satyanarayananan, A.K. 1967. Studies on the reduction of gypsum to calcium sulphide. Chem. Age (India). **18** (4): 282.

Rochelle, G.T. and King, C.J. 1979. Process alternatives for stack gas desulfurization with H_2S regeneration to produce sulfur. Amer. Inst. Chem Eng. Symposium series. **188** (75): 48-61.

Roode, Q.I. 1996. The crystallography of synthetic gypsum and rare-earth-doped gypsum. MSc Thesis. University of the Witwatersrand. Johannesburg. South Africa.

Saeed, M., Khaliquw, A., Mansoor, S. and Bhatty, M.K. 1983. Pak. J. Sci. Ind. Res. **26** (4): 274.

Satoh, H., Yoshizawa, J. and Kametani, S. 1988. Bacteria help desulphurize gas. Hydrocarbon Processing. pp 76.

Savostianoff, D. 1990. The phosphate rock producers in strong position, Inf. Chim. **314**: 131-151.

Schoeman, J.J. and Steyn, A. 2001. Investigation into alternative Water Treatment Technologies for the treatment of underground mine water discharged by Grootvlei Proprietary Ltd into the Blesbokspruit in South Africa. Desalination. **133**: 13-30.

Senum, G.I. and Yang, R.T. 1977. Rational approximations of the integral of the Arrhenius function. J. Therm Anal. **11**: 445-448.

Sestak, J. and Berggren G. 1971. Study of the kinetics of the mechanism of solid - state reactions at increasing temperatures. Thermochim. Acta. **3**: 1-12.

Sestak, J., Satavo, V. and Wendlandt, W.W. 1973. The study of heterogeneous. processes by thermal analysis.Thermochim. Acta. **7**: 333-336.

Sharp, J.H., Brindley, G.W. and Achar, B.N. 1966. Numerical data for some commonly used solid state reaction equations. J. Amer. Ceram. Soc. **49**: 379

Shimadzu Corporation, www.shimadzu.com.

Shimin, T., Dalla Lana, I.G. and Chuang, K.T. 1997. Ind. Eng. Chem. Res. October. **36**: 4087-4093.

Simonyi, T., Ackers, D. and Grady, W. 1977. The Character and Utilization of the Sludge from Acid Mine Drainage Treatment Facilities. Coal Research Bureau and the College of Mineral and Energy Resources of West Virginia University, Report No. 165, Morgantown, WV.

Smith, D.K., Johnson Jr. G.G. Scheible, A. Wimms, A.M, Johnson, J.L and Ullmann, G. 1987. Quantitative X-Ray Diffraction method using the Full Diffraction Pattern, Powder Diffraction. **2** (2): 73-77.

Smit, J.P. 1999. The purification of polluted mine water. Proceedings of the International Symposium on Mine, Water and Environment for the 21st Century. Seville, Spain.

Spiegler, K.S. 1966. Principles of Desalination. Academic Press. 2nd edition. New York. pp 345.

Taylor, H.F.W. 1990. Cement Chemistry, Academic Press, London. pp 233-234.

Toerien D.F. and Maree J.P. 1987. Reflections on anaerobic process biotechnology and its impact on water utilisation in South Africa. Water SA. **13**: 137-144.

Valerdi-Perez, R., Lopez-Rodriguez, M. and Ibanez-Mengual, J.A. 2001. Characterizing and electrodialysis reversal plant. Desalination. **137**: 199-206.

Van der Merwe, E.M., Strydom, C.A. and Potgieter, J.H. 1999. Thermogravimetric analysis of the reaction between carbon and $CaSO_4.2H_2O$, gypsum and phosphogypsum in an inert atmosphere. Thermochim. Acta. **340**: 431-437.

Van Grieken, R. E. and Markowicz, A. A. 2002. Handbook of X-Ray Spectrometry. 2nd edition. Marcel Dekker Inc, New York.

Van Houten, R. T. 1996. Biological sulphate reduction with synthesis gas. PhD thesis. Wageningen Agricultural University. Wageningen. Netherlands.

Vasan, S. 1975. The citrex process for SO_2 removal. Chem. Eng. Prog. **71**: 61-65.

Verhoef, L.H. 1982. The chemical pollution of waters resulting from mine activities. Ground water '82. Johannesburg. pp 141-147.

Visser, A. 1995. The anaerobic treatment of sulphate containing wastewater. PhD thesis. Agricultural University Wageningen, The Netherlands.

Vyazovkin, S.V and Lesnikovich, A.I. 1990. An approach to the solution of the inverse kinetic problem in the case of complex processes. Part I. Methods employing a series of thermoanalytical curves. Thermochim. Acta. **165**: 273-280.

Vyazovkin, S.V and Lesnikovich, A.I., 1987. Some aspects of mathematical statistics as applied to nonisothermal kinetics. J. Therm. Anal. **32**: 909-918.

Vyazovkin, S.V., Goryachko, V.I. and Lesnikovich, A.I. 1992. An approach to the solution of the inverse kinetic problem in the case of complex processes. Part III. Parallel independent reactions. Thermochim. Acta. **197**: 41-51.

Wagner J.C and Van Niekerk, A.M. 1987. Quality and treatment of effluents originating from mine and municipal waste sites. Proceedings of the International Conference on Mining and Industrial Waste Management. Johannesburg. pp 283-286.

Wewerka, E.M., Williams, J.M. and Wagner, P. 1982. The Use of Multi-Media Environmental Goals to Evaluate Potentially Hazardous Trace Elements from High Sulphur Coal Preparation Wastes. Report LA-9189 MS, UC-90i, Los Alamos National Laboratory: Los Alamos, NM, USA, April.

WHO, 1996. Guidelines for drinking water quality. 2nd edition. World Health Organization, Geneva.

Wiles, D.B. and Young, R.A. 1981. A new computer program for Rietveld analysis of X-Ray powder diffraction patterns. J. Appl. Cryst. **14**: 149-151.

Wirsching, F. 1978. Gypsum. English translation of a contribution to Ullmanns Encyklopedia der Technischen Chemie. **12**: 1-28.

Zeman, L.J., Zydney, A.L. 1996. Microfiltration and Ultrafiltration: Principles and Applications, Marcel Dekker: New York.